DIAGNOSTIC IMAGING

of the Loggerhead sea turtle, *Caretta caretta*

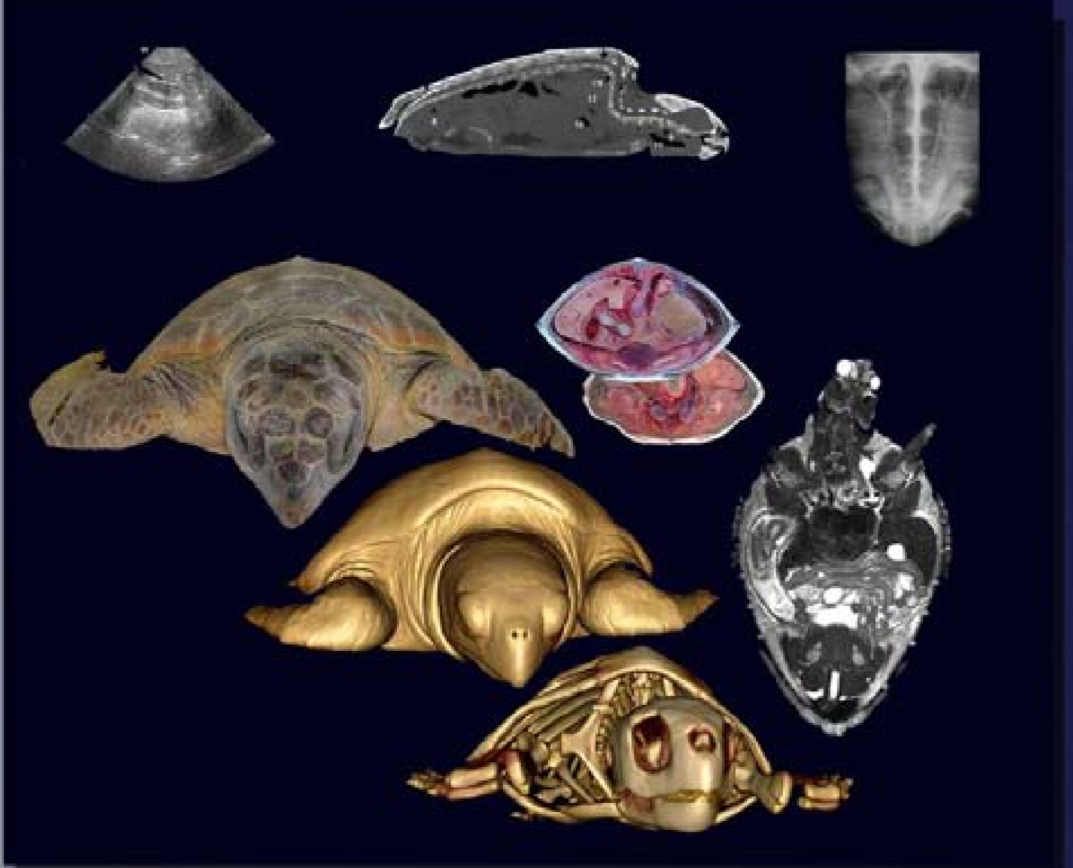

Ana Luísa Schifino Valente

PhD Thesis - 2007

UAB

Universitat Autònoma de Barcelona

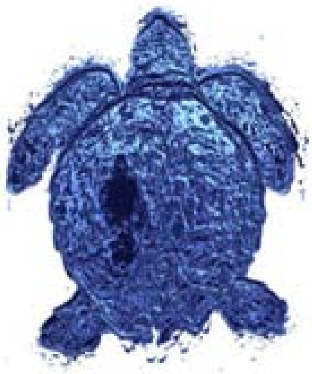

DIAGNOSTIC IMAGING OF THE LOGGERHEAD SEA TURTLE (*Caretta caretta*)

Memoria presentada por

Ana Luisa Schifino Valente

Para optar al grado de Doctor en Veterinaria

Directores

Prof. Dr. Rafaela Cuenca Valera   Prof. Dr. Ignasi Marco Sanchez

Dep. de Medicina i Cirurgia Animal – Facultat de Veterinaria

Universitat Autonoma de Barcelona

Bellaterra, 2007

ACKNOWLEGMENTS (in Spanish)

Una tesis doctoral, a pesar de estar firmada por un solo autor, no es un trabajo individual, sino el fruto de un esfuerzo colectivo que sólo es posible gracias a la colaboración y el apoyo de varias personas, tanto en el aspecto científico e institucional como personal. Por esto, quiero aquí dejar expreso mis agradecimientos a estas personas, algunas de Brasil y otras que han estado a mi lado durante estos cuatro años en Barcelona.

A la Universidade Federal de Pelotas (UFPel - Brasil) por haberme concedido la oportunidad de realizar este trabajo, estando ausente de mis actividades de enseñanza en esta institución. Al Instituto de Biología y a los colegas del Departamento de Morfología por haber apoyado mi excedencia para cursar el doctorado fuera del país. En especial al Prof. Dr. Althen Teixeira Filho, por apoyarme la excedencia asumiendo la responsabilidad de impartir mis clases en la asignatura de Anatomía de los Animales Domésticos I.

Quería agradecer también al Prof. Luis Fernando Minello (Dep. de Morfología, IB, UFPel), por asumir la dirección del Núcleo de Reabilitação de Fauna Silvestre y representarme legalmente en la UFPel durante mi ausencia.

Al Prof. Dr. Santiago Lavín (Dep. de Medicina i Cirugía Animal, Facultat de Veterinaria de la UAB) por la acogida, amistad, compañerismo y confianza depositados en mí durante estos cuatro años de convivencia.

Al Prof. Dr. Ignasi Marco (Dep. de Medicina i Cirugía Animal, Facultat de Veterinaria de la UAB) por su interés e incentivo. Por su amistad y orientación en la realización de esta tesis.

A mi amiga y directora de tesis Profa. Dra. Rafaela Cuenca (Dept de Medicina i Cirugía Animal, Facultat de Veterinaria de la UAB). Te agradezco el hacerme sentir capaz, tu perseverancia, cariño e incentivo y sobretodo por los lazos de amistad y confianza que hemos creado.

Al Prof. Dr. Josep Pastor por la amistad, por su paciencia y habitual disponibilidad a ayudar. Por los apoyos técnicos y los momentos divertidos que compartimos.

A la Dra. María Angeles Zamora, neuróloga de Diagnosis Médica (Barcelona), por su dedicación, paciencia y motivación por este trabajo. Por facilitarnos el acceso a la tomografía computerizada y resonancia magnética, pruebas sin las cuales no podríamos haber desarrollado este trabajo.

Al director del Centro de Recuperación de Animales Marinos, Sr. Ferran Alegre (CRAM), por permitir que utilizáramos los animales atendidos por el centro.

A la María Luz Parga MSc., veterinaria del CRAM, por su compañerismo, apoyo y por poner a nuestra disposición sus pacientes para la realización de esta tesis. Al biólogo del CRAM, Alex Bartolí, por ayudarnos en el manejo de las tortugas. A los muchos voluntarios del CRAM que ayudaran en algunas de las etapas de este trabajo, por su disponibilidad y entusiasmo.

Al Dr. Jaume Martorell, Clínico de animales exóticos del Hospital Veterinario de la UAB, por su ayuda en la ejecución de las radiografías digitales.

Al Prof. Dr. Jordi Franch (Dep. de Medicina i Cirugía Animal, Facultat Veterinaria de la UAB) por las sugerencias y apoyo técnico en las radiografías de las tortugas.

A la Profa. Dra. Yvonne Espada (Dep. de Medicina i Cirugía Animal, Facultat Veterinaria de la UAB) por la realización de las ecografías y por su apoyo técnico en este área.

Al Prof. Dr. Francisco Reina (Dep. de Anatomía, Facultat Medicina de la UAB) la realización de los cortes anatómicos de las tortugas.

A los Profs. Drs. Manel López Bejar y Carlos López Plana (Dep. de Sanitat i Anatomia Animal, Facultat Veterinaria de la UAB) y al Museo de Zoología de Barcelona por poner a nuestra disposición esqueletos de tortuga utilizados como referencia en este estudio.

Al Prof. Dr. Thomas Dellinguer, Universidade da Madeira, Portugal, por aceptar mi propuesta de cooperación en su proyecto, permitiendo mi estancia de 3 meses en esta Universidad.

A los revisores anónimos de los artículos por sus críticas constructivas.

A los amigos del Servicio de Ecopatologia de Fauna Salvaje (SEFaS), Encarna Casas, Gregorio Mentaberre, Carlo Siracusa, Ester Bach, Francesc (Kiko) Closa, Montse Mesalles, Cintia Mastrorilli, Pancha Alcayaga y Jordi López. En esta corta jornada que es la realización de la tesis, tuvimos momentos para reírnos juntos, llorar, alegrarnos, cansarnos, quejarnos, lamentarnos y consolarnos por los tropiezos de la vida. Os agradezco de todo corazón el cariño con que me recibieron.

A la Dra. Roser Velarde, histopatológa del SEFaS, que a pesar del poco tiempo de convivencia hemos despertado muchas cosas en común.

A la Profa. Dra. Teresa Mora por los momentos relajados que pasamos en compañía de Rafi en la hora de la comida y en aquel típico “cafezinho” en la salida del restaurante de la facultad.

A mi amigo Prof. Dr. Luis Carlos Guerreiro (Universidade da Madeira) por el apoyo logistico durante mi estancia en Funchal, Portugal.

A mi amigo Juan García Marqués por su colaboración en la edición de esta tesis. A las señoras María Antonia y Eulalia Blanch Piera por el cariño de la acogida y por hacer parte de mi familia en España.

A mis amigas Ana Paula Albano, Rosa Massaro y Neila Moraes por ser una prolongación mía en Brasil y a Patricia Vives por ser la segunda madre de mis perros mientras estuve ausente.

A mis padres, Nestor Saraiva Valente y Elci Schifino Valente, por soportar mi ausencia en silencio, por desear lo mejor para mí, aunque que implicase un dolor en sus corazones. Os agradezco por la paciencia de la espera y por apoyar mis ideales incondicionalmente. En memoria a mi tía, Eldi Schifino Fonseca, para quien la espera fue demasiado larga, lamento no haber estado a tu lado en el momento en que nos dejaste. Que Dios esté contigo, donde estés.

A mi pareja Lluís Doutres Blanch por su cariño y amor. Por preocuparse por mí en los momentos críticos de adaptación al cambio de cultura y país. Por su constante estímulo a mi avance y por la comprensión en los momentos que dejé de estar en el hogar por estar en la Universidad. Por fin, me faltarían líneas para explicar cuánto una persona puede ser importante en la vida de otra. A ti cariño, y a nuestras “buppies” (perritas Tosca y Cane) os agradezco por los momentos de felicidad que compartimos.

A aquellos que colaboraron directa o indirectamente en la realización de este trabajo y que por ventura no fueron mencionados en este apartado, por favor, sepáis que tengo mi profundo reconocimiento.

A ti, lector, si terminas la lectura.

A las tortugas...
Sí. A las tortugas...
Sin tu sufrimiento no habría el motivo,
Sin tu amenaza no habría preocupación en conservarte
Sin tu existencia no habría tesis y...
Lo más importante, los océanos no serian tan sabios.
Lo siento por retardar tu retorno al mar
Tu alma pertenece a las corrientes
Pues tu libertad es azul.
Perdóname por transportarte, por sujetarte, pincharte...
Ojala podamos redimir tu sufrimiento
a través de nuestro auxilio.

INTRODUCTION

1. INTRODUCTION

Human activity causes constant and increasing threats to wildlife. From oil spills and boat strikes to habitat loss and entanglement with potentially fatal debris, marine animals in crisis are a sadly common worldwide feature (IUCN, 2006). The Loggerhead sea turtle (*Caretta caretta*) in the Mediterranean faces an imminent threat of extinction due to accidental captures and habitat loss (Margaritoulis et al., 2003; Gómez de Segura et al., 2006). Each year, marine rescue centers along the Mediterranean coast have become inundated with juvenile and subadult turtles, the majority of which are injured as a result of human activities. Between 1994 and 2005, 527 Loggerhead sea turtles were rescued in the *Centre de Recuperació de Animals Marins de Catalunya* (CRAM) in Premià de Mar (Barcelona, Spain), accounting for 88% of the admissions caused by fishery interactions, most of them related with the ingestion of fishhooks (CRAM, 2006). Veterinary Healthcare and Education Programs designed to specifically address the medical and biological issues that accompany reintroduction programs have been performed by this center in scientific agreement with the Servei d'Ecopatologia de Fauna Salvatge of the Universitat Autònoma de Barcelona.

Chelonian medicine represents a great challenge to veterinarians. A major part of the unusual anatomy and physiology of the turtles and tortoises is scarcely known and routine clinical examination usually applied to domestic animals provides little information about their health status (MCarthur et al., 2004). Injured sea turtles usually display few clinical signs of illness and therefore diagnosis in this species is frequently poor. Diagnostic imaging techniques are routinely applied in human medicine and increasingly so in companion animal medicine. However, because of differences in anatomy, physiology, physiopathology, indications, specificity and sensibility of these techniques in sea turtles, the medical references can not be directly deduced from those of dogs/cats or even other reptilian species (Silverman and Jansen, 2006). Specialized medical databases for radiology, ultrasonography, computed tomography and magnetic resonance for Loggerhead sea turtles are needed in order to provide references for image interpretation. These techniques provide a good view of anatomical structures and organs, are non-invasive, and suitable for accurate diagnosis as well as assessing biological data in this endangered species.

The most widely-used imaging techniques in current veterinary medicine are radiography and ultrasonography. Although the use of computed tomography and magnetic resonance imaging are usually limited to specialized facilities, use of them is imperative when dealing with endangered species such as the Loggerhead sea turtle. In this work we have studied Loggerhead sea turtles admitted and kept temporarily at the *Centre de Recuperació de Animals Marins de Catalunya* (CRAM) between 2004-2005. The normal parameters for radiology, ultrasound, computed tomography and magnetic resonance of this species were studied and described in the five scientific papers presented in this thesis. Additionally, two other papers concerning the use of Doppler ultrasonography and evaluation of the ingesta passage times in the Loggerhead sea turtle are also included as annex documents. The last paper, although not related to a specific imaging technique, was included due to the use of specialized radiographic markers required to dog and cat testing. Clinically healthy animals were subjected to radiographic and ultrasonographic examination at the facilities of the Veterinary Hospital of the Universitat Autònoma de Barcelona; the computed tomography and resonance magnetic scans were performed in a private human radio-diagnostic clinic in Barcelona.

1.2. OBJECTIVES

The aims of this work are:

1. To provide the normal cervical and coelomic radiographic appearance of the Loggerhead sea turtle, in the dorso-ventral view, as well as other useful landmarks, to allow for correlation of shell scutes with internal anatomic structures.

2. To provide the normal radiographic anatomy of the limbs of the Loggerhead sea turtle in combination with data obtained from computed tomography - osteological, gross anatomical and histological data.

3. To describe the normal ultrasonographic appearance of cervical structures and coelomic organs of the Loggerhead sea turtle, and to provide the respective images of frozen cross-sections for anatomical reference.

4. To provide normal computed tomographic images of the vertebral column and coelomic structures of the Loggerhead sea turtle, by establishing reference standards for organ size and position in this species; to provide images of virtual tracheo-bronchoscopy and 3D reconstructions of the respiratory tract and bone structures.

5. To provide the normal magnetic resonance imaging (MRI) appearance of coelomic structures of Loggerhead sea turtles in T1 and T2-weighted scans via comparison with cross-sectional anatomic sections of this species.

1.3. LITERATURE REVIEW

1.3.1. Evolution of sea turtles

The oldest turtle fossils found date from the Jurassic period (210 million years ago). *Proganochelys* is the most primitive turtle known; it was a heavily-armoured animal with some of the features seen in the turtles today, such as presence of the shell consisting of a large number of bones including the ribs that are fused to form a single solid plate (Gaffney, 1990). In the middle Jurassic period, the main lineage of turtles had split into two branches: the side-neck turtles (pleurodires), which protect the head by folding the neck and head over to one side, and the hidden-neck or arch-neck turtles (cryptodires), which pull the neck into a vertical S-curve and retract the head straight back between the shoulders (Perrine, 2003). The side-necked turtles produced many sea-going species during the Cretaceous period (145 to 65 million years ago), but all of these died out. Modern pleurodires live in freshwater. Sea turtles date from the Cretaceous and belonged to the hidden-neck group, to which the majority of turtles belong today. The hidden-neck group comprised many families, most of which had died out by the early Cretaceous period. Fossil records of chelonioids before the Late Cretaceous have been poorly documented. The Cretaceous sea turtle *Archelon ischyros* was first recorded based on fossils found in South Dakota, E.U.A. (Wieland, 1896). However, according to Hirayama (1998) the oldest sea turtle known dates from the Early Cretaceous stage (about 110 million years ago), the fossil being found in eastern Brazil. Four important families of hidden-neck sea turtles did survive into the mid-Cretaceous period. Two of these families, the Dermochelyidae and the Cheloniidae, have modern descendants. The genera and eight species of sea turtles known today all originated within the last 60 to 10 million years. The leatherback sea turtle is the only surviving member of the Dermochelyidae. The Loggerhead sea turtle and other remaining modern sea turtles belong to the Cheloniidae.

1.3.2. Taxonomy of sea turtles

The eight species of modern sea turtles are found within two families: Dermochelyidae and Cheloniidae. The first family has only one species: the Leatherback sea turtle (*Dermochelys coriacea*). The Cheloniidae family comprises six species of sea turtles: the Green turtle (*Chelonia mydas*), Loggerhead sea turtle (*Caretta caretta*), Hawksbill turtle (*Eretmochelys imbricata)*, Kemp's ridley (*Lepidochelys kempii),* Olive ridley (*Lepidochelys olivacea)* and the Flatback sea turtle (*Natator depressus)* (Perrine, 2003).

The name Caretta is a latinized version of the French word 'caret', meaning 'turtle, tortoise, or sea turtle' (Smith and Smith, 1980). The name 'caret' or 'carey' (Spanish) is usually associated in colloquial language with the Hawksbill turtle rather than the Loggerhead, and the name probably resulted from Linnaeus' confusion over the identity of these species (Brongersma, 1961; Wallin, 1985).

Taxonomy of the Loggerhead sea turtle

Phylum Chordata

Subphylum Vertebrata

Superclass Tetrapoda

Class Reptilia

Subclass Anapsida

Order Testudines (Linnaeus 1766)

Suborder Cryptodira (Gray 1825)

Superfamily Chelonioidae

Family Cheloniidae

Caretta caretta (Linnaeus, 1758)

1.3.3. Morphological features of the Loggerhead sea turtle

The Loggerhead sea turtle is named for its relatively large and triangular head, which support powerful jaws that enable the species to feed on hard-shelled prey, such as whelks and conch. The neck and flippers are usually brown to reddish, being brown on top and pale yellow on the sides and bottom. Front flippers are short and thick with 2 claws while the rear flippers can have 2 or 3 claws (Brongersma, 1961; Pritchard and Trebbau, 1984).

Some aspects of the external morphology of this species change depending on the size of the specimen. Based on the carapace length, different age categories for Loggerhead turtles have been established (Dood, 1988). Morphological features are different in the hatchlings, in which the external colour pattern varies from light to dark brown to dark gray dorsally. Flippers are dark gray to brown above with white to white-gray margins. The coloration of the plastron is generally yellowish to tan. At emergence, hatchlings average 45 mm in length and weigh approximately 20 g (Caldwell et al., 1955). The category ‘hatching’ includes the turtles from their hatching to the first few weeks of life as they begin rafting on currents for the life stage known as the ‘lost year’ (Carr, 1986). This latter category includes turtles up to 10 cm straight-line carapace length (SLCL) and is characterized by the presence of the umbilical scar (Dood, 1988) (Fig. 1A).

Juveniles are those in the pelagic rafting life stage and have an SLCL of approximately 40 cm. The center of the dorsal scutes is elevated into a sharp keel or spine (Dood, 1988) (Fig. 1B). Subadults are those between the end of the pelagic rafting stage to the onset of sexual maturity (Fig. 1C), which occurs about 70-90 cm SLCL, depending on the population (Dood, 1988). In the Western Atlantic, the adult Loggerhead sea turtle typically has a 73-107cm carapace length and weighs up to 180 kg (Bjorndal et al., 1983). In the Mediterranean sea, adults are smaller than those from the Atlantic, showing a carapace length of about 90 cm and weighing less than 100 Kg (Fig. 1D) (Pritchard and Mortimer, 1999). The size at sexual maturity for males is assumed to be similar to that for females.

Figure 1. Loggerhead sea turtle: A, Hatchling; B, carapace of small juvenile - arrows indicate dorsal keels; C, subadult; D, male (top) and female (bottom) adult turtles.

In adults and sub-adults, the carapace is moderately wide, slightly heart-shaped and reddish-brown; the plastron is generally a pale yellowish colour (Fig. 1C-D). The carapace is composed of bone covered by large, non-overlapping, rough keratinized scutes. The carapace scutes are numbered from front to back and identified as nuchal (n=1), vertebral (n=5), lateral or costal (n=5), marginal (n=6) and inframarginal or bridge scutes (variable in number), (Pritchard and Mortimer, 1999) (Fig. 2A). The carapace bones are flat, thick and do not coincide with the scutes. They are identified as nuchal, neural, pleural, suprapygal, pygal or peripheral bones according to carapace localization. The nuchal bone is large and notched laterally. The neural bones (usually 7-11) are narrow, forming a continuous series over the vertebral column. Each neural bone usually has a vertebral *centrum* attached to the ventral surface (Wyneken, 2001). Pleural bones are fused with the ribs and contact the peripheral bones by way of free tips at the end. A single pygal bone and a pair of suprapygal bones form the caudal edge of the carapace (Wyneken, 2001) (Fig.2B).

The plastron is also covered by keratinized scutes under which lie nine bones (Fig. 2D). The hyoplastra and hypoplastra are similar in shape. Interdigitating projections are present on the antero-lateral faces of the hyoplastra and postero-lateral faces of the hypoplastra. The epiplastra are reduced, and the entoplastron is elongated. The xiphiplastra are also elongated and nearly straight (Wyneken, 2001).

The heavily-keratinized scutes of the carapace and plastron of the Loggerhead provide a protective barrier against attacks and abrupt environmental changes. The epidermis contains the pigment cells, and is much thicker on the plastron of the Loggerhead than that of the Green turtle. The keratin is of the hard variety and assists in reducing frictional drag in water (Solomon et al., 1986).

The carapace and plastron undergo substantial changes after hatching. Growth is allometric because different parts of the body grow at different rates. Hatchlings have three dorsal keels on a roughly heart-shaped carapace and there are two longitudinal ridges on the plastron that disappear with age. In both hatchlings and juveniles, the vertebral scutes are wider than they are long, but as the turtle grows, there is greater increase in length relative to width. Although the increase in length does not occur simultaneously in all scutes or at the same rate (Brongersma, 1972) the vertebral scutes V1 to V4 tend to increase length relative to width. The vertebral scutes of juveniles are keeled with a knob-like process on the posterior portion of each keel, which is most distinct on the anterior scutes. At a length of 35.0 cm, the knobs generally disappear although the keels are still present, and at 58.0 cm the keels also disappear (Brongersma, 1972).

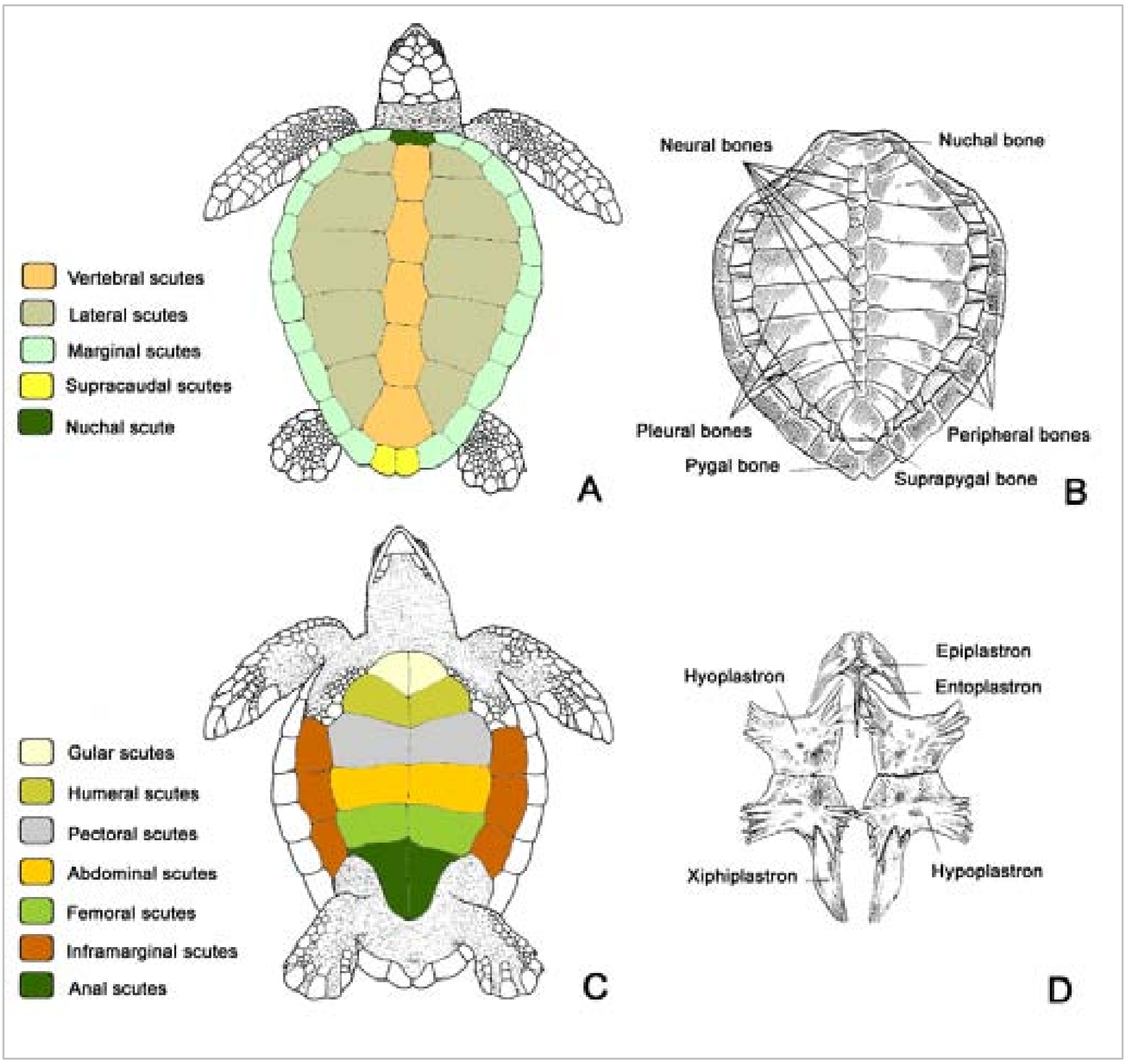

Figure 2: Morphology of the carapace and plastron of Loggerhead sea turtles. A, Dorsal view of the carapace; B, Dorsal view of carapace bones; C, Ventral view of plastron; D, Ventral view of plastron bones. Scutes are indicated in the legend. Drawings adapted from Pritchard et al., 1999 and Wyneken, 2001.

The bones of the forearm and hand of the Loggerhead sea turtle are illustrated by Walker (1973) and especially the humerus, by Zangerl (1958) and Zug et al. (1986). Rhodin (1985) noted similarities in patterns of skeletal growth between the Loggerhead and freshwater turtles. In both groups, non-calcified cartilage remains avascularised, and a subphyseal plate is formed causing transient isolation of a metaphyseal cartilage cone. However, in the Loggerhead, the central cartilaginous zone does not hypertrophy and remains uncalcified even as the peripheral zone of the subphyseal plate becomes ossified. Also, the basophilic network of Suzuki's tissue is localized in the zone of cartilaginous expansion in the center of the subphyseal plate rather than in the epiphysis (Rhodin, 1985). These modifications may be related to the rapid growth in the uncalcified portion of the subphyseal plate.

There are three comprehensive guides to Loggerhead sea turtle anatomy currently available. Rainey (1981) used black-and-white photographs to illustrate the locations of organ systems in a juvenile male Loggerhead and three other species of sea turtles. Wolke and George (1981) presented a guide for conducting necropsies under field conditions. Line drawings supplement a description of dissection methods, and information on fixatives, equipment, and data forms is provided. In a comprehensive publication, Wyneken (2001) provided a systematic description of sea turtle anatomy which includes the Loggerhead.

The main morphological features of the Loggerhead sea turtle distinguishing it from other sea turtle species are the presence of two pairs of prefrontal scales; elongated carapace, somewhat tapered posteriorly, and thickened above the caudal region; non-imbricated dorsal scutes (except in some young specimens); smooth adult vertebral scutes, although small turtles have projections toward the rear of lateral and vertebral scutes (more conspicuous on the latter); five pairs of pleural scutes, with first contact at the pre-central; usually three or four infra-marginal enlarged and poreless laminae; two claws on each flipper as hatchlings; very broad triangular head with powerful jaws; reddish-brown carapace; yellowish-white to yellowish-brown plastron (Pritchard and Mortimer, 1999). Detailed descriptions are also to be found in Smith and Smith (1980) and Pritchard and Trebbau (1984).

1.3.4. Distribution

Loggerheads are circumglobal, inhabiting continental shelves, bays, lagoons, and estuaries throughout the temperate, subtropical and tropical regions of the Atlantic, Pacific, and Indian oceans as well as the Mediterranean, Red and Black seas. In the Atlantic, the Loggerhead turtle's range extends from Newfoundland (Canada) to as far south as Argentina (Dood, 1988; FAO, 1990). The limit of distribution of the Loggerhead sea turtle is temperature-dependent. The species is widely distributed in coastal tropical and subtropical waters with temperatures between 16°- 20°C. The species rarely survives in water below 10°C. Therefore, in the winter turtles may remain buried in the mud of quite deep water. During warm years they may reach northern waters looking for thermal comfort (e.g. Murmansk and Barents Sea) and in the spring and summer juveniles, sub-adults and some adults are found in feeding grounds (Lutz and Musick, 1996). Adult Loggerheads are known to make extensive migrations between foraging areas and nesting beaches. During the summer, nesting occurs primarily in the subtropics (Dood, 1988).

In the Western Atlantic, during non-nesting years, adult females from U.S. beaches are distributed in waters off the Eastern U.S. and throughout the Gulf of Mexico, Bahamas, Greater Antilles, and Yucatán. Along the Brazilian cost, the species nest from the north of Rio de Janeiro to the state of Sergipe. Areas in southern Brazil are used as feeding grounds (Marcovaldi and Marcovaldi, 2004). In the North-eastern Atlantic, there are widespread records of Loggerheads from Europe, especially from the British Isles. Strandings have been summarized by Brongersma (1972) and are primarily of juvenile and subadult turtles. Loggerheads do not nest anywhere on the Atlantic coast of Europe.

In the Mediterranean, the Loggerhead sea turtle has been recorded from Spain, including the Balearic Islands (Salvador 1978, 1985; Pascual 1985; Carr 1986b), France, Corsica, Italy (including Sicily and Lampedusa Island), Sardinia, Greece, Bulgaria, Turkey, Israel, Cyprus, Egypt, Libya and Tunisia (Dood, 1988). Nestlings occur in the easternmost part of the Mediterranean while the western part consists of feeding areas. Individuals from the Mediterranean and North Atlantic populations congregate annually for feeding in a broad area around the Balearic Islands.

In the Eastern Pacific, Loggerheads have been reported as far north as Alaska, and as far south as Chile. In the United States, occasional sightings are reported from the coasts of Washington and Oregon, but most records are of juveniles off the coast of California. The west coast of Mexico, including the Baja Peninsula, provides critically important developmental habitats for juvenile Loggerheads. In the North Pacific, nesting areas for Loggerheads are found only in southern Japan.

1.3.5. Life cycle

Loggerheads occupy three different ecosystems during their lives: the terrestrial zone, the oceanic zone, and the neritic zone. Loggerheads nest on ocean beaches, generally preferring high energy, relatively narrow, steeply sloped, coarse-grained beaches (Dood, 1988). Immediately after hatchlings emerge from the nest, they begin a period of hyperactivity. During this period, hatchlings move from their nest to the surf, swim and are swept through the surf zone and continue swimming away from land for about one to several days.

After this swim frenzy period, post-hatchling Loggerheads take up residence in areas where surface waters converge to form local downwellings. These areas are often characterized by accumulations of floating material, such as seaweed (e.g., *Sargassum*). Post-hatchling Loggerheads may remain for months in waters just off the nesting beach or else are carried by ocean currents.

Once individuals are carried further offshore by ocean currents, they enter the oceanic zone. Within the North Atlantic, juvenile Loggerheads have been primarily studied in the waters around the Azores and Madeira (Bolten, 2003). Other populations exist (e.g., in the region of the Grand Banks off Newfoundland), but data on these populations are limited. The juvenile turtles around the Azores and Madeira spend the majority of their time at the top of the water column (depth of 5 m).

Somewhere between the ages of 7 to 12 years (about 40 cm SLCL), oceanic juveniles migrate to near shore coastal areas (neritic zone) and continue maturing until adulthood. In the Western Atlantic, subadult developmental habitats include lagoons, estuaries, and the mouths of bays and rivers, rich in food resources. Adult Loggerheads are best known from shallow coastal waters adjacent to nesting beaches (Dood, 1988).

1.3.6. Feeding

The Loggerhead is primarily carnivorous, feeding on a wide variety of food items, especially molluscs. They eat horseshoe crabs, clams, mussels, and other invertebrates (Plotkin et al., 1993). The broad head and substantial jaw muscles seem particularly well-adapted for crushing hard-shelled prey (Hendrickson, 1980). Adults and juveniles feed in shallow waters of the continental shelves, often in water only a few meters deep. They spend much of their time around reefs, or along the bottom. Adults sometimes travel for thousands of kilometers. Hatchlings and young juveniles do not dive, staying near the surface, often in association with mats of floating seaweed (Dood, 1988).

1.3.7. Reproductive aspects

Sexual dimorphism is apparent only in adults. Hughes (1974) reported that sexual differentiation begins to become apparent in turtles with SLCL from 60.0 cm to 67.0 cm. Adult males have a longer tail than females and larger, curved claws (Figs. 1D and 3). Males also have a shorter plastron, presumably to accommodate their large muscular tail (Geldiay et al. 1982). Adult females have a more domed carapace than males, but males appear to be wider, and have a more gradually tapering carapace (Carr, 1952). Males also show a tendency to have a wider head (Hughes 1974; Pritchard and Trebbau, 1984). Sexual distinction of hatchlings, juveniles, and the smaller subadults is not possible through external examination; distinction is possible only through dissection, laparoscopy, histological examination, or radioimmunological assays (Owens, 1999; Wyneken, 2000; Brooke, 2005).

Age at first maturity has not been clearly determined yet. Data from researches in captivity indicate ages from 6 to 20 years; the back calculation from capture - recapture data of tagged nesting females in the Southeastern coast of the United States, analyzed through logistic and von Bertalanffy growth curves, produce ranges from 12 to 30 or more years, for minimum (74 cm) and maximum (92 cm) straight carapace lengths (FAO, 1990). However, age at sexual maturity may vary between populations, or even within populations, since growth rates show considerable variation within and between populations (Limpus, 1985).

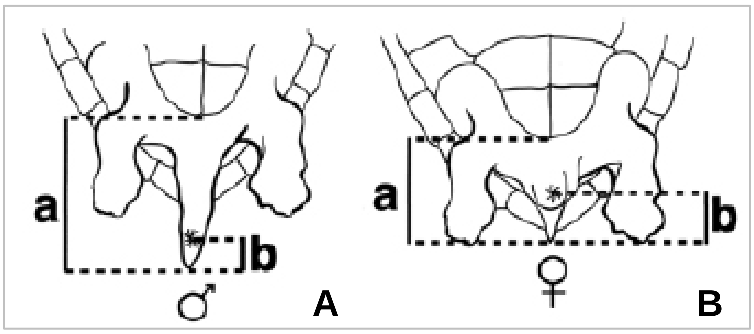

Figure 3. Ventral view of the caudal region of the adult Loggerhead sea turtle. A, Male; B, Female. a, distance between plastron edge and tail tip (greater in males); b, distance between cloaca and tail tip (shorter in males). Drawings from Bolten, 1999.

There is a considerable body of literature on the sizes of nesting females, showing that the populations with the smallest mature females occur in the Mediterranean (over the curve measurements, 69.5-95 cm) and Natal, South Africa (Dood, 1988). The largest average-sized females occur in the Southeastern United States. Frazer and Schwartz (1984) provided an age estimation of 16 -17 years old in 2 sexually-mature Loggerheads raised in captivity in North Carolina. In Florida, other studies performed in wild turtles and based on measurements of recaptured individuals or growth annuli of humeral bones gave estimates of 10-15 year old to reach sexual maturity (Mendonça, 1981).

Continental beaches (primarily) and beaches (secondarily) are preferred for nesting. Scattered Loggerhead nesting occurs regularly on some islands, such as those in the Mediterranean, the Bahamas, and Cuba. The nesting season of the Loggerhead is confined to the warmer months of the year in temperate zones - that is, from May through August in the Northern Hemisphere and from October through March in the Southern Hemisphere. Nesting often occurs several hours after sunset (Caldwell, 1959), but may occur at any time of night. Loggerheads are known to nest from one to six times in a nesting season (Lund, 1986), the record being seven nests in a single season by a female in Georgia (Lenarz et al., 1981). The inter-nesting interval varies, but is generally about 14 days depending on location. Lays average 100 to 126 eggs at each nest. The eggs are incubated for about 60 days.

Hughes (1974) and Limpus (1985) have shown that females may have a cycle extending from 2 years to a longer or shorter one. The specific periodic nesting cycles observed on any given beach are dependent, in part, on the annual survival rates of the nesting females (Frazer, 1984). Females show a high degree of philopatry to nest in a specific area when remigrating in subsequent years.

1.3.8. Population trends

The most recent reviews show that two Loggerhead nesting beaches - South Florida (U.S.) and Masirah Island (Oman) accout for more than 10,000 females nesting per year. The status of the Oman nesting colony has not been evaluated recently. Total estimated nesting in the U.S. is approximately 68,000 to 90,000 nests per year. Recent analyses of nesting data from the Index Nesting Beach Survey Program in Southeast Florida show the population is declining. Similarly, long-term nesting data show that there was no statistical evidence of an increasing or decreasing trend in numbers of clutches laid per year in North Carolina, although a significant decrease in the number of turtles nesting and number of clutches laid per year was found from 1991 (Hawkes et al., 2005).

In the Eastern Atlantic, the Cape Verde Islands support an intermediate-sized Loggerhead nesting assemblage. In 2000, researchers tagged over 1,000 nesting females on just 5 km of beach on Boa Vista Island (Ehrhart et al., 2003). In the Western Atlantic (excluding the U.S.), Brazil supports an intermediate-sized Loggerhead nesting assemblage. Reports provide an estimate of about 4,000 nests per year in Brazil (Ehrhart et al., 2003). Loggerhead nesting throughout the Caribbean is sparse.

In the Mediterranean, Loggerhead nesting is confined almost exclusively to the eastern portion of the Mediterranean Sea. The main nesting assemblages occur in Cyprus, Greece, and Turkey. However, small numbers of Loggerhead nests have been recorded in Egypt, Israel, Italy, Libya, Syria, and Tunisia. Based on the recorded number of nests per year in Cyprus, Greece, Israel, Tunisia and Turkey, Loggerhead nesting in the Mediterranean ranges from about 3,300 to 7,000 nests per season (Margaritoulis et al., 2003).

Loggerheads nest throughout the Indian Ocean and, with the exception of Oman, the number of nesting females is small. Most trends in Loggerhead nesting populations in the Indian Ocean are unknown.

Loggerhead populations in Honduras, Mexico, Colombia, Israel, Turkey, Bahamas, Cuba, Greece, Japan, and Panama have been declining. This decline continues and is primarily attributed to incidental capture in fishing gear, directed harvest, coastal development, increased human use of nesting beaches, and pollution (NOAA, 1991).

1.3.9. Mortality, conservation, threats to survival, and protection

Hatchlings of Loggerhead sea turtles are preyed on primarily by ghost crabs, sharks, predatory bony fishes, as well as a variety of mammals, including the water mongoose, genets, raccoons, foxes, dogs, and cats (Heithaus et al., 2002). A variety of birds also take hatchlings that emerge during daylight hours. Mortality from non-predatory animals, including disease, starvation, and cold-stunning undoubtedly occurs, but nothing is known about the effects on specific populations. Juvenile, subadult and adult Loggerheads are preyed on by sharks, particularly tiger sharks (*Galeowdo cuvieri*).

In the wild, juveniles, subadult and adult Loggerhead sea turtles are known to be affected by two main diseases - spirorchidiasis and fibropapillomatosis - that may be responsible for significant debilitation and mortality. The latter was first described in captured adult Green turtles but similar tumours have been found in Loggerheads (Lackovich et al., 1999). Externally, the lesions are characterized by small to large multiple areas of minimal to mild epidermal hyperplasia forming arborizing tumours (Jacobson et al., 1989). Internal nodules may be found at multiple visceral sites such as the liver, kidney, lung and gastrointestinal tract. A herpes-like virus has been identified and associated with the tumour occurrence (Jacobson et al., 1991; Lackovich et al., 1999). Although a worldwide disease, its prevalence ranges from 0% to 92% in some areas. The parasitic infection by spirorchids is common in Loggerhead sea turtles, mainly in turtles from the east coast of the United States of America (Wolke et al., 1982). Species representing three genera, *Carettacola*, *Hapalotrema* and *Neospirorchis* have been reported in the heart or blood vessels of the Loggerhead sea turtle (Manter and Larson, 1950). The infected turtles present granulomatous gastritis, enteritis, hepatitis, pneumonitis and nephritis. Acute and chronic vasculitis accompanied by metastasis of eggs is present and severe hepatic hemosiderosis is caused by the anemia (Wolke et al., 1982). Adult parasites may cause endocarditis, arteritis and thrombosis of the blood vessels (Gordon et al., 1998). Recently, Jacobson et al. (2006) have recorded the presence of *Neospirorchis* associated with neurological disorders in Loggerhead sea turtles found in waters off south Florida. There are no records of fibropapilloma or spirorchidisis in Loggerhead sea turtles in the Mediterranean Sea.

In addition to the natural causes of mortality and typical diseases, sea turtles are widely exploited by man for their eggs, meat and shells. Their survival is seriously threatened by many anthropologic factors such as fishing activities, pollution, loss of nesting sites, and tourism.

In the Mediterranean, general anthropogenic degradation has been noted at some significant nesting sites, while some historic host nesting areas have either been lost to turtles (e.g. Malta) or become severely degraded (e.g. Israel). The main anthropogenic threats affecting marine turtle nesting areas include tourism and recreational activities, increasing human presence, vehicular and pedestrian traffic, beachfront lighting and noise, uncontrolled development and construction, beach pollution, marine pollution, planting of vegetation, boat strikes, near-shore fishing and the use of underwater explosives (Margaritoulis et al., 2003).

Mediterranean fisheries have an enormous impact on the local Loggerhead sea turtle stock. About 20,000 Loggerhead turtles are estimated as being caught each year by Spanish longline fisheries, with a mortality rate of at least 34% (Aguilar et al., 1995). Fisheries are characterized by: (i) multispecificity; (ii) a high level of interaction between trawls and set gears (both use the same fishing areas and resources); (iii) the major importance of artisanal fisheries, and (iv) the increasing size of tuna fleets. The demersal species of greatest commercial interest are: hake (*Merluccius merluccius*), blue whiting (*Micromesistius poutassou*), red shrimps (*Aristeus antennatus*), Norway lobster (*Nephrops norvegicus*), red mullet (*Mullus surmuletus* and *Mullus barbatus*), octopuses (*Octopus vulgaris* and *Eledone cirrhosa*) and sole (*Solea vulgaris*). Of the small pelagic species, sardine (*Sardina pilchardus*) and anchovy (*Engraulis encrasicolus*) are the most significant. Blue-fin tuna (*Thunnus thynnus*) and swordfish (*Xyphias gladius*) are the most important large pelagic species and albacore (*Thunnus alalunga*) ranks third in importance.

The problems related to the interaction between fisheries and turtles in the Mediterranean are common to all fisheries. However, local features can affect reproduction, feeding or wintering populations of turtles differently in different areas (Tudela, 2000). Bottom trawl, surface longline and driftnet, along with coastal gillnet and entangling net fisheries have a large bycatch causing fishery-related mortality (Argano and Baldari, 1983; De Metrio et al., 1983; Deflorio et al., 2005).

The Barcelona Convention adopted an Action Plan for the Conservation of Mediterranean Marine Turtles in 1989, acknowledging that catches by fishermen are the most serious threat to the turtles at sea (Tudela, 2000).

Loggerhead turtles are protected by various international treaties and agreements as well as national laws. These are listed in Appendix I of the Convention on International Trade in Endangered Species of Wild Flora and Fauna (CITES), which means that international trade of this species is prohibited. Loggerheads are listed in Appendices I and II of the Convention on Migratory Species (CMS) and are protected under the following auspices of CMS: the Memorandum of Understanding on the Conservation and Management of Marine Turtles and their Habitats of the Indian Ocean and South-East Asia (IOSEA) and the Memorandum of Understanding Concerning Conservation Measures for Marine Turtles of the Atlantic Coast of Africa. Loggerheads are also protected under Annex II of the Specially Protected Areas and Wildlife (SPAW) Protocol of the Cartagena Convention. Additionally, the U.S. is a party to the Inter-American Convention for the Protection and Conservation of Sea Turtles (IAC), which is the only binding international treaty dedicated exclusively to marine turtles.

1.3.10. Diagnostic imaging techniques and application to reptilian medicine and biology

Reptilians usually show very poor clinical signs of most diseases, and frequently physical examination does not provide sufficient information for correct diagnosis. Diagnostic imaging techniques such as radiography, ultrasonography, computed tomography (CT) and magnetic resonance (MRI) are reliable techniques for the purposes of accurate diagnosis. These techniques are particularly useful in chelonians, due to the physical limitations imposed by the carapace and plastron, which make traditional methods of clinical examination difficult to use. Although designed primarily for diagnosis in humans, over the past few decades sophisticated techniques such as CT and MRI have been more frequently applied in veterinary medicine, especially in small animals, in which they play an important role in the diagnosis of a range of pathologies.

1.3.10.1. Radiology

Radiology is the most common and inexpensive diagnostic imaging method used in veterinary medicine, providing good overall information about the skeleton and respiratory system. However, in the case of reptiles (particularly chelonians) the overlying shell or epidermal scales normally compromise image quality. Information about restraint and positioning, body systems descriptions, interpretation and clinical findings in reptiles is available in various review articles and book chapters on reptile medicine (Rubel et al., 1991; Beymon et al., 1992; Gaudron et al., 2001; Hernandez-Divers and Hernadez-Divers, 2001; MCarthur et al., 2004; Girling and Raiti, 2004; Mader, 2006). In reptiles, radiographs are very useful for the diagnosis of bone fractures, osteometabolic disturbance, osteomyelitis, urinary bladder calculi, pneumonia and swallowing of foreign bodies. Additionally, the radiograph reveals the presence of the calcified shell of eggs, therefore being an important tool for reproductive studies too (Wilkinson et al., 2004). In turtles, radiographs have been used to verify swallowing of fishhooks (Hyland, 2002; Alegre et al., 2006) and to evaluate the digesta transit time in animals with presumptive diagnosis of intestinal obstruction (Di Bello et al., 2006).

Most high-capacity radiographic units can be set to produce good quality radiographs of reptilian patients. Three standard views are used to examine chelonians: dorso-ventral (top-to-bottom) using a vertical beam, plus lateral (side) and cranio-caudal (head-to-tail) using a horizontal beam. According to Silverman and Janssen (2006) and Gaudron et al. (2001) the dorso-ventral approach using a vertical beam is recommended in reptiles to evaluate the digestive and genitourinary systems, axial and limbs skeleton, and carapace and plastron (in chelonians). Of all reptilian patients, chelonians are the least difficult to restrain for radiography. They tend to lie quietly on the film cassette, offering no resistance (Rübel et al., 1991). The dorso-ventral view is obtained by placing the animal directly onto the film cassette. Since small chelonians tend to move off the cassette, adhesive tape may be attached to the rear edge of the carapace; the head and limbs should be extended out of the shell so that the limb structures are not superimposed on the internal structures (Siverman, 2006). Because chelonians have no diaphragm, in lateral and cranio-ventral views the head of the x-ray machine should be adjusted to give a horizontal beam; this allows the animal to be examined in the upright position, preventing the intestines from descending into the lung area and thus obscuring the view of the lung fields (Silverman and Janssen, 2006).

Mammography radiographic units, which provide better detail and resolution than standard radiographic equipment, may also be used for the radiography of reptiles (Hernandez-Divers and Hernandez-Divers, 2001). De Shaw et al. (1996) compared the use of various radiographic techniques in sand boa (*Eryx colubrinus loveridgei*), bearded dragon (*Pogona vitticeps*) and red-eared slider (*Trachemys scripta elegans*). The authors concluded that film produced using the matched mammography film-screen combination had greater resolution and detail and were superior to standard Bucky and table-top radiographs in the evaluation of bone and soft tissues.

According to Jackson and Sainsbury (1992), when interpreting reptile radiographs, as for any other animal, it is important that the clinician follow a protocol in order to reach a correct diagnosis. The criteria to be considered are:

1. Organ position, shape, size, density and homogeneity.
2. Comparative size of the various organs.
3. State of nutrition of the reptile with respect to the gradation of density between skeleton, muscle mass, soft tissues, gastrointestinal organs and their contents.

Description of the normal radiographic anatomy is scarce for most reptilian species. Mader (2006) presents some common body forms and a general overview of the various reptilian body parts, including a snake, a common green iguana (*Iguana iguana*), Malayan water monitor (*Varanus salvator*) and a non-specified tortoise. A large range of anatomic features may be observed over more than 6,000 reptile species; therefore specialized literature should be made available for each individual species in order to provide normal references and help in radiographic interpretation.

Over the past decade, radiography has also been used in studies of digestive physiology. A set of serial radiographs has been taken to locate radiodense barium-impregnated pills (BIPS®) or solution (barium sulphate or Gastrografin®) travelling with food, so as to evaluate the digestive transit time in dogs and cats. In chelonians, digesta passage time has been calculated using a solution of barium sulphate and Gastrografin® (Di Bello et al., 2006; Meyer, 1998; Taylor et al., 1996), and other markers (Barboza, 1995; Hailey, 1997; Hatt et al., 2002). Digesta passage times in the Loggerhead sea turtle are unknown, and BIPS® to verify transit, retention, and gastric emptying times have never been tested in any other chelonian species.

1.3.10.2. Ultrasound

Ultrasonography is a practical, rapid and non-invasive technique enabling real-time visualization of soft-tissue differentiation. As is the case in mammals, ultrasonography in reptiles has potential applications in the monitoring of reproductive function (Morris et al., 1996; Henen and Hofmeyr, 2003), disease diagnosis as well as being coadjuvant to other diagnostic techniques, such as ultrasound-guided biopsy. Sedation is not usually required to scan reptiles, although several handlers may be necessary to restrain lively large animals (Jackson and Sainsbury, 1992). General information about the application of ultrasonography and image interpretation in some species of reptiles is provided by previous authors (Gaudron et al., 2001; Hernandez-Divers and Hernandez-Divers, 2001; Wilkinson et al., 2006; Mader, 2006). More specifically in reproductive function, the technique is recommended for assessment of ovary activity, and also for distinguishing between pre- and post-ovulatory egg stasis (Casares et al., 1997). Clinically, ultrasonography has not been widely utilized in reptile diagnostics, and in research for a limited number of species only. For disease diagnosis, the liver and gallbladder, kidneys and urinary bladder, any tissue soft mass, ocular and retrobulbar disease and cardiac disease may be accessed (Hernandez-Divers and Hernandez-Divers, 2001). Size limitation plus the physical barrier imposed by the carapace and plastron is a restriction in the case of chelonians. In these reptiles there are few imaging acoustic windows, the most widely-used being the cervicobrachial and prefemoral. Due to the reduced area of these points of ultrasound beam access, small-tipped probes must be used. In ultrasonographic examinations of small chelonians, 7 – 10MHz sector transducers are normally used (Gaudron et al., 2001), whereas in the large ones 2.5 – 3.5 MHz transducers may be needed (Rostal et al., 1989,1990). Doppler ultrasound is widely used in medicine for measuring blood velocity and is therefore reliable in the diagnosis of cardio-vascular disorders. Use of this technique in reptilians is relatively new, being used mainly in monitoring patients in comatous or anesthetized conditions (Murray, 2006).

In sea turtles, ultrasound examination has been performed almost exclusively to assess the reproductive status. Rostal et al. (1994) concluded that this technique is totally non-invasive and significantly lowers the risk to turtles; it allows accurate measurement of structures such as follicles and eggs, and enables more frequent monitoring of the turtle's condition without increasing the stress factor. With a view to clinical practice, there is a need for more information about the normal aspect, shape and volume of the coelomic structures viewed through ultrasonography to supplement the current sparsity in the literature. No description of normal ultrasonographic features of coelomic organs and Doppler parameters of blood flow in Loggerhead sea turtle currently exists.

1.3.10.3. Computed Tomography

Computed tomography (CT) uses special x-ray equipment to obtain image data from different angles around the body and then uses computer processing of the information to provide cross-sections of body tissues and organs. A radiographic source and detector rotating around the patient produce the scans that are usually performed in transverse direction, with 1-5mm slice thickness and distance pre-set by the examiner. Computer programs are able to build 3-dimensional models of these slices. Unlike other imaging methods, CT scanning offers detailed views of many types of tissue including the lungs, bones, some soft tissues and blood vessels and therefore has been shown to be a cost-effective imaging tool for wide range of clinical problems. CT examinations are often used to diagnose pulmonary and osseous diseases, plan and properly administer radiation treatment for tumours, guide biopsies and other minimally-invasive procedures, as well as plan surgery and determine surgical respectability.

In reptile medicine, CT has potential application in chelonians because of the limits of physical and ultrasonographic examinations, and superimpositions in the conventional radiographs caused by the shell. As in other areas of veterinary medicine, the high cost of the equipment and restriction of use to large animals (gantry ranges from 60 to 70 cm in diameter) limit its usefulness in exotic and wild animals. CT technology is usually available only in selected medical centers or large referral veterinary hospitals.

Examinations are usually performed rapidly (a few minutes) and in most cases chelonians do not need to be sedated. Horizontal scans are similar to common dorsoventral radiographs. However, lateral recumbency of the animal causes displacement of the inner organs (Gumpenberger and Henninger, 2001).

Since CT enables detailed visualization of bony structures, it is the best technique for diagnosis of skeletal injuries in chelonians. In a gravid Leopard tortoise (*Geochelone pardalis pardalis*) with metabolic bone disease, the use of CT was imperative to visualize a dystrophic calcification of the left hepatic lobe and the presence of preovulatory follicles (Raiti and Haramati, 1997). Abou-Madi et al. (2004) detected axial and appendicular fractures in a Snapping turtle (*Chelydra serpentina*) that were not visualized during plain film radiography. Garland et al. (2002) highlighted the application of CT in wild animals and recommended the use of 3D reconstruction with volume rendering for expanding the imaging possibilities in this difficult group of patients. The authors of the study mentioned diagnosed a nodal mass in the chest, granulomas in the lungs and a ball in the stomach in a Hawksbill sea turtle that showed failure to thrive. In a Loggerhead sea turtle with carapace fracture produced by propellers, the use of CT and 3D reconstructions and magnetic resonance imaging of the affected area were decisive in evaluating the extent of vertebral damage and spinal cord section (Parga et al., 2005). Other pathologies diagnosed with CT scan include pneumonia in chelonians; abscesses in cranial lung and mid-coelomic cavity in red-eared sliders (*Trachemys scripta elegans*); urinary bladder stone in African spurred tortoise (*Geochelone sulcata*) and secondary hyperparathyroidism in Hermann's tortoise (*Testudo hermanni*) (Wilkinson et al., 2004). Arencibia et al. (2006) have described the normal CT images of the head of the Loggerhead sea turtle based on comparison with anatomical cross-sections.

Over the past few years, there have been major technological developments in the field of diagnostic imaging, CT units particularly having been equipped with multiple rows of detector arrays. This new generation technology, called Multidetector Computed Tomography (MDCT), allows for very fast examinations and more precise multiplanar and 3D reconstructions, and is therefore an excellent diagnostic tool also for scientific research into endangered species.

1.3.10.4. Magnetic Resonance Imaging

Like CT, magnetic resonance imaging (MRI), provides cross-sectional images of the body. MRI uses a strong magnetic field to measure the energy released by hydrogen atoms in tissue cell-water. By altering the timing and strength of the radio frequency pulses, it is possible to detect differences in proton characteristics within different parts of the tissue. The most widely used sequence is known as Spin-Echo. Here radio waves released are transmitted to a computer which displays a highly-detailed image showing up any abnormality of anatomy, mass lesions and tissue inflammation. Images are produced using two parameters based on repetition times, called T1 and T2-weighted images. Substances such as fat, proteinaceous fluids and lipid-rich molecules produce a bright (white) image in T1-weighted scans because they show a high signal, with the same bright aspect being produced by water-rich tissues in T2-weighted images. Alterations in the properties of cellular membranes change tissue appearance in T1 and T2-weighted images due to intracellular bulk water. Tumours, inflammation, oedema, pure fluids and cerebro-spinal fluid produce black, T1-weighted image areas (Wilkinson et al., 2004). The primary application of MRI technology had been in the diagnosis of neurological diseases such as tumours, stroke and inter-vertebral disc injuries. In veterinary practice, MRI has also been valuable in diagnosing musculoskeletal diseases and for mapping and staging tumours prior to surgery.

A number of pathologic disorders that cannot be visualized by standard imaging techniques in reptiles can be diagnosed with MRI (Straub and Jurina, 2001). However, MRI in veterinary is still limited due to its high cost. High noise levels are produced in the gantry during the 30-45 minute examination during which the animal must be immobile, entailing the use of general anaesthesia. Although MRI cannot provide images of calcified tissues, bone marrow, cartilage, or muscle, nonetheless blood vessels and intra-articular fat all show up well, so that it is possible to detect subtle orthopaedic pathologies (Wilkinson et al., 2004). As in mammals, MRI is the best choice for imaging the nervous system, being suitable for evaluation of the chelonian spinal cord for evidence of trauma, infection or tumours (Wilkinson et al., 2004). Image interpretation requires in-depth knowledge of the species' topographical anatomy and the MRI appearance of each structure in each sequence. Cardiovascular structures, lung fields, liver, kidneys, urinary bladder and intestinal and reproductive tracts have all been imaged in detail in tortoises (Wilkinson et al., 2004). Normal morphological and T1 and T2-weighted images have been reported on mainly in Herman's, Aldabra and Greek tortoises (Straub and Jurina, 2001; Rübel and Kuoni, 1991; Wilkinson et al., 2004).

In the case of sea turtles, their size limits the application of this technique. Adults do not pass through the gantry. Hidalgo et al. (2006) provided an overview of the normal cross-sectional anatomy of the head of the Loggerhead sea turtle using MR images. Spin-echo T1-weighted MR images of the head have provided details of clinically relevant anatomy and discrimination of both soft and mineralized tissues. In Green turtles, Croft et al. (2004) described the gross sectional anatomy and tested the use of MRI to detect internal tumors in animals with cutaneous fibropapillomatosis. The normal appearance of the coelomic organs of the healthy Loggerhead sea turtle in T1 and T2-weighted images is unknown.

1.4. CITED REFERENCES

Abou-Madi, N.; Scrivani, P.; Kollias, G.V. and Hernandez-Divers, S.M. 2004. Diagnosis of skeletal injuries in chelonians using computed tomography. *Journal of Zoo and Wildlife Medicine* 35: 226-231.

Alegre, F.; Parga, M.; Castillo, C. and Pont, S. 2006. Study on the long-term effect of hooks lodged in the mid-esophagus of sea turtles. Twenty-sixth Annual Symposium on Sea Turtle Biology and Conservation. April 3-8, Creta, Greece, p. 234 [abstract].

Aguilar, R.; Mas, J. and Pastor, X. 1995. Impact of Spanish swordfish longline fisheries on the loggerhead sea turtle *Caretta caretta* population in the Western Mediterranean. In Proceedings of the 12th annual workshop on sea turtle biology and conservation: Richardson, J.I. and Richardson, T.H. (Eds.). NOAA Technical memorandum NMFS-SEFSC-361. Miami. US Department of Commerce. Pp 1-6.

Arencibia, A.; Rivero, M.A.; De Miguel, I.; Contreras, S.; Cabrero, A.; Oros, J. 2006. Computed tomographic anatomy of the head of the loggerhead sea turtle (*Caretta caretta*). *Research in Veterinary Science* 2: 165-169.

Argano, R. and Baldari, F. 1983. Status of Western Mediterranean sea turtles. *Rapport d'Commission International de la. Mer Méditerranée* 28: 233-235.

Barboza, P.S. 1995. Digesta passage and functional anatomy of the digestive tract in the desert tortoise (*Xerobates agassizii*). *Journal of Comparative Physiology B* 165: 193-202.

Bjorndal, K.A.; Meylan, A.B. and Turner, B.J. 1983. Sea turtles nestilng at Melbourne beach, Florida, I. Size, growth and reproductive biology. *Biological Conservation* 26: 65-77.

Bolten, A. B. 1999. Techniques for measuring sea turtles. In: Research and Management Techniques for the Conservation of Sea Turtles. *K. L. Eckert, K. A. Bjorndal, F. A. Abreu-Grobois, M. Donnelly (Editors)*. IUCN/SSC Marine Turtle Specialist Group Publication 4: 1-5

Bolten, A.B. 2003. Active Swimmers – Passive Drifters: The Oceanic Juvenile Stage of Loggerheads in the Atlantic System. In: Bolten, A.B. and B.E. Witherington (eds). Loggerhead Sea Turtles. Smithsonian Books, Washington D.C. Pp 63-78.

Brongersma, L.D. 1961. Notes upon some sea turtles. *Zoologische Verhandelingen* (Leiden) 51:1-45.

Brooke, L. 2005. Sex determination of loggerhead sea turtles (*Caretta caretta*) via hormonal analysis by high performance liquid chromography. Master dissertation, Florida Atlantic University. 66pp.

Caldwell, D.K. 1959. The loggerhead turtles of cape Romain, South Carolina. *Bulletin of the Florida. State Museun. Biological. Science.* 4: 319-348.

Caldwell, D.K.; Carr, A. and Hellier, T.R.Jr. 1955. Natural history notes on the Atlantic loggerhead turtle, *Caretta caretta*. *Quarterly Journal of Florida Academic Science* 18: 292-302.

Camiñas, J.A. and de la Serna, J.M. 1995. The loggerhead distribution in the Western Mediterranean Sea as deduced from captures by the Spanish long-line fishery. In: Scientia herpetological. Llorente, G.A., Montori, A.; Santos, X. and Carretero, M.A. (eds). Asociación Herpetologica Española, Barcelona. Pp 316-323.

Carr, A. F. Jr. 1986a. Rips, FADS, and little loggerheads. *Bioscience* 36: 92-100.

Carr, A.F.Jr. 1986b. New perspectivas on the pelagic stage of sea turtle development. NOAA Tech. Mem. NMFS-SEFC-190, 36 pp.

Casares, M.; Rübel, A. and Honegger, R.E. (1997) Observations on the female reproductive cycle of captive Giant Tortoises (*Geochelone* spp.) using ultrasound scanning. *Journal of Zoo and Wildlife Medicine* 28: 267-273.

Ciampa, M.; Ferreti, L.; Treglia G. and Bentivegna, F. 2006. Treatment of trauma, fractures, wounds and lesions in injured sea turtles. In: *26th Annual Symposium on Sea Turtle Biology and Conservation 2006; Book of Abstracts*, International Sea Turtle Society, Crete, Greece. Pp 67-68 [abstract].

CRAM, 2006. Clínica y recuperación. Estadísticas de ingresos. Webpage available in: www.cram.org. Accessed in March 2007.

Croft, L.A.; Graham, J.P.; Schaf, S.A. and Jacobson, E.R. 2004. Evaluation of magnetic resonance imaging for detection of internal tumors in green turtles with cutaneous fibropapillomatosis. *Journal of American Veterinary Medical Association* 225: 1428-1435.

De Metrio, G.; Petrosino, G.; Matarrese, A.; Tursi, A. and Montanaro, C. 1983. Importance of the fishery activities with drift lines on the populations of *Caretta caretta* (L.) and *Dermochelys coriacea* (L.) (Reptilia, Testudines), in the Gulf of Taranto. *Oebalia* 9: 43-53.

Deflorio, M.; Aprea, A.; Corriero, A.; Nicoleta, S. and De Metrio, G. 2005. Incidental captures of sea turtles by swordfish and albacore longline in the Ionian Sea. *Fisheries Science* 71: 1010-1018.

DeShaw, B.; Schoenfeld, A.; Cook, R.A. and Haramati, N. 1996. Imaging of reptiles: a comparison study of various radiographic techniques. *Journal of Zoo and Wildlife Medicine* 27: 364–370.

Di Bello, A.; Valastro, C.; Staffieri, F. and Crovace, A. 2006b. Contrast radiography of the gastrointestinal tract in sea turtles. *Veterinary Radiology & Ultrasound* 47: 351-354.

Dodd, CK Jr. 1988. Synopsis of the biological data on the loggerhead sea turtle *Caretta* (Linnaeus 1758). U.S. Fish and Wildlife Service Biological Report 88: 35-82.

Ehrhart, L.M.; Bagley, D.A. and Redfoot, W.E. 2003. Loggerhead Sea Turtles in the Atlantic Ocean: Geographic Distribution, Abundance and Population Status. In: Bolten, A.B. and B.E. Witherington (eds). Loggerhead Sea Turtles. Smithsonian Books, Washington D.C. Pp 157-174.

FAO. 1990. Species catalogue. Sea turtles of the world. Márquez M., R. (ed.) *FAO Fisheries Synopsis* 125, Vol. 11. Rome. 81 pp.

Frazer, N.B. and Schwartz, F.J. 1984. Growth curves for captive loggerheads, *Caretta caretta*, in North Carolina, USA. *Bulletin of Marine Science 34*: 485-489.

Frazer, N.B. 1984. A model for assessing mean age-specific fecundity in sea turtle populations. *Herpetologica* 40: 281-291.

Gaffney, E.S. 1990. The comparative osteology of the Triassic turtle *Proganochelys*. *Bulletin of. American Museum of Natural. History.* 194: 1-263.

Garland, M.R.; Lawler, L.P.; Whitaker, B.R.; Walker, I.D.F.; Corl, F.M. and Fishman, E.K. 2002. Modern CT applications in Veterinary Medicine. *Radiographics* 22 : 55-62.

Gaudron, C. ; Lignereux, Y. and Ducos de Lahitte, J. 2001. Imagerie médicale appliquée a l'anatomie clinique des chéloniens en consultation. In: Proceedings of the International Congress on *Testudo* Genus, Toulosse. Pp 161-179.

Geldiay, R.; Koray, T. and Balik, S. 1982. Status of sea turtle populations (*Caretta c. caretta* and *Chelonia m. mydas*) in the northern Mediterranean Sea, Turkey. In: K. Bjorndal (Ed), Biology and Conservation of sea turtles. Smithsonian Institution Press, Washington, DC. Pp 425-434.

Girling, S. and Raiti, P. 2004. BSAVA Manual of Reptiles. British Small Animal Veterinary Association, Kingsley House, Gloucestershire. 350pp.

Gómez de Segura, A.; Tomás, J.; Pedraza, S.N.; Crespo, E.A. and Raga, J.A 2006. Abundance and distribution of the endangered loggerhead turtle in Spanish Mediterranean waters and the conservation implications. *Animal Conservation* 9: 199-206.

Gordon, A.N.; Kelly, W.R. and Cribb, TH. 1988. Lesions caused by cardiovascular flukes (Digenea: Spirorchidae) in stranded green turtles (*Chelonia mydas*). *Veterinary Pathol*ogy 35: 21-30.

Gumpenberger, M. and Henninger, W. 2001. The use of computed tomography in avian and reptile medicine. *Seminars in Avian and Exotic Pet Medicine* 10: 174-180.

Hailey, A. 1997. Digestive efficiency and gut morphology of omnivorous and herbivorous African tortoises. *Canadian Journal of Zoology* 75: 787-794.

Hatt, J.M.; Gisler, R.; Mayes, R.W.; Lechner-Doll, M.; Clauss, M.; Liesegang, A. and Wanner, M. 2002. The use of dosed and herbage n-alkanes as markers for the determination of intake, digestibility, mean retention time and diet selection in Galapagos tortoises (*Geochelone nigra*). *The Herpetological Journal* 12: 45-54.

Hawkes, L.A.; Broderick, A.C., Godfrey, M.H. and Godley, B. 2005. Status of nesting loggerhead turtles *Caretta caretta* at a Bald Head Island (North Carolina, USA) after 24 years of intensive monitoring and conservation. *Oryx* 39: 65-72.

Heithaus, M. R.; Frid, A. and Dill, L. M. 2002. Shark-inflicted injury frequencies, escape ability, and habitat use of green and loggerhead turtles. *Marine Biology* 140: 229-236.

Hendrickson, J.R. 1980. The ecological strategies of sea turtles. *American Zoologist* 20: 597-608.

Henen, B.T. and Hofmeyr, M.D. 2003. Viewing Chelonian Reproductive Ecology through Acoustic Windows: Cranial and Inguinal Perspectives. *Journal of Experimental Zoology* 297A: 88-104.

Hernandez-Divers, S. and Hernandez-Divers, S. 2001. Diagnostic imaging of reptiles. *In Practice* july/august: 370-391.

Hidalgo, M.R.; Contreras, S.; Orós, J.; Rivero, M.A.; Casal, A.B.; Monagas, P. and Arencibia, A. 2006. Magnetic resonance imaging anatomy of the head of the loggerhead sea turtle (*Caretta caretta*). Twenty-sixth Annual Symposium on Sea Turtle Biology and Conservation. April 3-8, Creta, Greece, p. 60 [abstract].

Hirayama, R. 1998. Oldest known sea turtle. *Nature* 16: 705-708.

Hughes, G.R. 1974. The sea turtles of south-east Africa. I. Status, morphology and distributions. *Oceanographic Research Institute. Investigational Report.* 35. 144pp.

Hyland, R.J. 2002. Surgical removal of a fish hook from the oesophagus of a turtle. *Australian Veterinary Journal* 80: 54-56.

IUCN 2006. IUCN Red List of Threatened Species. <www.iucnredlist.org>. Accessed on 08 March 2007.

Jackson, O.F. and Sainsbury, A.W. 1992. Radiological and related investigations. In: P.H. Beynon, Lawton, M.P. and Cooper, J.E. BSAVA Manual of Reptiles. British Small Animal Veterinary Association, Kingsley Hourse. Gloucestershire. Pp 63-72.

Jacobson, E. R.; Buergelt, C.; Williams, B. and Harris, R.K. 1991. Herpesvirus in cutaneous fibropapillomas of the green turtle, *Chelonia mydas*. *Diseases of Aquatic Organisms* 12: 1-6.

Jacobson, E.R. 1997. Buoyancy problems in sea turtles: causes and diagnosis. Proceedings 17th Annual Sea Turtle Symposium, 4-8 March, Orlando, Florida. p. 67 [abstract].

Jacobson, E. R.; Mansell, J. L.; Sundberg, J.P.; Hajarr, L.; Reichmann, M.E.; Ehrhart, L.M.; Walsh, M.and Murru. F. 1989. Cutaneous fibropapillomas of green turtles, *Chelonia mydas*. *Journal of Comparative Pathology*. 101: 39-52.

Jacobson, E.R.; Homer, B.L.; Stacy, B.A.; Greiner, E.C.; Szabo, N.J.; Chrisman, C.L.; Origgi, F.; Coberley, S.; Foley, A.M.; Landsberg, J.H., Flewelling, L., Ewing, R.Y.; Moretti, R.; Schaf, S.; Rose, C.; Mader, D.R.; Harman, G.R.; Manire, C.A.; Mettee, N.; Mizisin, A.P. and Shelton, G.D. 2006. Neurological disease in wild loggerhead sea turtles *Caretta caretta*. *Diseases of Aquatic Organisms* 70: 139-154.

Lackovich, J. K; Brown, D.R.; Homer, B.L.; Garber, R. L.; Mader, D.R.; Moretti, R.H.; Patterson, A.D.; Herbst, L.H.; Oros, J.; Jacobson, E. R.; Curry, S. S. and Klein, P.A. 1999. Association of herpesvirus with fibropapillomatosis of the green turtle *Chelonia mydas* and the loggerhead turtle *Caretta caretta* in Florida. *Diseases of Aquatic Organisms* 37: 89-97.

Lenarz, M.S.; Frazer, N.B.; Ralston, M.S. and Mast, R.B. 1981. Seven nest recorded for loggerhead turtle (*Caretta caretta*) in one season. *Herpetological Review* 12: 9.

Limpus, C.J. 1985. A study of the loggerhead sea turtle, *Caretta caretta*, in eastern Australia. PhD dissertation. University of Queensland, St. Lucia, Australia.

Lund, F. 1986. Nest production and nesting-site tenacity of the loggerhead sea turtle, *Caretta caretta*, on Jupiter Island, Florida. M.S. Thesis. University of Florida, Gainesville, 32 pp.

Lutz, P. L. and Musick, J. A. 1996.The Biology of Sea Turtles. CRC Press, Boca Raton, Fla. 432pp.

Mader D. 1996. Radiographic anatomy. In: Mader D.R. (ed.). Reptile Medicine and Surgery. W.B. Saunder Co. USA. Pp. 485-489.

Mader, D.R. 2006. Reptile Medicine and Surgery. 2nd edition. Elsevier Inc. 1242pp.

Manter, H.W. and Larson, M.I. 1950. Two new blood flukes from a marine turtle, *Caretta caretta*. *Journal of Parasitology* 21: 274-276.

Marcovaldi, M.A.; Marcovaldi, G.G.1999. Marine turtles of Brazil: the history and structure of Projeto TAMAR-IBAMA. *Biological Conservation* 91: 35-41.

Margaritoulis, D.; Argano, R.; Baran, I.; Bentivegna, F.; Bradai, M.N.; Camiñas, J.A.; Casale, P.; De Metrio, G.; Demetropoulos, A.; Gerosa, G.; Goodley, B.; Haddoud, D.; Houghton, J.; Laurent, L. and Lazar, B. 2003. Loggerhead turtles in the Mediterranean. Present knowledge and conservation perspectives. In: Bolten, A. y Witherington, B.E. (eds.). Ecology and Conservation of Loggerhead sea turtles. Smithsonian Institution Press. Washington D.C., USA.

MCarthur, S.; Wilkinson, R.; Barrows, M. and Meyer, J. 2004. Introduction. Diagnostic Imaging. In: McArthur, S.; Wilkinson, R. and Meyer, J. (eds.). Medicine and Surgery of tortoises and turtles. Victoria, Australia: Blackell Publishing Ltd. Pp 1-34.

Mendonça, M.T. 1981. Comparative growth rates of wild immature *Chelonia mydas* and *Caretta caretta* in Florida. *Journal of Herpetology* 15: 447-451.

Meyer, J. 1998. Gastrofin as a gastrointestinal contrast agent in the Greek tortoise (*Testudo hermanni*). *Journal of Zoo and Wildlife Medicine* 29: 183-189.

Morris, P. J. and Allison, A.C. 1996. Determination of sex in White-throated monitors (*Varanus albigularis*), Gila monsters (*Heloderma suspectum*), and Beaded Lizards (*H. horridum*) using two-dimensional ultrasound imaging. *Journal of Zoo and Wildlife Medicine* 27: 371-377.

Murray, M.J. 2006. Cardiology. In: Mader, D.R (Ed.), Reptile Medicine and Surgery. Elsevier Inc., Philadelphia. Pp 181-195.

NOAA, 1991. Endangered Species Act Biennial Report. Pp. 33-36. Available on line: http://www.nmfs.noaa.gov/pr/pdfs/laws/esabiennial1991.pdf

Orós, J. and Torrent, A. 2000. Unusual tumors in three loggerhead sea turtles (*Caretta caretta*) stranded in the Canary Islands, Spain. *Marine Turtle Newsletter* 88: 6-7.

Orós, J.; Déniz, S. and Calabuig, P. 2004. Digestive pathology of sea turtles stranded in the Canary Islands between 1993 and 2001. *Veterinary Record* 155: 169-174.

Orós, J.; Torrent, A.; Calabuig, P. and Déniz, S. 2005. Diseases and causes of mortality among sea turtles stranded in the Canary Islands, Spain (1998-2001). *Diseases of Aquatic Organisms* 63: 13-24.

Owens, D.W. 1999. Reproductive Cycles and Endocrinology. Research and Management Techniques for the Conservation of Sea Turtles. IUCN/SSC Marine Turtle Specialist Group Publication 4: 1-5.

Parga M.L.; Valente, A.L.; Zamora, M.A.; Lavin, S.; Alegre, F.; Cuenca, R. and Marco, I. 2005. Carapace trauma associated with hind limb paralysis in a loggerhead sea turtle (*Caretta caretta*). Proccedings of the Spring Meeting of the British Veterinary Zoolological Society. P. 41 [abstract].

Pascual, X. 1985. Contribuición al studio de las Tortugas en las costas Españolas. I. Distribuición. *Miscellania Zoologica* 9: 287-294.

Perrine, D. 2003. Sea Turtles of the World. Voyageur Press. Stillwater, MN. 144pp.

Plotkin, P.T.; Wicksten, M.K. and Amos, A.F. 1993. Feeding ecology of the loggerhead sea turtle *Caretta caretta* in the Northwestern Gulf Mexico. *Marine Biology* 115: 1-5.

Pont, S. G. and Alegre, F. N. 2000. Work of the Foundation for the Conservation and Recovery of Marine Life. *Marine Turtle Newsletter* 87: 5-7.

Pritchard, P.C.H. and Mortimer, J.A. 1999. Taxonomy, External Morphology, and Species Identification. In: K. L. Eckert; Karen, A.; Bjorndal, F.; Abreu, A. G. and Donnelly, M.A. (eds.). Research and Management Techniques for the Conservation of Sea Turtles. IUCN/SSCMarine Turtle Specialist Group Publ. No. 4. Washington, D.C. Pp 21-38.

Pritchard, P.C.H. and Trebbau, P. 1984. The turtles of Venezuela. *SSAR Contribution to Herpetology* 2. Pp 1-403

Rainey, W.E. 1981.Guide to sea turtle visceral anatomy. NOAA Tech. Mem. NMFS-SEFC-82. 82pp.

Raiti, P. and Haramati, N. 1997. Magnetic Resonance Imaging and Computerized Tomography of a Gravid Leopard Tortoise (*Geochelone pardalis pardalis*) with metabolic bone disease. *Journal of Zoo and Wildlife Medicine* 28: 189-197.

Rhodin, A.G.J. 1985. Comparative chondro-osseous development and growth of marine turtles. *Copeia* 1985: 752-771.

Rostal, D.; Robeck, T.; Owens, D.; Louis, E. and Kraemer, D. 1989. Ultrasonic imaging of ovaries and eggs in sea turtles. Proceedings of the Ninth Annual Symposium on Sea Turtle Biology and Conservation. NOAA Technical Memorandum NMFS-SEFC 232, Georgia, February 7 to 11. Pp 257-258.

Rostal, D.C.; Robeck, T.R.; Owens, D.W. and Kraemer, D.C. 1990. Ultrasound imaging of ovaries and eggs in Kemp's ridley sea turtles (*Lepidochelys kempi*). *Journal of Zoo and Wildlife Medicine* 21: 27-35.

Rübel, A.; Kuoni, W. and Frye, F. 1991. Radiology and Imaging. In: F. Frye (ed.). Biomedical and surgical aspects of captive reptile husbandry. Krieger Publishing Co. Florida. Pp.185–208.

Salvador, A. 1985. Guia de campo de los anfibios y reptiles de la Península Iberica, Islas Baleares y Canarias. Unigraf, S.A. Fuenlabrada, Madrid.

Silverman, S. 2006. Dignostic imaging. In: D.R. Mader (ed.). Reptile Medicine and Surgery. W.B. Saunder Co. Pp 471-489.

Silverman, S. and Janssen D. 1996. Diagnostic Imaging. In: D.R. Mader (ed.). Reptile Medicine and Surgery. W.B. Saunder Co. Pp 258-264.

Smith, H. M. and Smith, R. B. 1980. Synopsis of the Herpetofauna of Mexico. Vol. 6: Guide to Mexican turtles. Bibliographic addendum III. John Johnson, North Bennington, Vermont. 1044 pp.

Solomon, S.E.; Hendrickson, J.R. and Hendrickson, L.P. 1986. The structure of the carapace and plastron of juvenile turtles, *Chelonia mydas* (the green turtle) and *Caretta caretta* (the loggerhead sea turtle). *Journal of Anatomy* 145: 123-131.

Straub, J. and Jurina, K. 2001. Magnetic Resonance Imaging in Chelonians. *Seminars in Avian and Exotic Pet Medicine* 10: 181-186.

Taylor, S.K.; Citino, S.B.; Zdziarski, J.M. and Bush, R.M. 1996. Radiographic anatomy and barium sulphate transit time of the gastrointestinal tract of the leopard tortoise (*Testudo pardalis*). *Journal of Zoo Wildlife Medicine* 27: 180-186.

Tudela, S. 2000. Ecosystem effects of fishing in the Mediterranean: an analysis of the major threats of fishing gear and practices to biodiversity and marine habitats. FAO Project for the preparation of a Strategic Action Plan for the conservation of biological biodiversity in the Mediterranean region. 45 pp.

Walker, W.F. 1973. The locomotor apparatus of Testudines. In: C. Gans and T. Parsons (eds.). Biology of the reptilian IV. Academic Press, New York. Pp 1-100.

Wallin, L. 1985. A survey of Linnaeus's material of *Chelone mydas*, *Caretta caretta* and *Eretmochelys imbricata* (Reptilia, Chelonidae). *Zoological Journal of the Linnaean Society* 85: 121-130.

Wieland, G.R. 1896. *Archelon ischyros*: a new gigantic crytodire testudinate from the Fort Pierre Cretaceous of South Dakota. *American Journal of Science* 12: 399-412.

Wilkinson, R.; Hernandez-Divers, S.; Lafortune, M.; Calvert, I.; Gumpenberger, M. and Mcarthur, S. 2004. Diagnostic Imaging. In: McArthur, S.; Wilkinson, R. and Meyer, J. (eds.). Medicine and Surgery of tortoises and turtles. Victoria, Australia: Blackell Publishing Ltd. Pp 187-238.

Wolke, R.E. and George, A. 1981. Sea turtle necropsy manual. NOAA Tech. Mem. NMFS-SEFC-24, 24pp.

Wolke, R.E.; Brooks, D.R. and George, A. 1982. Spirorchidiasis in loggerhead sea turtles (*Caretta caretta*): Pathology. *Journal of Wildlife Diseases* 18: 175-185.

Wyneken, J. 2001. The Anatomy of Sea Turtles. U.S. Departament of Commerce NOAA Technical Memorandum NMFS-SEFSC 470: 1-172.

Zug, G.R. 1986. Age determination of loggerhead sea turtles, *Caretta caretta*, by incremental growth marks in the skeleton. *Smithsonian Contribution to Zoology* 427: 1-34.

SUMMARY OF RESULTS AND DISCUSSION

2. SUMMARY OF RESULTS AND DISCUSSION

Dorsoventral radiographs taken of the neck and body of 30 Loggerhead sea turtles using analog and digital radiography showed image distortion or superimposition at various points, due to the natural curvature of the neck and the shell which hindered the accuracy of interpretation. The pectoral and pelvic girdles were easily recognized. Important external landmarks included the vertebral and lateral scutes, and important internal landmarks included bronchi, coracoid bones, caudal border of the pulmonary fields, and the acetabulum.

Bones from the distal part of the fore- and hind flippers were seen in detail in radiographs using mammography film-screen combination. Pectoral and pelvic girdles, superimposed by the carapace bones, were better seen on the standard radiographs using rare-earth intensifying screens. Mammographic radiographs of the manus of 5 small juvenile turtles showed active growth zones. Visualization of bone contours on the distal part of the limbs was clearer compared with mammals due to the very low number of superimpositions. The presence of a massive cartilage in the epiphyses produced better visibility of limb-ends.

Ultrasonographically, the fourth and fifth cervical vertebrae, spinal cord, and the venous sinuses of the external jugular vein were clearly seen through the cervical-dorsal acoustic window. From the cervical-ventral acoustic window, the esophagus and the heart were imaged. The stomach was more frequently seen through the left axillary acoustic window. Although the liver could be imaged from both sides, the right axillary acoustic window provided a better view of the gallbladder. The large and small intestines and the kidneys could be seen in the right and left prefemoral acoustic windows; the latter were easily identified due to intense renal vasculature.

Computed tomography provided detailed information mainly of the respiratory system and skeleton. With regard to skeletal structures, multiplanar sagittal reconstruction of the vertebral column enabled evaluation of the vertebrae and vertebral canal. Three-volume reconstruction renderings of the carapace and plastron provided a detailed view of respective bones. Clinically relevant organs including the oesophagus, stomach, trachea, bronchi, lungs, liver, gallbladder, heart, spleen, kidneys were also identified in CT images. In the neck, the topographic relationships between oesophagus and trachea at each cervical vertebra were identified, and the tracheal mucosa could be inspected using virtual bronchoscopy. The morphology of the lungs, bronchi and pulmonary blood vessel could be clearly seen.

As for the MRI study, the general view on the 3 oriented planes (sagittal, dorsal and transverse) provided for good understanding of cross-sectional anatomic features and their identification on T1 and T2-weighted images. Likewise, major anatomic structures such as the esophagus, stomach, lungs, intestine (duodenum and colon), liver, gallbladder, spleen, kidneys, urinary bladder, heart, bronchi, and vessels could be imaged in detail principally in T2-weighted images. It was not possible to recognize the ureters or reproductive tract due to their small size.

The use of diagnostic imaging techniques in Loggerhead sea turtles involves certain aspects that should be considered: they include costs, viability, equipment and logistics, applicability to the diagnosis, time invested and the effects of handling on the patient's health status. Some imaging techniques, such as conventional/analog radiography, are often available in small veterinary clinics and even in some rescue centers. A portable x-ray apparatus in this case seems to be most recommended for sea turtles since different views may be obtained by moving the machine around the animal and adjusting the x-ray to provide a vertical, horizontal or oblique beam. In more specialized centers and in some veterinary hospitals radiography has already been improved with the advent of digital systems. In this study we have used two systems (analog and digital). To assess the coelomic cavity structures we have used 55-70Kv and 100 mA with a 0.2-second time exposure. Due to the low respiratory frequency observed in this species, the long exposure did not cause motion artefacts, and provided satisfactory contrasted images. Obtaining the same radiographs with the digital system had the added advantage of enabling adjustment of the brightness and contrast settings on the monitor screen before impression, thus avoiding unnecessary repetition of the x-ray. As to radiographs of the limbs, betters results were observed when the conventional system was performed using mammographic film. Because of the small size, thinness and low bone density of the flippers of juvenile and subadult turtles, mammographic film was more suitable for visualisation of bone structures in detail. Radiography is the cheapest diagnostic imaging method, examination time is short, and no sedation or anaesthesia of the turtle is required. We recommend its routine use in marine rescue centers because it is the best method for detecting the presence of a swallowed fishhook and for evaluating skeleton integrity. The drawback with this method is superimposition of the internal bony structures over the carapace and plastron, which may compromise diagnosis in some cases.

The second most-affordable technique for rescue centers is ultrasonography. Many portable models are available. Ultrasonographic examination of Loggerhead sea turtles was very useful in evaluating soft tissues such as the heart, liver, kidneys and intestines. Once access points to the organs and the topographic anatomy are known (both are reported in this work), examination may proceed easily and rapidly. The method has proved to be safe, with the added advantage of providing an overview of the organs functioning in real time using only physical restraint. More particularly in sea turtles, an ultrasongraphic scan of the gastrointestinal tract provided detailed visualisation of the normal appearance and thickness of layers of the intestinal wall, as well as identification of small and large intestines. This is important since most disorders found in injured sea turtles are fisheries-related and are caused by swallowed fishhooks or monofilament lines in the intestines that produce a range of types of enteritis including intestinal necrotising enteritis associated with intussusception (Orós et al., 2004). Because chelonians have few body parts not covered by the carapace or plastron which are internally limited by the bone of the proximal end of the limbs, the spaces of the acoustic windows are very small, thus limiting the scan to one plane. Other drawbacks include low ultrasound beam penetration in turtles with large amounts of fat in the subcutaneous tela and gas in the lumen of the gastrointestinal tract. In this study we used 5.0, 6.0 and 7.0 MHz sector phased array transducers. To assess internal organs, such as the heart, liver and stomach in large subadult turtles, lower-frequency transducers than those used in juveniles are needed, and in general they produce lower-resolution images. Lungs cannot be examined with this technique.

The use of computed tomography and magnetic resonance requires substantial logistical support, currently unavailable to small veterinary centers because of the price of equipment and the specialized facilities in which to house it. This does not mean that these techniques are not suitable for sea turtles, but rather that the trade-off between the cost and effects of handling and transporting the sick turtle to a specialized center and the need for an accurate diagnosis must be considered. Arrangements between diagnostic imaging and rescue centers may be one way of making examinations financially viable while providing support for scientific research in return. In specialized human centers the two techniques are often available, and if so required may be performed consecutively, entailing less handling of the turtle. In this study we first carried out an MRI scan of the turtles under anaesthesia for as long as 50 minutes. This initial scan was followed by the faster (under 5 minutes) CT examination. Information obtained with MRI is different from that provided by CT, and its use is indicated in special cases in which the diagnosis cannot be established with radiographs or ultrasonography. For instance, a CT scan followed by a MRI examination could be strongly recommended in turtles with carapace fractures displaying neurological symptoms. Carapace fracture - caused by collision with boat propellers - is one of most common causes of sea turtle admissions (Pont and Alegre, 2000; Parga et al., 2005; Ciampa et al., 2006). The multiplanar and 3D reconstruction of the spine in these cases provides detailed indications of the vertebrae affected and the extent of the fracture, whereas T1 and T2-weighted MRI images will show integrity of the spinal cord (Parga et al., 2005). Computed tomography is also indicated in those animals with suspected pulmonary lesions such as those related to abnormal buoyancy, pneumonia, oedema or presence of pulmonary fibropapillomatosis (Orós et al., 2004; Jacobson, 1997; Croft et al., 2004; Garland et al., 2002). Additionally, the oesophageal wall, plus the hepatic, splenic and renal parenchyma and vessels are better visualized using MRI, as has been shown in the present study. This finding could justify the use of this technique in helping in the diagnosis of certain pathologies which to date have been identified only at necropsy, such as necrotising and multifocal granulomatous hepatitis and splenitis, as well as the presence of internal tumours (Orós et al., 2004; Orós and Torrent, 2000; Croft et al., 2004).

CONCLUSIONS

3. CONCLUSIONS (in portuguese)

1. Tanto as radiografias convencionais utilizando filme standart e chassis de terras raras como as radiografias digitais proporcionam uma boa visualização das estruturas ósseas da região cervical e da cavidade celomática, incluindo os ossos do plastrão e carapaça. No entanto a última permite otimizar o tempo empregado na realização dos exames. Em ambos os casos, a visualização das ultimas vértebras cervicais e dorsais está comprometida pela curvatura normal da carapaça e sobreposição com os ossos pelvianos, respectivamente.

2. A radiografia convencional usando a combinação de filme e chassi para mamografía apresenta melhor detalhamento das estruturas ósseas da extremidade distal dos membros do que aquela obtida pelo método digital. Ao contrário, a extremidade proximal dos membros é mais bem visualizada em placas standart com chassis de terras raras ou usando a radiografia digital, porem utilizando kv mais altos.

3. A ultrasonografia é o método de eleição para avaliar o funcionamento do coração, parênquima hepático, vesícula biliar, rins, bexiga e intestino delgado e grosso, através de 4 janelas acústicas, que são: janela acústica cervical-dorsal e cervical-ventral, cervico-braquial, axilar e pré-femoral.

4. A tomografia computadorizada tem grande potencial para diagnosticar patologias que afetam o sistema respiratório e esqueleto solucionando os problemas de superposição das estruturas esqueléticas que ocorre nas placas radiográficas.

5. A ressonância magnética proporciona imagens excelentes da maioria dos órgãos internos sendo de grande valor para a inspeção detalhada das estruturas anatômicas. No entanto, a técnica está limitada a tartarugas de tamanho pequeno (até 40 cm de SCLmim), sendo necessário anestesiar o animal.

ARTICLES

4.1. CERVICAL AND COELOMIC RADIOLOGY OF THE LOGGERHEAD SEA TURTLE (CARETTA CARETTA)

Valente, A.L.; Cuenca, R.; Parga, M.L.; Lavín, S.; Franch, J. y Marco, I. (2006). Cervical and coelomic radiology of loggerhead sea turtle (*Caretta caretta*). Can. J. Vet. Res. 70: 285-290.

Cervical and coelomic radiologic features of the loggerhead sea turtle, *Caretta caretta*

Ana Luisa Valente, Rafaela Cuenca, Maria Luz Parga, Santiago Lavín, Jordi Franch, Ignasi Marco

Abstract

Many investigators have undertaken radiologic studies in chelonians. However, descriptive papers focusing on the radiographic anatomy are limited to only a few species. The purpose of this article is to provide the normal cervical and coelomic radiographic appearance of the loggerhead sea turtle (*Caretta caretta*), in the dorsoventral view, and to indicate useful landmarks to identify internal anatomic structures. Dorsoventral radiographs were taken of the neck and body of 30 loggerhead sea turtles by means of analog and digital radiography. At various points, distortion or superimposition of images due to the natural curvature of the shell hindered the accuracy of interpretation. The pectoral and pelvic girdles were easily recognized. Important external landmarks included the vertebral and lateral scutes, and important internal landmarks included the bronchi, coracoid bones, the caudal border of the pulmonary fields, and the acetabulum.

Résumé

Plusieurs chercheurs ont entrepris des études radiologiques chez les chéloniens. Toutefois, les articles descriptifs portant sur l'anatomie radiographique sont limités à seulement quelques espèces. Le but du présent article est de fournir l'apparence radiographique cervicale et coelomique normale, en vue dorso-ventrale, de la caouanne (Caretta caretta) *et d'indiquer les repères utiles pour identifier les structures anatomiques internes. Des radiographies dorso-ventrales du cou et du corps de 30 caouannes ont été prises à l'aide de radiographies analogiques et digitales. À certains endroits, une distorsion ou une superposition des images causée par la courbure naturelle de la carapace interféra avec la précision de l'interprétation. Les gaines pectorale et pelvienne étaient facilement reconnaissables. Les repères externes importants incluaient les scutelles vertébrale et latérale, et les repères internes importants incluaient les bronches, les os coracoïdes, le bord caudal des champs pulmonaires et l'acétabulum.*

(Traduit par Docteur Serge Messier)

Introduction

Reptilian species often show the same nonspecific symptoms with a variety of diseases. Radiologic studies in chelonians have been described by many authors (1–7). However, owing to the great variability of species, papers dealing with radiographic anatomy are limited to a representative number of species of each order of *Reptilia* (8). In sea turtles, traumatic injuries of the shell and the ingestion of fishhooks are the most frequent causes of admission to marine-animal rescue centers (9). In most cases, physical examination does not give sufficient information, and dorsoventral radiography is usually the 1st option as an ancillary test to determine the diagnosis (10). Radiography gives a good overview of the skeletal system and in sea turtles is the most inexpensive and noninvasive method to detect ingested fishhooks and fractures (7). Nevertheless, as with many chelonian species, the image is often compromised by the overlying shell, which makes accurate interpretation difficult if the standard radiographic features are not well known. Detailed radiographic studies focusing on endangered sea turtles, such as the loggerhead (*Caretta caretta*), have not been available in the scientific literature and are needed as reference material for aquariums and marine-animal rescue centers.

In medicine, anatomic landmarks are used to indicate the location of biologic features (11). True landmarks are placed according to a biologic hypothesis of equivalence, or homology; pseudo-landmarks are placed on a surface according to a mathematical rule, such as a series of points distributed evenly along a given surface (12). The palpable external anatomic landmarks usually employed in veterinary medicine, such as the xyphoid tip, costal arch, intercostal spaces, and coxal tuberosity (13), are not helpful in chelonians because their body is protected by a rigid shell. Radiographic anatomic landmarks could help the interpretation of x-ray-film images of sea turtles and provide better determination of the diagnosis when other imaging modalities are not available.

The purpose of this investigation was to provide the normal cervical and coelomic radiographic appearance of the loggerhead sea turtle, in the dorsoventral view, as well as other useful landmarks, to allow for the correlation of shell scutes with internal anatomic structures.

Servei d'Ecopatologia de Fauna Salvatge (Valente, Cuenca, Lavín, Marco) and Departament de Medicina i Cirurgía Animals (Franch), Facultat de Veterinària, Universitat Autònoma de Barcelona, 08193 — Bellaterra, Barcelona, Spain; Centre de Recuperació d'Animals Marins, Camí Ral 239, 08330 — Premià de Mar, Barcelona, Spain (Parga).

Address all correspondence and reprint requests to Dr. Ana Luisa Valente; telephone: +34 93 581 19 23; fax: +34 93 581 20 06; e-mail: schifinoval@hotmail.com

Received November 9, 2005. Accepted March 6, 2006.

Materials and methods

Dorsoventral radiographs were taken of the neck and body of 15 juvenile and 15 subadult loggerhead sea turtles; 17 were alive and 13 dead. All had been accidentally caught in pelagic longline sets and fishing nets along the northwestern Mediterranean coast (40°31′ to 42°26′ north and 0°32′ to 3°10′ east). Juvenile turtles were considered to be those with a minimum straight carapace length (SCLmin) of 21 to 40 cm and subadults those with an SCLmin of 41 to 65 cm (14). Live turtles were temporally housed in the rehabilitation facilities of the Rescue Centre for Marine Animals (CRAM), Premià de Mar, Barcelona, Spain. Only clinically normal animals were included in the study.

No sedation was necessary for the examination. The animals were manually restrained, blindfolded, and positioned in ventral recumbency. At least 2 dorsoventral radiographs were taken of each turtle. Analog radiography was performed in 14 animals and digital radiography in the other 16. Tabletop images were taken with a Rotanode x-ray tube (model E7239; Toshiba Electron Tubes and Devices Company, Tokyo, Japan) at a focal distance of 68 cm. Analog radiography was performed with medical x-ray films used for mammography (UM-MA hc, 24 × 30 cm) and a Fuji AD-MA screen (UM MAMMO fine) and with Super HR-GB films 30 × 40 cm and rare-earth intensifying screens (Fuji ECD 30 × 40 cm), all from Fuji Photo Film Company, Tokyo, Japan. The radiographs were digitized on a flatbed scanner at a minimum resolution of 300 dots per inch. Digital radiography was performed with a digital flat-panel detector system (Regius cassette 14 × 17, Konica Minolta, Tokyo, Japan) and a Regius CR reader (model 170). All images were analyzed with Adobe Photoshop, version 5.5 (Adobe Systems, San Jose, California, USA); normal and inverted (negative) images were compared.

To correlate the external scutes with internal structures, we painted the union lines among the carapace scutes of 6 dead turtles with a radio-opaque product (anticorrosive paint with red lead oxide) before the radiographs were taken. Additionally, 3 dead turtles were injected with a solution of barium sulfate (Bario-dif Suspension, Rovi SA, Madrid, Spain) via the femoral vein to show the position of the kidneys. To visualize the jugular venous sinus and the large-intestine position, 2 other dead turtles were injected with the same contrast agent via the jugular vein and the cloaca, respectively. The anatomic terminology applied corresponds to that of the *Nomina Anatomica Veterinaria*. However, specific terminology for turtles (15) and sea turtles (16) was also applied.

Results

In the cervical region of the vertebral column, only the first 3 vertebrae were clearly imaged. The 4th cervical vertebra was partially seen because it is just below the cranial edge of the carapace (Figure 1). The contour of the 5th, 6th, and 7th cervical vertebrae could not be visualized. Although superimposed, the contour of the vertebral arches of these vertebrae (Figure 2B) could be identified in the juvenile turtles. The 10 dorsal vertebrae that form the carapace were visible, with a slim body, slightly broader in the extremities because the articular surface opposes the head of the ribs (Figure 3B). The vertebral bodies were seen to be elongated from the 2nd to the 6th dorsal vertebrae. The body contour of the 7th and 8th dorsal vertebrae was not clearly visible. In the costovertebral joints, from the 4th to the 10th dorsal vertebrae, each rib head was seen to be slightly caudal to the junction of 2 vertebral bodies (Figure 2A). The intervertebral space was visualized as a very fine and discrete radiolucent line, and the joint between the distal end of the ribs and the peripheral bones was clearly visible when mammographic film or digital radiography was used (Figure 3B). The 1st pair of ribs was seen to be very close to the 2nd pair, and the ribs were slimmer (Figure 3B). The 9th and 10th pairs of ribs were inconspicuous but seen caudal to an imaginary line transversely crossing the acetabulum. The 9th rib was seen to be short and caudally curved and the 10th rib shorter, pointed, and floating (Figure 4). The sutures between the pleural bones were easily identified on plain films as transverse radiolucent lines in the middle of the intercostal spaces (Figure 3). In 2 small juvenile turtles this suture was widely open. The fontanelles, the intercostal spaces not ossified in the distal third of the ribs, were

Figure 1. Dorsoventral radiographic view of the cranial end of a subadult loggerhead sea turtle. 1 — atlas; 2 — axis; 3 — 3rd cervical vertebra; 4 — 4th cervical vertebra; 5 — trachea; 6 — left bronchus; 7 — right bronchus.

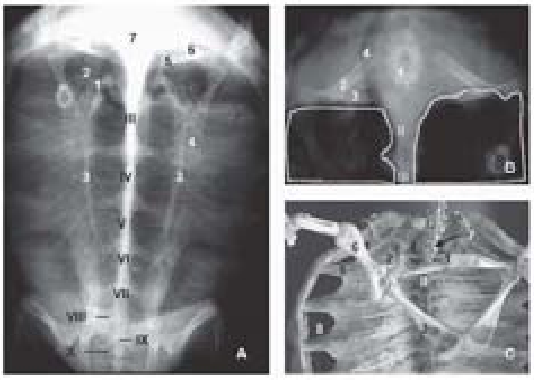

Figure 2. Dorsoventral radiographic views of subadult loggerhead sea turtles (A and B) and a ventral view of an adult loggerhead sea turtle's skeleton. Roman numerals indicate the respective dorsal vertebrae. A: 1 — bronchus; 2 — epiplastron; 3 — pulmonary blood vessels; 4 — coracoid bone; 5 — scapula; 6 — acromion; 7 — area of high radiodensity because of superimposition of osseous structures. B: 1 — cervical vertebral arches (superimposed); 2 — acromion; 3 — scapula; 4 — trachea. The cranial border of the pulmonary fields is delineated. C: 1 — scapula; 2 — acromion; 3 — coracoid bone; 4 — 1st pair of ribs; 5 — 2nd pair of ribs; 6 — humerus; 7 — 12th cervical vertebra; 8 — fontanelle.

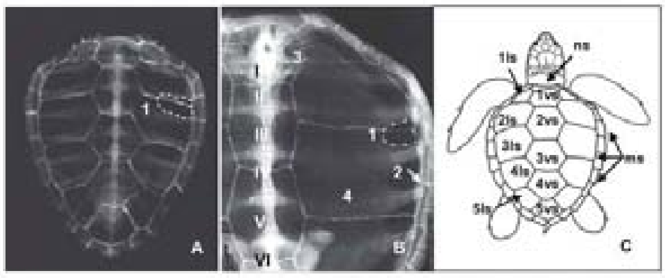

Figure 3. Digital dorsoventral radiographic views of the carapace of a juvenile loggerhead sea turtle of minimum straight carapace length (SCLmin) 23 cm (A) and a subadult of SCLmin 56 cm (B). Schematic drawing indicates the external scutes. A: 1 — widely opened fontanelle. B: 1 — partially ossified fontanelle; 2 — joint between rib and peripheral bone; 3 — 1st pair of ribs; 4 — sutures between the pleural bones. Roman numerals indicate the respective dorsal vertebrae. C: ls — lateral scute; ns — nuchal scute; vs — vertebral scute; ms — marginal scutes.

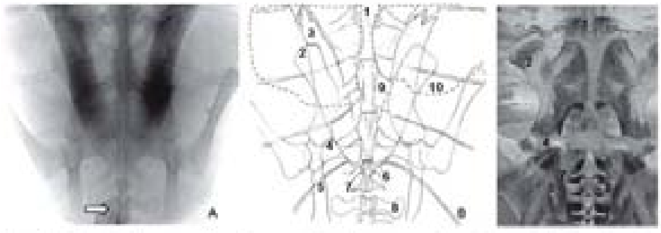

Figure 4. Negative image of the dorsoventral radiographic view of the pelvis of a subadult loggerhead sea turtle (A) and its interpreted drawing (B) and the ventral view of a skeletal pelvis (C). A: arrow indicates a fishhook in the rectum. B and C: 1 — 6th dorsal vertebra; 2 — lateral pubic process; 3 — xiphiplastron; 4 — ischium; 5 — ilium; 6 — 9th pair of ribs; 7 — 10th pair of ribs; 8 — transverse process of the 1st sacral vertebra; 9 — 7th pair of ribs; 10 — caudal border of the right pulmonary field.

extensively opened in all the turtles, but partial ossification was visible in 1 large subadult turtle (SCLmin 61 cm) (Figure 3).

The painted outline of the scutes was clearly visible in the radiographs. The images showed that the external keratinized scutes did not coincide with the pleural and neural bones (Figure 3). Each of the 5 vertebral scutes except the first and last (which are more caudal) completely covered 1 dorsal vertebra and half of the body of the preceding and following vertebrae, and each lateral scute covered 2 pairs of ribs (Figure 3). A difference in the ratio of length and width of the vertebral scutes was observed between the juvenile and subadult turtles, the scutes being wider than longer in the former (Figure 3). The relationship between the vertebral and lateral scutes and the osseous structure of the axial skeleton was constant and proportional in all of the turtles studied, independent of their size. The 3 sacral vertebrae were observed just below the 5th vertebral scute. Their bodies were shorter than those of the last dorsal vertebrae and showed a spatula-shaped transverse process articulating with the ilium (Figures 4 and 5). These vertebrae were not clearly visible in the juvenile turtles. Caudal vertebrae were variable in number.

The pectoral girdle was easily recognized in all films. It is formed by a union of 3 bony structures: scapula, acromion, and coracoid bone. These structures are jointed, forming about a 90° angle (Figure 2C). The acromion was seen to be completely ossified to the scapula, forming a single bone, and was identified as the most cranial of the 3 bones, followed caudally by the scapula (Figure 2B), which articulates with the carapace near the 1st dorsal vertebra. The Y-shaped structure thus formed is positioned horizontally on each side of the axial skeleton, just below the 1st vertebral scute, where the superimposition of the image of the cervical vertebrae forms an undefined central radio-opaque area (Figure 2A). The coracoid bone, caudal to the shoulder joint, has a flatter and wider shape at its caudal end (Figure 2). In all the turtles a radiolucent line could be seen at the union of the coracoid bone with the scapula.

The pubis and ischium form the ventrally positioned part of the pelvis, which was not clearly visible in the radiographs taken. Only the lateral pubic process and the articular end of the pubis could be clearly identified (Figure 4). The ischium was identified as an osseous bridge joining the acetabulum side to side. The image of this bone was usually superimposed by the silhouette of the 8th dorsal vertebra (Figure 4). The ilium was seen to be oriented dorsoventrally, articulating with the sacral vertebrae, which were easily recognized, as were the articular surfaces of the acetabular cavity (Figure 4).

The joint between the epiplastron and the hyoplastron was seen in the 1st third of the turtle's body as an oblique radiolucent line crossing the coracoid–acromion angle (Figure 6). The entoplastron could not be recognized owing to the great superimposition of the last cervical vertebrae. The suture between the hyoplastron and the hypoplastron was visible at the level of the 5th pair of ribs (5th dorsal

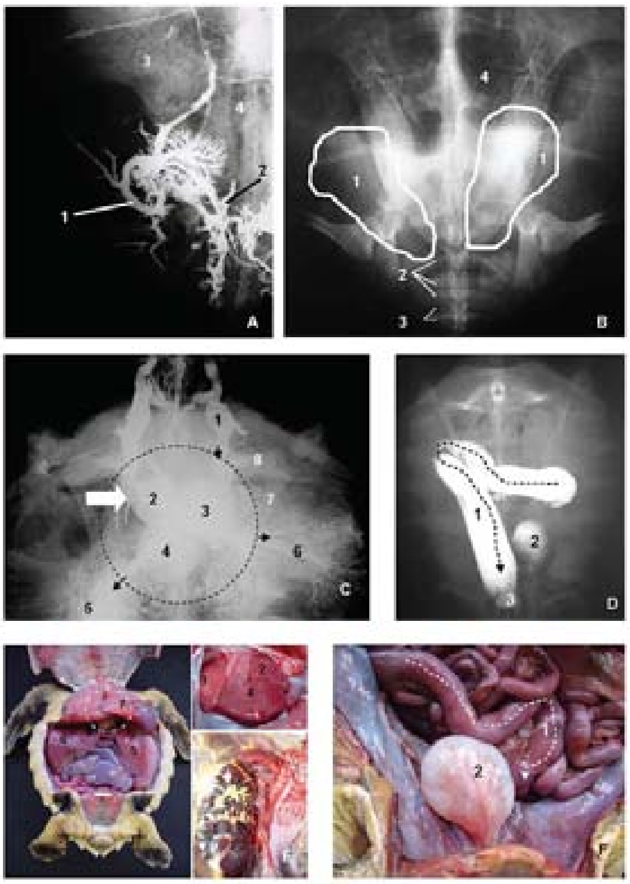

Figure 5. Dorsoventral radiographic views (A to D) and anatomic dissections (E and F) of subadult loggerhead sea turtles. A: renal vasculature injected with contrast agent; 1 — iliac vein; 2 — circumflex iliac vein; 3 — 4th costal scute; 4 — 4th vertebral scute. B: 1 — kidney positions; 2 — sacral vertebrae; 3 — caudal vertebrae; 4 — right pulmonary field. C: dorsoventral view of the cranial half of a dead juvenile loggerhead sea turtle injected with contrast agent; the heart position is delineated; 1 — sinus of the jugular vein; 2 — left atrium; 3 — right atrium; 4 — ventricle; 5 — left hepatic lobe; 6 — right hepatic lobe; 7 — scapula; 8 — coracoid. Small arrows indicate the jugular vein and the hepatic veins. White arrow indicates a fishhook. D and F: 1 — descending colon (enlarged in D by contrast injection); 2 — urinary bladder; 3 — cloacae. E: ventral view of a dissected turtle: 2 to 7 — same structures as shown in C; 9 — kidney.

vertebra) (Figure 6). The xiphiplastron images were superimposed with the images of the pubic bones, which produced some image distraction (Figure 6).

The position of the heart was recognized in relation to the skeleton and the sinus of the jugular vein in the dead animals injected with barium solution (Figure 5C and 5E). The heart was between the 1st to 3rd intercostal spaces, in the triangular area delineated by the coracoid bone and scapula (Figure 5C), and thus at the level of the 2nd vertebral scute. The trachea was easily identified on the left side of the cervical column (Figure 1), and its bifurcation to form the 2 long and extrapulmonary bronchi was visible at the level of the 2nd dorsal vertebra (Figure 2). The entrance of the right and left bronchi into the lungs was identified as 2 circular radiolucent areas at the level of the 1st dorsal vertebra (Figures 1 and 2). The pulmonary fields were very clearly imaged in all 17 live turtles and extended from the 1st to the 8th dorsal vertebrae. Although 9 of the turtles had symmetric lung fields, slight asymmetry between the right and left fields was observed in 8 turtles (Figures 2A and 5B). The pulmonary vasculature was very obvious, and the large pulmonary artery and vein were seen superimposed. They extended longitudinally in each lung (Figure 2A), and the collateral vasculature was frequently identified.

Visceral coelomic structural detail was often poor, and, in general, the clinically important organs, such as stomach, intestines, liver, and kidneys, were not imaged. Radio-opaque contents such as mollusk shells and fishhooks (Figure 4A), and even ingested coarse sand,

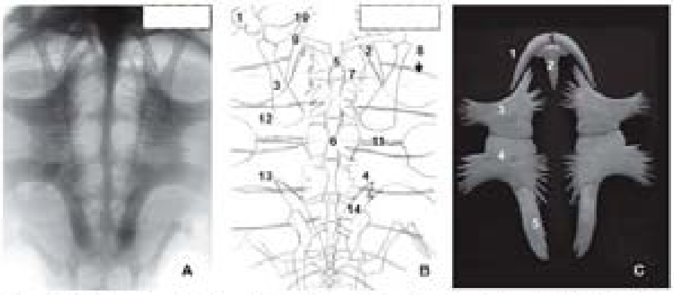

Figure 6. Negative image of the dorsoventral radiographic view of the whole body of a loggerhead sea turtle (A) and its interpreted drawing (B) and a ventral view of the plastron bones (C). B: 1 — humerus; 2 — epiplastron; 3 — coracoid bone; 4 — suture between the hypoplastron and the xiphiplastron; 5 — 2nd dorsal vertebra; 6 — 4th dorsal vertebra; 7 — 3rd pair of ribs; 8 — suture between the pleural bones; 9 — scapula; 10 — acromion; 11 — suture between the hyoplastron and the hypoplastron; 12 — hyoplastron; 13 — hypoplastron; 14 — xiphiplastron. C: 1 — epiplastron; 2 — endoplastron; 3 — hyoplastron; 4 — hypoplastron; 5 — xiphiplastron.

were identified in the gastrointestinal tract of some clinically healthy turtles. Intestinal loops were recognized when filled by radio-opaque digestive content or luminal gas and were interpreted as normal. Radio-opaque contrast material injected via the cloaca in dead turtles allowed visualization of the caudal part of the large intestine and identification of the urinary bladder (Figures 5D and 5F).

The position of the kidneys was recognized only once their vasculature was filled with contrast agent (Figures 5A, 5B, and 5E). They were seen at the level of the 8th to 10th dorsal vertebrae, below the 4th vertebral scute and the 4th and 5th left and right lateral scutes.

Discussion

Radiography is a useful tool to diagnose diseases of the skeleton and alimentary disorders in reptiles (1). In chelonians, pulmonary diseases, nutritional osteofibrosis, fractures, dystocia, and alimentary obstructions are the most important indications for radiographic diagnosis (7). According to previous studies (3), dorsoventral radiographs are the most suitable views for evaluating major organ systems in chelonians. In this study, we have verified that with careful adjustments to the kilovoltage potential (kVp) and the milliamperage-seconds (mAs) it is possible to gain much valuable information from dorsoventral radiography in loggerhead sea turtles. Digital radiography improves contrast and makes these adjustments easier. In reptiles, images produced with the matched mammography film–screen combination have greater resolution and better detail than standard tabletop radiographs (4). The film–screen combination was not as useful in evaluating coelomic structures in loggerhead sea turtles as in other chelonian species owing to the small screen size and the great thickness of the turtle's body, as well as the high radiodensity of their osseous structures, which made it necessary to increase the kVp to obtain more penetrability, thus causing loss of contrast. In addition to the use of digital images, the adjustment to a negative view was a reliable way of having ossified structures stand out, which made the recognition of the skeleton easier.

As a result of the variability of radiodensity in the different tissues and parts of the body, it was necessary to increase the kVp in the cranial third of the carapace and decrease it in the caudal third. Generally, individual identification of the vertebral bodies in the chelonians was difficult because of the superimposition of their images with those of the neural bones of the carapace. In addition, the intervertebral spaces (intercentral joints), easily recognized on radiographs in mammalian (17) and other reptilian species, is seen in chelonians as a very narrow and discrete radiolucent line that cannot be clearly imaged if a suitable kVp is not used. In large turtles, we recommend taking radiographs by sectors and using anatomic landmarks that allow spatial location of the affected areas, minor distortion or magnification, and better set-up of the adjustments.

In dorsoventral screening of the turtle's body, one must take into account the distortion caused by the natural curvatures of the body, which are seen at 2 points in the vertebral column: the S-shaped curvature of the cervical region, which causes the superimposition of images of the 5th and 6th cervical vertebrae, and the ventral flexion of the vertebral column from the 6th to the 10th dorsal vertebrae, which produces distortion in the length and partial superimposition of images of the vertebral bodies.

Knowledge of the relationship between the external scutes (used as external landmarks) and the vertebral column allows for efficient radiographic evaluation of traumatic injuries of the carapace, mainly those caused by propellers that affect the vertebral column and cause neurologic symptoms, once the injured vertebrae have been accurately identified (18).

Other anatomic landmarks useful in interpreting radiographs of the loggerhead sea turtle include the bronchi, coracoid bones, caudal border of the pulmonary fields, and acetabulum. Unlike that in most species of chelonians (1), the pulmonary field in healthy loggerhead sea turtles was easily identified in the dorsoventral view. Although in chelonian medicine, lateral and craniocaudal views are the most informative in assessing pulmonary disease (7,19), these views are often limited in the loggerhead sea turtle owing to the large size and high radiodensity of the body. Dorsoventral views are of reliable value because they allow clear recognition of any alteration in form, size, or appearance of the pulmonary field.

The morphologic differences observed in the turtle's pelvis (16) as compared with a mammalian pelvis (20) should be taken into account to avoid misinterpretation in identifying the pelvic bones. In the loggerhead sea turtle, the pubis is visible cranial to the acetabulum, in a position analogous to that of the mammalian ilium, the ischium is visible in a position analogous to that of the mammalian pubis, and the ilium is visible caudal to the acetabulum, in a position analogous to that of the mammalian ischium.

In conclusion, we have presented the standard radiologic appearance of the cervical and coelomic structures of the loggerhead sea turtle to help clinicians in evaluating radiographic abnormalities.

Acknowledgments

We thank Dr. Jaume Martorell, Departament de Medicina i Cirurgía Animals, Facultat de Veterinària, Universitat Autònoma de Barcelona, for his help with the radiography. We also thank CRAM volunteers and veterinary students Meritxell Clavell, Carolina García, Loana Fraga, and Olga Nicolas for their help with the turtle procedures. Thanks also go to Drs. Manel López Bejar and Carlos López Plana, Departament de Sanitat i Anatomia Animals, Facultat de Veterinària, Universitat Autònoma de Barcelona, for generously supplying the turtle skeleton. We also thank the anonymous peer reviewers.

References

1. Rübel A, Kuoni W. Radiology and imaging. In: Frye FL, ed. Biomedical and Surgical Aspects of Captive Reptile Husbandry. 2nd ed. Melbourne, Florida: Krieger Publishing, 1991:185–208.
2. Jackson OF, Sainsbury AW. Radiological and related investigations. In: Beynon PH, ed. Manual of Reptiles. Quedgeley, England: British Small Animal Veterinary Association, 1992:63–72.
3. Silverman S, Janssen D. Diagnostic imaging. In: Mader DR, ed. Reptile Medicine and Surgery. Philadelphia, Pennsylvania: W.B. Saunders, 1996:258–264.
4. DeShaw B, Schoenfeld A, Cook RA, Haramati N. Imaging of reptiles: a comparison study of various radiographic techniques. J Zoo Wildl Med 1996;27:364–370.
5. Meyer J. Gastrografin as a gastrointestinal contrast agent in the Greek tortoise (*Testudo hermanni*). J Zoo Wildl Med 1998;29: 183–189.
6. Gaudron C, Lignereux Y, Ducos de Lahitte J. Imagerie médicale appliquée à l'anatomie clinique des chéloniens en consultation. Proc Int Meet *Testudo* Genus 2001:161–182.
7. Wilkinson R, Hernandez-Divers S, Lafortune M, Calvert I, Gumpenberger M, McArthur S. Diagnostic imaging. In: McArthur S, Wilkinson R, Meyer J, eds. Medicine and Surgery of Tortoises and Turtles. Victoria, Australia: Blackwell Publishing, 2004:187–238.
8. Mader D. Radiographic anatomy. In: Mader DR, ed. Reptile Medicine and Surgery. Philadelphia, Pennsylvania: W.B. Saunders, 1996:485–489.
9. Pont SG, Alegre FN. Work of the Foundation for the Conservation and Recovery of Marine Life. Marine Turtle Newsl 2000;87: 5–7.
10. McArthur S. Problem-solving approach to conditions of marine turtles. In: McArthur S, Wilkinson R, Meyer J, eds. Medicine and Surgery of Tortoises and Turtles. Victoria, Australia: Blackwell Publishing, 2004:301–307.
11. Maudgil DD, Free SL, Sisodiya SM, Lemieu L, Woermann FG, Fish DR. Identifying homologous anatomical landmarks on reconstructed magnetic resonance images of the human cerebral cortical surface. J Anat 1998;193:559–571.
12. Bookstein FL. Morphometric Tools for Landmark Data: Geometry and Biology. New York, Cambridge University Press, 1991.
13. Radostits OM, Mayhew IG, Houston DM. Examen y diagnóstico clínico en veterinaria. 2nd ed. Madrid, Spain: Ediciones Harcourt, SA, 2002:409–467.
14. Dodd CK Jr. Synopsis of the Biological Data on the Loggerhead Sea Turtle *Caretta caretta* (Linnaeus 1758). US Fish and Wildlife Service Biological Report 1988:88(14).
15. Holz P, Barker IK, Crawshaw GJ, Dobson H. The anatomy and perfusion of the renal portal system in the red-eared slider (*Trachemys scripta elegans*). J Zoo Wildl Med 1997;28:378–385.
16. Wyneken J. The Anatomy of Sea Turtles. US Department of Commerce NOAA Technical Memorandum NMFS-SEFSC 2001;470:43–58.
17. Smallwood JE, Spaulding KA. Radiographic anatomy of the dog and horse. In: Thrall DE, ed. Textbook of Veterinary Diagnostic Radiology. 2nd ed. Philadelphia, Pennsylvania: W.B. Saunders, 1994:556–602.
18. Parga ML, Valente AL, Zamora MA, et al. Carapace trauma associated with hind limb paralysis in a loggerhead sea turtle (*Caretta caretta*). Proc Spring Meet Br Vet Zool Soc 2005:41.
19. Hernandez-Divers S, Hernandez-Divers S. Diagnostic imaging of reptiles. In Practice 2001;23:370–391.
20. Newton CD. Fractures of the pelvis. In: Newton CD, Nunamaker MJB, eds. Textbook of Small Animal Orthopaedics. Philadelphia, Pennsylvania: J.B. Lippincott, 1985.

4.2. RADIOGRAPHIC ANATOMY OF THE LIMBS OF THE JUVENILE AND SUBADULT LOGGERHEAD SEA TURTLES (CARETTA CARETTA)

Valente, A.L.; Marco, I; Zamora, M.A.; Parga, M.L.; Lavín, S.; Alegre, F. y Cuenca, R. (2007). Radiographic anatomy of the limbs of the juvenile and subadult loggerhead sea turtles (*Caretta caretta*). Can. J. Vet. Res. Aceptado para publicación.

RADIOGRAPHIC ANATOMY OF THE LIMBS OF THE JUVENILE AND SUBADULT LOGGERHEAD SEA TURTLES (*Caretta caretta*).

A. L.Valente, I. Marco, M. Zamora, M. L. Parga, S. Lavin, Alegre F. and
R. Cuenca

Address of authors:
Servei d'Ecopatologia de Fauna Salvatge. Facultat de Veterinària, Universitat Autònoma de Barcelona; 08193-Bellaterra, Barcelona, Spain (Valente, Cuenca, Lavin, Marco).
Diagnosis Médica, Córcega, 345, Barcelona, Spain (Zamora)
Centre de Recuperació d`Animals Marins; Camí Ral 239, 08330 - Premià de Mar, Barcelona, Spain (Parga, Alegre)

Corresponding author: Ana Luisa Valente.
Servei d'Ecopatologia de Fauna Salvatge, Facultat de Veterinària, Universitat Autònoma de Barcelona; 08193-Bellaterra, Barcelona, Spain.
Telephone number: +34 93 581 19 23;
Fax number: +34 93 581 20 06;

Abstract

This study aims to provide the normal radiographic anatomy of the limbs of the loggerhead sea turtle (*Caretta caretta*). Dorso-palmar (-plantar) radiographs were taken on the fore- and hindlimbs of 15 juvenile and 15 sub-adult loggerhead sea turtles, 17 alive and 13 deceased. Additionally, computed tomography (CT), gross anatomy, osteological and histological studies were performed on the limbs of 5 of them for comparison with radiological findings. Bones from the distal part of the fore- and hind flippers were seen in detail using mammography film-screen combination. Pectoral and pelvic girdles, superimposed by the carapace, were better seen on the standard radiographs using rare-earth intensifying screens. Mammographic radiographs of the manus of 5 small juvenile turtles showed active growth zones. Visualization of bone contours on the distal part of the limbs was clearer compared with mammals due to the very few superimpositions between them. The presence of a significant cartilage in the epiphyses produced better visibility of limb-ends. We have concluded that the use of mammographic film-screen combination is the best mode to evaluate the bony and joint structures of the fore- and hindlimbs of juvenile and subadult sea turtles. Radiographs provided reliable images for clinical purposes. Considering the low cost and logistics of this technique it is one of the more practical ancillary tests that marine animal rehabilitation centres can use.

Keywords: radiographic anatomy, loggerhead sea turtle, *Caretta caretta*, limbs, diagnostic imaging.

Introduction

Sea turtle populations have declined over the past few decades due to human activity. Boat-strike injuries, entanglement in fishing nets, the swallowing of hooks, fishing lines and crude oil are the main causes of sea turtle mortality around the Canary Islands and in the Western Mediterranean (1, 2). The loggerhead sea turtle (*Caretta caretta*) is listed as endangered (3) and is the most common species accidentally caught by fishing activities in the Mediterranean Sea. Juveniles and subadults are most commonly caught and most animals rescued from fishing nets have some degree of limb trauma which occurs when turtles become entrapped in nets, leading to strangulation of extremities (2). Once at the rehabilitation centre, proper physical assessment should be performed as should a minimum standard database including blood analysis and radiographs (4).

Different imaging methods are available today for veterinary practice. However, normal radiological parameters are scarce for most free-ranging animals, including sea turtles. Previous authors have reported radiological techniques applied to reptile species (5, 6, 7, 8, 9, 10). However, due to the wide morphologic variety of reptiles, further knowledge of the normal radiographic anatomy in a particular species is required.

This article forms part of a wide-ranging study on diagnostic imaging of the loggerhead sea turtle, its purpose being to provide the normal radiographic anatomy of the limbs of the loggerhead sea turtle. We have combined radiological information with computed tomography, osteological, gross anatomical and histological data of the apendicular skeleton of this species in order to provide useful information for increasing relevant clinical knowledge.

Materials and Methods

Dorso-palmar (-plantar) radiographs were taken on the fore- and hindlimbs of 15 juvenile and 15 sub-adult loggerhead sea turtles accidentally caught in pelagic longline sets and fishing nets along the North-Western Mediterranean coast. Juvenile turtles were considered to be those with a minimum straight carapace length (SCLmin) of 21 to 40 cm, and sub-adults those with a SCLmin of 41 to 65 cm (11). Seventeen of the animals were alive and thirteen deceased. Live turtles were temporally housed in the rehabilitation facilities of the Rescue Centre for Marine Animals (CRAM) (Premiá de Mar, Barcelona, Spain). Only turtles free of limb damage or skeleton pathology were considered for this study. The turtles were manually restrained in ventral recumbency, the limbs maintained with cellotape in a physiological position. No sedation was required; only the eyes were masked. Table-top images were taken using a Toshiba – Rotanode ^{tm} (Model E7239) x-ray tube at a 68-cm film-focal distance. Radiographs were taken using UM- MA hc, 24x30 cm for mammography medical x-ray film, a Fuji AD-MA screen (UM MAMMO fine, Fuji Photo Film Co., Ltd.; Tokyo 106-8620) and Super HR-GB, 30x40 cm film and rare-earth intensifying screens, (Fuji ECD). Using a negatoscope the radiographs were photographed and digitalized at a minimum resolution of 300dpi. Radiographs were evaluated and radiographic anatomy described when found to be consistent.

Multi-detector Computed Tomography (MDCT) of the whole body was performed in four juvenile and one subadult loggerhead sea turtles. Turtles were anaesthetized with the association of intravenous ketamine (15mg/K, Imalgene® 1000, Merial) and diazepam (0,5mg/Kg, Diazepam, Almirall Proderfarma, Prodes), injected into the dorsal cervical sinus to prevent flipper movement. Cardiac frequency was verified using a mini-doppler and the animals were carefully kept wet prior to the scan. MDCT studies were obtained by a sixteen-detector row CT scanner (Aquilion 16, Toshiba Medical, Tokyo, Japan) using the following parameters: 120 kVp, 250mA, 16 x 1mm detector configuration and a 512 x 512 matrix. The field of view ranged from 35cm to 52cm and total time examination took between 10-15 seconds, depending on the size of the turtle. The volumetric data of the limbs were reconstructed with a 1mm slice width and reconstruction interval of 0.8 mm. Three-dimension images were generated on a Vitrea computer workstation (Vitrea® version 3.0.1., Vital Images, Plymouth, MN).

In order to obtain anatomical information of the limbs from the dead turtles, five of them (2 juvenile and 3 subadult) were frozen at -80° C, and serial parallel sections from 18 to 20 mm thick were taken in the dorsal plane using an electric bone saw. The limb bones and associated joints were evaluated and samples of epiphyses of the humerus, radius, ulna, femur, tibia, fibula, metacarpal and metatarsal bones and phalanges were collected and fixed in neutral-buffered 10% formalin solution for histological study.

Five loggerhead sea turtle skeletons from the Museo de Zoología de Barcelona and the Departamento de Sanidad y Anatomía, Facultad de Veterinaria of UAB were photographed and radiographed for osteological data.

Radiologically visible structures were compared with those observed on osteological preparations, 3D CT reconstructions, gross anatomical sections and histological samples. All radiographic images were analyzed with Adobe Photoshop® (Adobe Photoshop® v 5.5, Adobe Systems Incorporated; USA) and normal and inverted (negative) images were compared.

The anatomical terminology used in this study is that of the *Nomina Anatomica Veterinaria*. In addition, specific terminology for sea turtles (12) was also applied.

Results

Bones from the distal part of the fore and hind flippers were seen in detail in radiographs using the mammography film-screen. CT reconstructions images showed best definition to examine the cortical bone, density of the matrix and trabeculas. The pectoral and pelvic girdles were better seen in the standard table-top radiographs using rare-earth intensifying screens than the mammographic film-screen combination. These regions will be not described here since they were included in a previous publication on the coelomic cavity (13). Bones from juvenile and subadult loggerhead sea turtles did not differ in form or structure; however some bony features such as the head and greater tuberosity of the humerus and the head and major trochanter of the femur were more pronounced in the subadults.

Radiographically, a large joint space was seen in all synovial joints of the limbs (Fig.1A). In the anatomical sections a thick hyaline cartilage cone plugged each bone forming the great part of the epiphyseal area (Fig. 1B). Mammographic radiographs of 5 small juvenile turtles showed a thin radiolucent line followed by a radiodense longitudinally striated and thicker band (Fig. 2A) mainly in the physes of the metacarpals, metatarsals, phalanges and distal physes of the humerus. Subcondral growth was observed in all bones. These findings were interpreted based on the histological analyses of the same animals, as active growth zones in the epiphyseal plate (Fig. 2D). Long bones consisted primarily of a core of cancellous bone bounded by a thin cortex of compact bone (Fig. 2 B-C). The histological study carried out in 2 juveniles showed that the epiphysis consisted of a mass of undifferentiated cartilage where the cells (condrocytes) of the layer next to the shaft forming the growth zone were flattened and arranged in longitudinal columns, showing different degrees of hypertrophy. Condrocytes nearest to the shaft were more vacuolated than those nearest the end of the epiphyses. In the 3 subadult turtles, the cellular arrangement in the growth area was similar to that observed in the 2 juvenile ones; however the longitudinal columns were not so well-defined. In all cases, mineralization of a cartilage template was observed and endocondral bone was set down on the eroded surface of the cartilage (Fig. 2D).

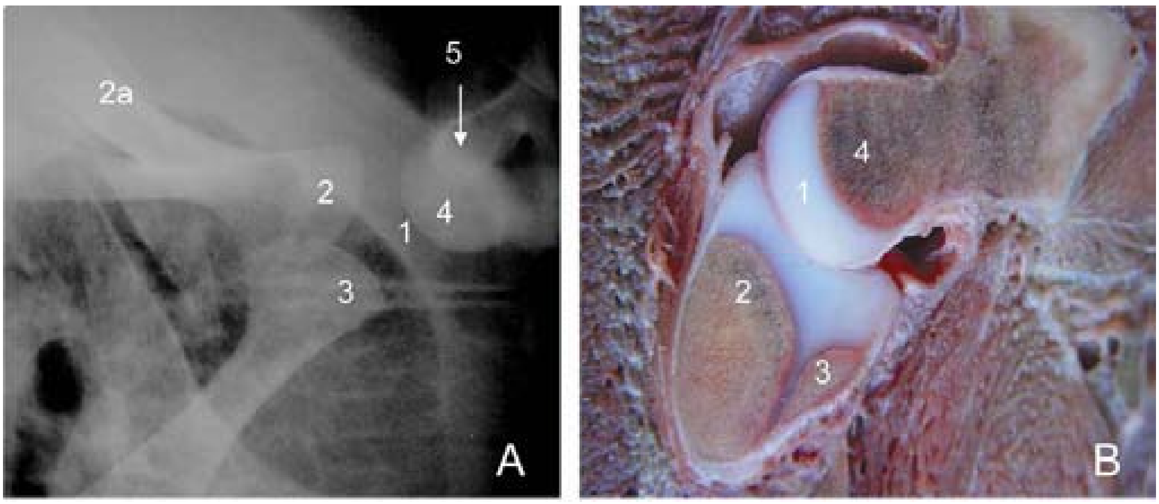

Figure 1. Dorsoventral radiographic view (A) and dorsal anatomical section (B) of the shoulder joint of a loggerhead sea turtle. 1, Cartilaginous part of humerus head. 2, articular end of the Scapula (cranial fused bone is the Acromion process – 2a); 3, articular end of the coracoid; 4, humerus head; 5, greater tuberosity.

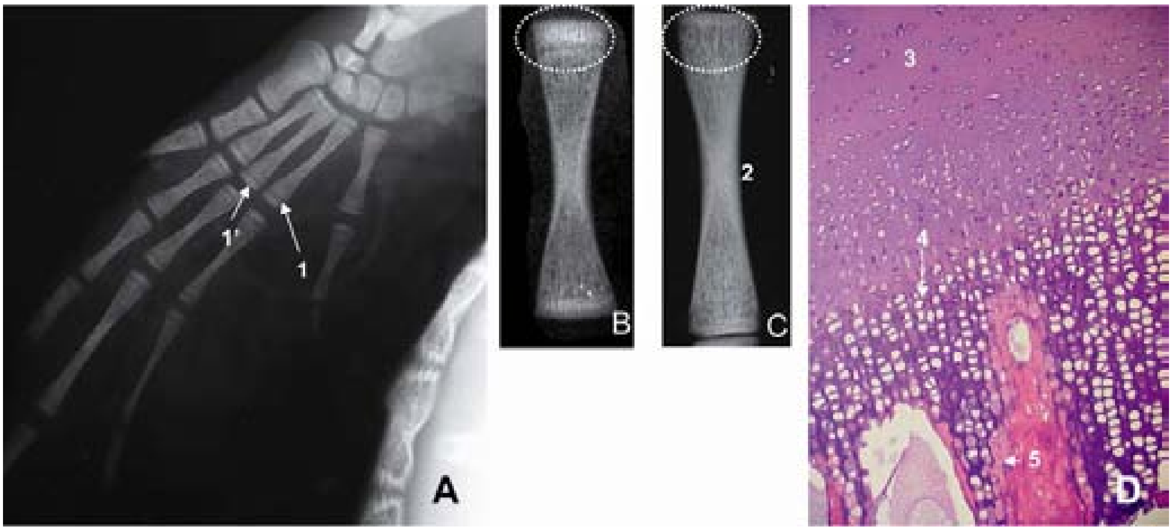

Figure 2. Dorsoventral radiographic view (A) of the manus of small juvenile loggerhead sea turtle. Close-up of proximal phalange of digit II of juvenile (B) and subadult (C) specimens. Histological survey of the growth area (C). 1, epiphyseal growth zone (1' epiphyseal plate); 2, ossified diaphysis; 3, undifferentiated cartilage; 4, longitudinal columns of hypertrophied condrocytes; 5, Mineralization of cartilage template, endocondral bone.

Humerus

The proximal epiphysis of the humerus was not clearly seen radiographically due to the superimposition of the carapace and plastron bones. The head of the bone was seen joined with the articular surface formed by the scapula and acromion and coracoid bones (Figs. 1A-B, 3A). Caudal to the head, the great and rounded medial process (greater tuberosity) was easily identified in all radiographs (Fig. 3A-C). The morphology of this structure in the radiographs was similar to the head of the humerus in both juvenile and subadult turtles (Fig. 3A, B).

However, in CT, osteological and anatomical dissections, this structure was more prominent than the head (Fig. 3C). A large fosa could be clearly seen in the radiographs as a radiolucent area immediately below the head and the greater tuberosity. The deltoid crest could be identified as a rounded projection of the bone contour on the cranial border of the humerus (Fig. 3A-C). In 3 subadult turtles, this crest was more prominent than in juveniles and, depending on the rotation of the limb at the moment of the examination, the structure was seen partially superimposed on the humeral head (Fig.1A). In one juvenile turtle a sharp process was seen in the caudal border of the crest (Fig. 3B). The nutrient foramen present on the ventral surface of the humerus (Fig.3C) could not be observed on all radiographs. In the distal epiphysis of the humerus, the medial and lateral condyles were recognisable due to the presence of the intertuberal groove between them (Fig. 3C, E).

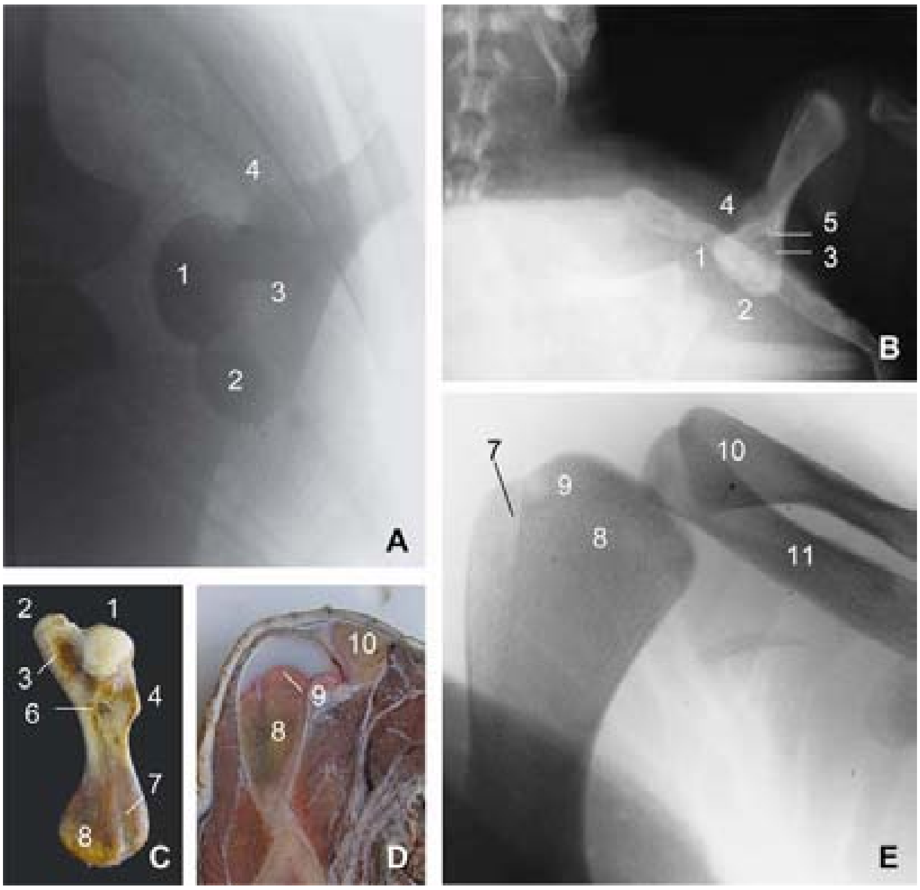

Figure 3. Negative image of dorsoventral radiographic view of humerus of sub-adult (A, E) and juvenile (B) loggerhead sea turtles; ventral view of humerus (C) and anatomical section of elbow joint (D). 1, humerus head; 2, greater tuberosity; 3, fossa between humerus head and greater tuberosity; 4, deltoid crest; 5, sharp process on deltoid crest; 6, nutrient foramen; 7, intercondylar sulcus; 8, medial condyle; 9, growth zone; 10, radius; 11, ulna.

Radius and ulna

The bones were seen partially superimposed, the radius, shorter than the ulna was seen cranial to it. The radius had a broad and triangular proximal epiphysis and its caudal border showed a concave curvature. The ulna was seen as straight and tubular shaped with its distal end superimposed on the ulnare and radiale carpal bones (Fig. 3E, 4A). No pronounced process or grooves were visualized in either bones and the cortices were markedly thickened in the mid-diaphyseal region but tapered proximally and distally (Figs. 3E, 4A).

Carpal bones

The nine carpal bones could be clearly recognized in the carpus due to scant superimposition (Fig. 4A-C). In the proximal row, the radiale was seen as a rectangular bone placed laterally. The ulnare showed a semilunar shape, with a great curvature pointed medially. The pisiform bone was seen standing out medially from the distal row. The small and rounded centrale bone was seen immediately ventral to the radiale and ulnare bones. In the distal row of the carpus, five carpal bones were identified, each one respective to a digit (Fig. 4C).

Metacarpals and phalanges

Metacarpals bones and phalanges have similarly-shaped digits except for the first, which shows a flattened articular surface on the physes and elongated, thin diaphyses. The first digit is prominent and consists of a short and strong metacarpal bone with only two sturdy phalanges, the proximal and distal ones (Fig 4A). The second digit has a shorter and thicker proximal phalange than those of the 3rd and 4th digits. The intermediate phalange of the third digit is the most slender and longest of all. The fifth digit has only two phalanges. In the radiographs and CT images, no sesamoid bones were seen associated with the flipper joints (Fig. 4 A, B).

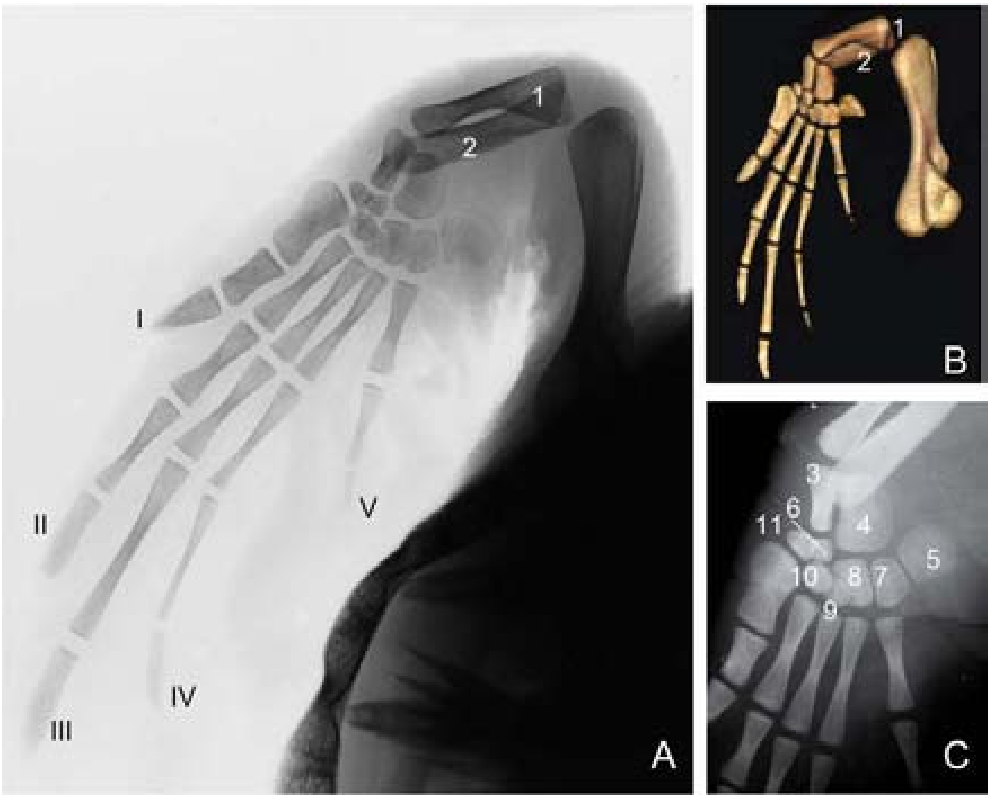

Figure 4. Negative image of dorsoventral radiographic view (A) and 3-D reconstruction (B) of *manus* of juvenile loggerhead sea turtle. Close-up of dorsoventral radiographic view of carpal region (C). 1, radius; 2, ulna; 3, radiale; 4, ulnare; 5, pisiform; 6, centrale bone; 7,8,9,10,11, carpal bones. Roman numbers in A indicate respective digit.

Femur

The joint of the head of the femur with the acetabulum superimposed on the carapace bones was clearly visible in all radiographs taken using conventional plain film (Fig. 5A, B). In juvenile turtles, most of the head was made up of cartilage. In the subadult animals the ossified head was stouter than in juvenile and was joined to the physes through a thick neck (Fig 5A-E). The prominent major trochanter was seen caudal to the head. The diaphysis was long and slender. The condyles on the distal epiphyses could not be differentiated because the distal epiphysis was superimposed on the marginal bones of the carapace. Neither the patella nor other sesamoid bones were visualized in the stifle joint (Fig. 5A, 6B).

Tibia and fibula

The tibia and fibula could be seen with scant superimposition of epiphyses. The tibia was thicker, cranial to the fibula, and with a convex articular surface at the proximal epiphysis. Both bones were elongated and fairly similar in length (Fig. 6A, B).

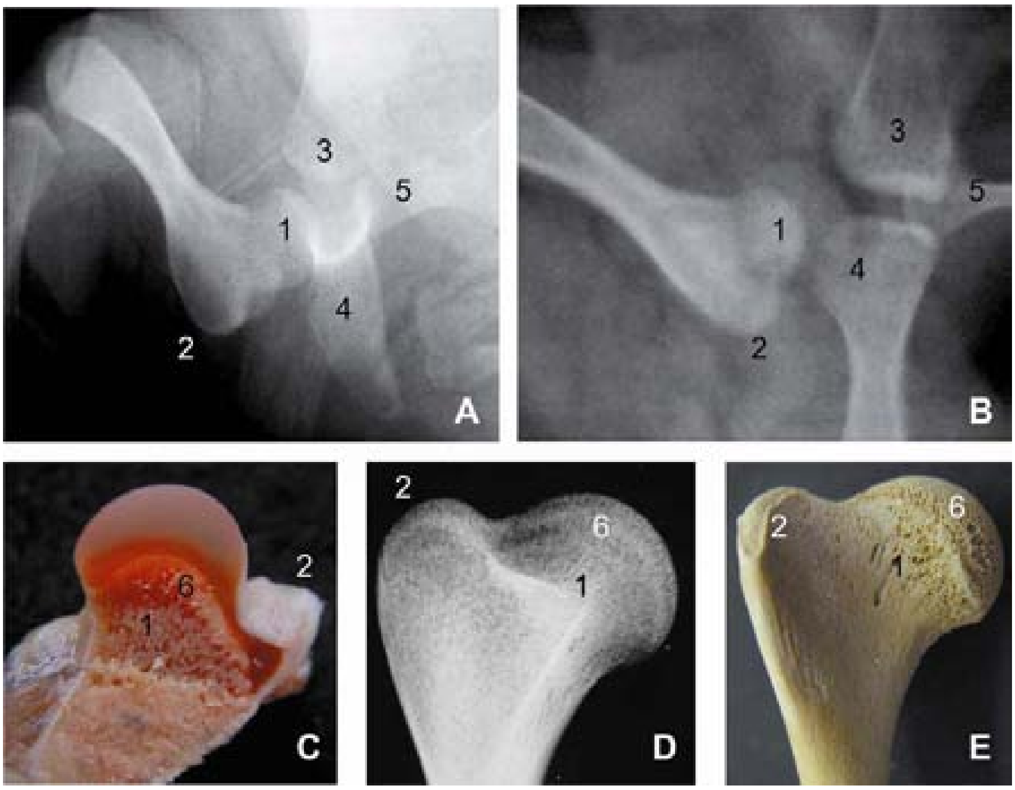

Figure 5. Dorsoventral radiographic view of hip joint of sub-adult (A) and juvenile (B) loggerhead sea turtles. Gross anatomy section (C), radiographic view (D) and osteological preparation (E) of proximal epiphysis of femur. 1, femoral head; 2, greater trochanter; 3, pubis; 4, ilium; 5, ischium; 6, growth zone.

Tarsal bones

Six tarsal bones were perfectly visualized in all radiographs. We have identified two rounded and bigger ones and four quite spherical and smaller ones (Fig. 6 A-C). On the proximal row the great astragalus was seen laterally below the tibia, and the calcaneum seen as a small rounded bone positioned medially below the fibula (Fig.6C). In the distal row, the V tarsal bone was articulated with the IV and V metatarsal bones and was prominent because of its heart shape and the large size related to other tarsal bones, which were spherical and positioned just proximal to each respective digit, I, II and III (Fig. 6C).

Metatarsals and phalanges

Similar to the forelimb, the first digit consisted of a short, flattened and strong metatarsal bone and only two sturdy phalanges. Digits II to V showed three somewhat proportioned phalanges. The V metatarsal bone is flattened and resembles the I metatarsal bone, though slightly smaller (Fig.6 A, B).

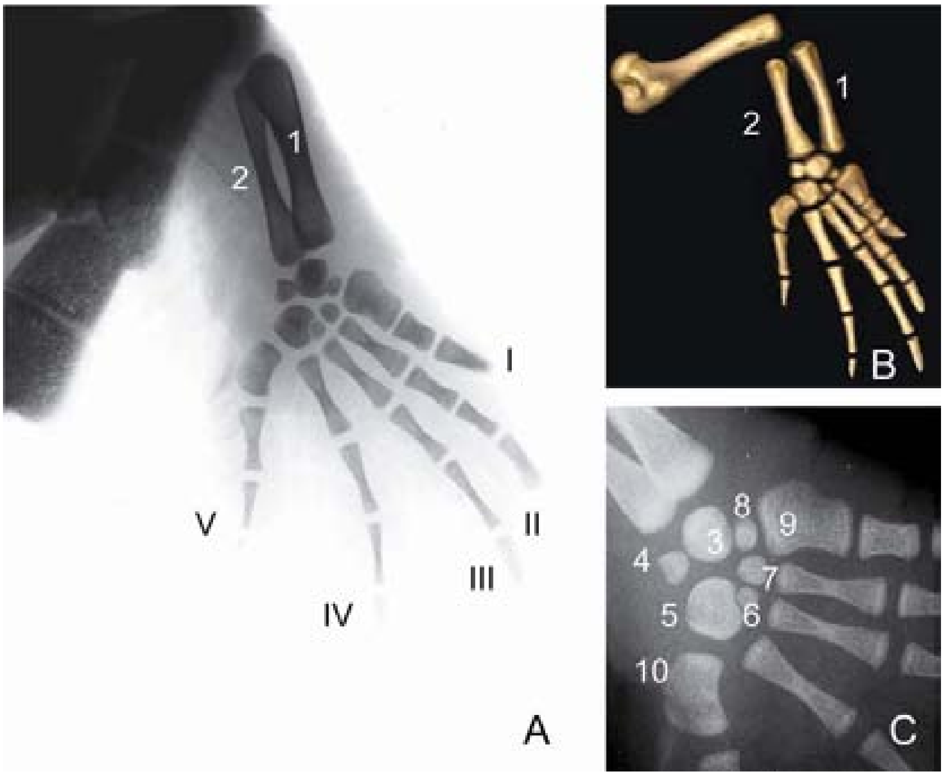

Figure 6. Negative image of dorsoventral radiographic view (A) and 3-D reconstruction (B) of *pedis* of juvenile loggerhead sea turtle. Close-up of dorsoventral radiographic view of tarsal region (C). 1, tibia; 2, fibula; 3, astragalus; 4, calcaneum; 5, V tarsal bone; 6, 7, 8, tarsal bones; 9, metatarsal bone from digit I; 10, metatarsal bone from digit V. Roman numbers in A indicate respective digit.

Discussion

Routine radiography of the limbs is usually performed in at least three views: dorso-palmar (or –plantar), lateral and oblique (14). The flattened shape and relative thinness of the loggerhead sea turtles' flippers when compared with the compact and quite cylindrical limbs of the terrestrial vertebrates precludes the use of other views except the dorso-palmar (-plantar). Size or morphological distortion was observed only at the proximal end of the humerus, where the great tuberosity was seen partially superimposed on itself showing an unreal shape in the radiographs. Numerous anatomical differences between the limbs of chelonians and those of mammalians, or even between turtles and other reptiles, make them a unique patient. When comparing radiographs of limbs of sea turtles with those of mammals, such as the dog or cat, there is a clearer visualization of the bone contours due to the scant superimpositions between them. Additionally, the presence of a massive cartilage in the epiphyses produced better visibility of the articular ends. According to previous information (15) these cartilaginous epiphyses become gradually thinner with age because the passage of undifferentiated cells into the growth zone and consequently the articular and growth zones come into close approximation; however growth may be retained even in aged animals. Easy visualization of the bone ends was a finding with practical clinical application because the diagnosis of bone disorders such as fractures, osteomyelitis, osteofibrosis and mainly joint pathologies could be easily made using a conventional and inexpensive x-ray technique.

Previous studies (8) have reported that the matched mammography film-screen combination was superior to standard Buchy and table-top radiographs in the evaluation of bone and soft tissues in small reptiles. The combination results in a resolution of 10-20 line pairs (lp)/mm as opposed to the 5-10 lp/mm resolution in standard radiographic techniques (8), which in this study permitted optimal visualization of the cancellous and compact bone arrangement in the long bones, and the epiphyseal growth areas. The growth areas observed in our animals as a radiopaque band at the end of the long bones were also observed in skeletally immature humans (16), where transverse trabecular bands of increased radiodensity appeared following a temporary slowdown or cessation of rapid longitudinal bone formation. When growth rates were normal, longitudinally-oriented trabeculae with interspersed marrow elements predominated at the zone of transformation of cartilage to bone (16).

Radiological examination of the long bone epiphyses together with evaluation of time of closure have been used as a chronological reference in various species of vertebrates (17, 18). In reptiles this methodology is not suitable because endocondral growth may be life-long (15). On the other hand, turtles and crocodiles do not have isolated ossification centres in the epiphysis (bony epiphysis) such as occurs with squamates (snakes and lizards) and mammals (15). Curiously, in our study only in 5 of 15 juvenile turtles was the presence of epiphyseal plates detected radiographically in the long bones of the manus. We are unaware of the reasons why these areas were not seen in all juvenile animals, as should be expected. Patterns of reptile growth have attracted considerable attention over the past few decades (19, 20, 21). The presence of growth rings in the transverse section of the humerus has been studied in reptiles, including sea turtles (22), as a method to calculate age. Turtles grow at different rates during the ontogenetic period, the rate being influenced quality and quantity of diet (15, 23). In their early years of life, oceanic-stage loggerhead sea turtles have relatively little control over their geographic position or movements and thus they have an extremely stochastic lifestyle with great variation in food availability and temperature (24). Temporary cessation of growth may occur even in relatively young turtles; it is resumed later, after perforation of the bony plates and renewal of activity by the marrow (15). The environmental variation results in variable growth rates, that could be directly associated with the inconsistent presence of a distinct growth area in the long bones of juvenile turtles of this study.

The shape and structure of bones is governed by many factors - genetic, metabolic and mechanical. In reptiles, the pectoral and pelvic arches appear to have a very anomalous position in the Chelonia, inasmuch as they seem to be situated inside and not outside the skeleton trunk (12). Modifications of the sea turtle pectoral limb into a semi-rigid elongated and flattened flipper for forelimb propulsion has resulted in proportional changes in the limb skeleton and shifts in the distributions of muscle tissue (25). This reduced presence of musculoskeletal elements includes the sesamoid bones, thus accounting for their absence in the radiographs of the present study. Although reptilian compact bone is quite similar to the other vertebrates, we have found the bone cortex to be relatively thinner in the case of turtles, with minor radiographic contrast between bones. Compared to the radiographic anatomy of well-known species such as the dog or cat (26), the diaphysis of turtle bones in general seems to show a smoother surface without pronounced processes, crests or tuberosities. As a result, there is a clearer radiographical image of the bone internal structure, with minimal superimposition of superficial bony elements. The response pattern of the bone to injury in reptiles differs significantly from that found in mammals. New periosteal bone production is less prominent in the former and it is common to see a radiolucent fracture line in clinically stable fractures that have healed with a fibrous callus (10, 27).

Mammographic radiographs and the multiplanar TC reconstructions were observed to provide similar information; the latter also involved greater cost and is a technique not readily available in rehabilitation centers. Also, more time is needed for image manipulation. Three-dimension reconstructions were useful to see the different views of the structures. However, this kind of virtual processing, when applied to extremely tight bone structures, as is the case with carpal or tarsal bones, may produce an artificial effect whereby the structures seems to be joined.

In this study we have concluded that the use of mammographic film-screen combination is the best radiographic modality to evaluate the bone and joint structures of the fore and hindlimbs of juvenile and subadult sea turtles. Radiographs provided reliable images for clinical purposes. Considering the low cost and logistics of this technique it is one of the more practical ancillary tests that marine animal rehabilitation centres can use.

Acknowlegments

The authors would like to thank Professor Dr. Francisco Reina and the laboratory technician Isabel Delgado Calvarro, Facultat de Medicina, UAB, for help with the anatomical sections, and the radio-diagnostic technician Montse March for technical support with the MDCT. Thanks also go to the Museo de Zoología de Barcelona and the Depto. de Sanidad y Anatomía, Facultad de Veterinaria of the UAB for providing the turtle skeletons. We are grateful to Dr. Jordi Franch, Depto de Medicina y Cirugia Animal, Facultad de Veterinaria of the UAB for the review of this paper.

References

1. Orós J, Torrent A, Calabuig P, Déniz S. Diseases and causes of mortality among sea turtles stranded in the Canary Islands, Spain (1998-2001). Dis Aquat Organ 2005;63:13-24.

2. Pont SG, Alegre FN. Work of the Foundation for the Conservation and Recovery of Marine Life. Marine Turtle Newsletter 2000;87:5-7.

3. IUCN. Red List of Threatened Species 2004.www.iucnredlist.org. Accessed February 22, 2006.

4. Wyneken J, Mader DR, Weber III ES, Merigo C. Medical care of sea turtles. In: Mader DR ed. Reptile Medicine and Surgery. Canada: Elsevier Inc., 2006:972-1007.

5. Wyneken J. Computed tomography and Magnetic resonance imaging anatomy of reptiles. In: Mader DR ed. Reptile Medicine and Surgery. Canada: Elsevier Inc., 2006:1088-1096.

6. Rübel A, Kuoni W. Radiology and Imaging. In: Frye FL ed. Biomedical and surgical aspects of captive reptile husbandry. 2nd ed. USA: Krieger Pub. Co., 1991:185-208.

7. Jackson OF, Sainsbury AW. Radiological and related investigations. In: Beynon PH, ed. BSAVA Manual of Reptiles. British Small Animal Association. Dorset: J. Looker Printers, 1992: 63-72.

8. DeShaw B, Schoenfeld A, Cook RA, Haramati N. Imaging of Reptiles: a comparison study of various radiographic techniques. J Zoo Wildl Med 1996;27: 364-370.

9. Hernandez-Divers S, Hernandez-Divers S. Diagnostic imaging of reptiles. In Practice 2001; july/august: 370-391.

10. Wilkinson R, Hernandez-Divers S, Lafortune M, Calvert I, Gumpenberger M, MCarthur S. Diagnostic Imaging. In: McArthur S, Wilkinson R, Meyer J, eds. Medicine and Surgery of tortoises and turtles. Victoria, Australia: Blackell Publishing Ltd., 2004:187-238.

11. Dodd CK Jr. Synopsis of the biological data on the loggerhead sea turtle *Caretta* (Linnaeus 1758). U.S. Fish and Wildlife Service Biological Report 1988;88:35-82

12. Wyneken J. The Anatomy of Sea Turtles. U.S. Departament of Commerce NOAA Technical Memorandum NMFS-SEFSC 2001;470:1-172.

13. Valente AL, Cuenca R, Parga ML, Lavin S, Franch J, Marco I. Cervical and coelomic radiology of the Loggerhead Sea turtle, *Caretta caretta*. Can J Vet Res (in press).

14. Morgan JP. Techniques of veterinary radiography. Iowa State University Press, Ames, Iowa, 1993.

15. Haines RW. Epiphyses and sesamoids. In: Gans C, d'A Bellairs A, eds. Biology of the Reptilia. New York: Academic Press,1969:81–115

16. Ogden JA. Growth slowdown and arrest lines. J. Pediatr Orthop 1984;4:409-415.

17. DiGiancamillo M, Rattegni G, Podestà M, Cagnolaro L, Cozzi B, Leonardo L. Postnatal ossification of the thoracic limb in striped dolphins (*Stenella coeruleoalba*) (Meyen, 1833) from the Mediterranean Sea. Can J Zool 1998;76:1286-1293.

18. Serrano E, Gállego L, Pérez JM. Ossification of the Appendicular Skeleton in the Spanish Bies *Capra pyrenaica* Schinz, 1838 (Artiodactyla: Bovidae), with Regard to Determination of Age. Anat Histo. Embryol 2004;33: 33-37.

19. Hailey A, Coulson IM. The growth pattern of the African tortoise *Geochelone pardalis* and other chelonians. Can J Zool 1999;77:181-193.

20. Bjorndal KA, Bolten AB, Martins HR. Somatic growth model of juvenile loggerhead sea turtles *Caretta caretta*: duration of pelagic stage. Mar Ecol Prog Ser 2000;202:265-272.

21. Arcos-García JL, Peralta MAC, Rosales VHR, Martínez GDM, Cerrilla MEO, Sánchez FC. Growth characterization of black iguana (*Ctenosaura pectinata*) in captivity. Vet Mex 2002;33:409-419.

22. Zug GR, Wynn A, Ruckdeschel C. Age Estimates of Cumberland Island Loggerhead Sea Turtles. Marine Turtle Newsletter 1983; 25:9-11.

23. Spencer RJ. Growth patterns of two distributed freshwater turtles and a comparison of common methods used to estimate age. Aust J Zoo 2002;50:477-490.

24. Bjorndal KA, Bolten AB, Dellinger T, Delgado C, Martins HR. Compensatory growth in oceanic loggerhead sea turtles: response to a stochastic environment. Ecology 2003;84:1237–1249.

25. Wyneken J. Comparative and functional considerations of locomotion in turtles. [PhD dissertation]. Urbana-Champaign. University of Illinois, 1988.

26. Konde LJ. Appendicular Skeleton – Companion Animals. Diseases of the Immature skeleton. In: DE Thrall, ed. Textbook of Veterinary Diagnostic Radiology. Philadelphia: WB Saunders, 1994:94-104.

27. Silverman S. Diagnostic Imaging. In: Mader DR, ed. Reptile Medicine and Surgery. USA: W.B. Saunders, 2006:471-489.

4.3. NORMAL ULTRASONOGRAPHIC IMAGING OF THE LOGGERHEAD SEA TURTLE (CARETTA CARETTA)

Valente, A.L.; Parga, M.L.; Espada, Y.; Lavin, S.; Alegre, F.; Marco, I. y Cuenca, R. (2007). Normal ultrasonographic imaging of the loggerhead sea turtle (*Caretta caretta*). Vet Rec. 160. Aceptado para publicación.

NORMAL ULTRASONOGRAPHIC IMAGING OF THE LOGGERHEAD SEA TURTLE (*Caretta caretta*)

A.L.Valente[1], DVM, MSc; M L. Parga[2], DVM, MSc; Y. Espada[3], DVM, PhD; S. Lavin[1], DVM, PhD; F. Alegre[2], DVM; I. Marco[1], DVM, PhD and R. Cuenca[1], DVM, PhD.

Address of authors:

[1]Servei d'Ecopatologia de Fauna Salvatge. Facultat de Veterinària, Universitat Autònoma de Barcelona, 08193-Bellaterra, Barcelona, Spain.

[2]Centre de Recuperació d`Animals Marins, Camí Ral, 239 - 08330 Premià de Mar, Barcelona, Spain.

[3]Departament de Medicina i Cirurgia Animal. Facultat de Veterinària, Universitat Autònoma de Barcelona, 08193-Bellaterra, Barcelona, Spain.

Correspondence address: MSc. Ana Luisa Valente. Servei d'Ecopatologia de Fauna Salvatge, Facultat de Veterinària, Universitat Autònoma de Barcelona, 08193-Bellaterra, Barcelona, Spain. Telephone number: +34 93 581 19 23; Fax number: +34 93 581 20 06; e-mail: schifinoval@hotmail.com.

Summary

This work describes the normal ultrasonographic appearance of cervical structures and coelomic organs of loggerhead sea turtles. Twenty live, and five dead juvenile and subadult loggerhead sea turtles were studied. Ten soft-tissue areas of integument were used as acoustic windows: cervical-dorsal and cervical-ventral, left and right cervicobrachial, left and right axillary, left and right prefemoral and left and right postfemoral acoustic windows. Anatomical cross-sections were performed on the dead turtles to provide reference data. The fourth and fifth cervical vertebrae, the spinal cord, and the venous sinuses of the external jugular vein are clearly seen on the cervical-dorsal acoustic window. On the cervical-ventral acoustic window, the esophagus and the heart were imaged. The stomach was more frequently seen through the left axillary acoustic window. Although the liver could be imaged through both sides, the right axillary acoustic window was the most indicated to see the gallbladder. The large and small intestines and the kidneys could be seen in the right and left prefemoral acoustic windows; the latter were easily identified due to the intense renal vasculature. This study shows that ultrasonography is a useful tool for diagnosis in juvenile and subadult loggerhead sea turtles.

Keywords: ultrasound, Loggerhead Sea Turtle, *Caretta caretta*, echoanatomy, anatomy

Introduction

The loggerhead sea turtle (*Caretta caretta*) is the most common species accidentally captured by fisheries in the western Mediterranean Sea. Juveniles and subadult animals are those most affected by the captures. According to (IUCN, 2004) the species is listed as endangered (EN A1abd) and the estimated annual number of subadult loggerhead sea turtles accidentally captured every year on the Spanish Mediterranean coast is more than 20,000 (Aguilar and Pastor 1995). Captured turtles are usually released back to the sea with a fish-hook still lodged, and it is estimated that between 20% and 30% of these individuals might die due to the lesions caused by them (Aguilar and Pastor 1995). The main cause of admission of sea turtles in the rescue centres is the ingestion of fishhooks; other causes include lesions by entanglement in fishing nets, collision with boat propellers and ingestion of garbage. As in other chelonian species, the shell severely limits examination of internal organs, and the diagnosis based only on a clinical examination is usually very poor.

Ultrasonography is well-established as a rapid, non-invasive and non-expensive method of assessing soft structures; therefore, it serves as a helpful tool for clinical diagnosis in turtle rehabilitation. Its main disadvantage is the lack of well-described ultrasonographic standards for sea turtles. Although general considerations on ultrasound in reptiles could be found in some chapters of wildlife medicine books (Jackson and Sainsbury 1992, Silverman and Janssen 1996, Whitaker and Krum 1999, Wilkinson and others 2004) and papers (Sainsbury and Gili 1991, Gaudron and others 2001, Schumacher and Toal 2001), only few works systematically describe the normal appearance and the best way to visualize the organs (Pennick and others 1991, Martorell and others 2004). Furthermore, anatomical differences among chelonian species have a reflective effect upon ease of scanning. The reproductive tract of adult female Olive Ridley (*Lepidochelys olivacea*) and Kemp's Ridley (*Lepidochelys kempii*) sea turtles has been studied by Rostal and others (1989, 1990 and 1994). These authors recommend ultrasound as a good technique to evaluate the gonad structure, egg development and presence of atretic follicles. To the authors' knowledge, published data about normal ultrasonography of the loggerhead sea turtle are not available.

The aim of this work is to describe the normal ultrasonographic appearance of cervical structures and coelomic organs of the loggerhead sea turtle and to provide images of frozen cross-sections for anatomical reference.

Materials and Methods

A total of 25 loggerhead sea turtles (*Caretta caretta*), with a minimum straight carapace length (SCLmin) of 26.0 cm to 58.5 cm and weights of 3.5 kg to 26.8 kg were used in this study. Twenty live turtles, eight juveniles and 12 subadults, were used for the ultrasound proposal, and five dead juvenile turtles were used to provide the anatomical information. Turtle measurements were based on Bolten (1999). According to Pont and Alegre (2000), turtles with a SCLmin of 21-40 cm, and those with 41-65 cm were considered juvenile and subadults, respectively. Sex could not be identified because they were sexually immature specimens. All animals were accidentally caught in pelagic long-line sets and fishing nets along the northwestern Mediterranean coast (40°31'- 42°26' N and 0°32'-3°10' E), Spain, and were temporally housed in the rehabilitation facilities of the Rescue Centre for Marine Animals (CRAM), Premiá de Mar, Barcelona, Spain. Only turtles in good condition, based on physical, radiographic and haematological parameters, were used in this study. From the turtles captured in longlines, we included only those in which the hook was superficially attached in the buccal cavity.

During the ultrasonographic examinations, the animals were manually restrained in ventral recumbency on a bucket, high enough to avoid the limbs contacting the table. No sedation was necessary. The head, neck or limbs were extended as needed. Eyes were kept blind through a mask and the body surface was kept wet using a sopping towel. Ten soft-tissue areas of integument were used as acoustic windows: cervical- dorsal and cervical-ventral, left and right cervicobrachial, left and right axillary, left and right prefemoral and left and right postfemoral acoustic windows (Figure 1). Colour and pulsed doppler were applied in the large vessels. Ultrasonographic examinations were performed with a real-time, B-mode scanner (Computed Sonography Siemens 128XP/10, Acuson) using sector electronic transducers and frequencies of 4.0, 5.0 and 7.0 MHz. Coupling gel (Polaris II, GE Medical Systems, Leonhard Lang GmbH, Archenweg 56, A-6020; Innsbruck, Austria) was placed on the surface of the transducer, which was oriented mainly on the horizontal plane (the one oriented parallel to the plastron and carapace). Other planes were not used due to size limitations of the acoustic windows and transducer. Images were recorded using videotapes. Records of the ultrasound images were made with a thermal printer.

Anatomical sections were performed on three frozen turtles, each one in an oriented plane: sagital plane, frontal plane and transverse plane. Two other dead turtles were dissected to improve the morphological data. Anatomical terminology followed Wyneken (2001).

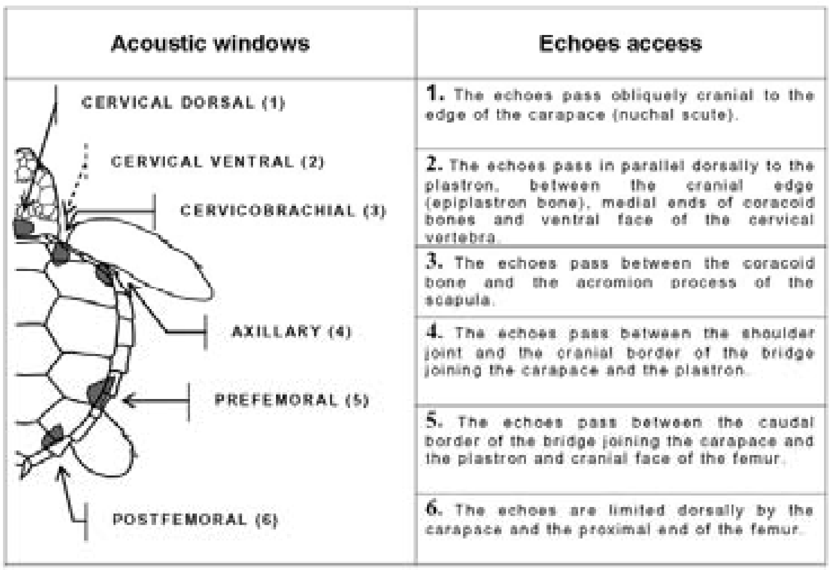

Figure 1. Acoustic-window and echo accesses used for the ultrasound scan of loggerhead sea turtles. The diagram shows only the right side

Results and Discussion

The fourth and fifth cervical vertebrae, the spinal cord, and the venous sinuses of the external jugular vein (also called cervical-dorsal sinus) were clearly seen in a transverse and transverse-oblique scan on the cervical-dorsal acoustic window (Figure 2, A-C). The ultrasonographic contour of the vertebrae was visible with echogenic borders followed by acoustic shadowing due to the strong reflection from the osseous tissue. The vertebral arch and the spinal cord were clearly recognized and could be used as landmarks to identify the right and left cervical-dorsal sinuses, which lay dorso-lateral to the vertebrae. The sinuses are broad dilatations of the external jugular vein (Figure 2, B-F) and were ultrasonographically identified as superficial, rounded, distensible hypo-echogenic structures connected to the venous vessels. The connection between left and right cervical sinuses was seen through the anastomosis with the vertebral vein, which lay centrally on the vertebral arch (Figure 2: B, D). The echoes of the circular blood flow inside the sinuses were sometimes visible. The dimensions of the sinuses were variable but, in general, relatively greater than those cited by Whitaker and Krum (1999). These authors stated that the dorsal-cervical sinus in 25-kg turtle was about 1 x 2 cm in a transverse section, while we found measurements of about 2.5 x 3.5 cm and 1.8 x 4.2 cm in a 26.8-kg and 58.5-cm SCLmin turtle, and in an 8.6-kg and 39- cm SCLmin turtle, respectively. The disparity could be related to different factors. Because reptiles are ectothermal animals, and the sinuses are vascular structures related to thermo-regulation, changes in their flow and dimensions are expected due to external temperature variation, as occurs in the front flippers (Hochscheid and others 2001). The turtles used in this study were scanned in the summer, and consequently underwent relatively high temperatures (25°C to 35°C) during the transportation and the procedure. Therefore, an increase in sinus size could be due to a vasodilatation response. Additionally, the inclination angle of the transverse oblique scan could also be related to the larger size found because of the longitudinally slanted section of the vessels, which could justify the greater length. On the other hand, compared to the anatomical sections, it was observed that the sinuses were not only a single dilation of the jugular vein, but also a complex of small cavities separated by fine membranous walls (Figure 2: D, F), which could not be completely visualized ultrasonographically.

Through the cervical-ventral acoustic window, the heart was dorso-ventrally flattened and located between the two hepatic lobes. The atria, during diastole, could be identified as oval anechogenic-paired structures with a fine echogenic wall (Figure 3, A). The ventricle had a homogenously echogenic appearance, with distinction of a thick wall with trabecular lining (Figure 3: A, B, D). Due to the slow heart rate, the echoes corresponding to blood flow and atrial diastole were easily recognized during ventricular systole. Only an atrioventricular valve was clearly seen as a short horizontal echogenic line centrally placed between the atria and ventricle. In juvenile specimens the best way to see the heart was the cervical-ventral acoustic window. Through this point, all three chambers and the large vessels on the cardiac base could be identified on a horizontal plane. By this access the scan usually passes along the dorsal aspect of the heart, where the pulmonary and subclavian arteries could be seen together with the aortic arches (Figure 3, A-D).

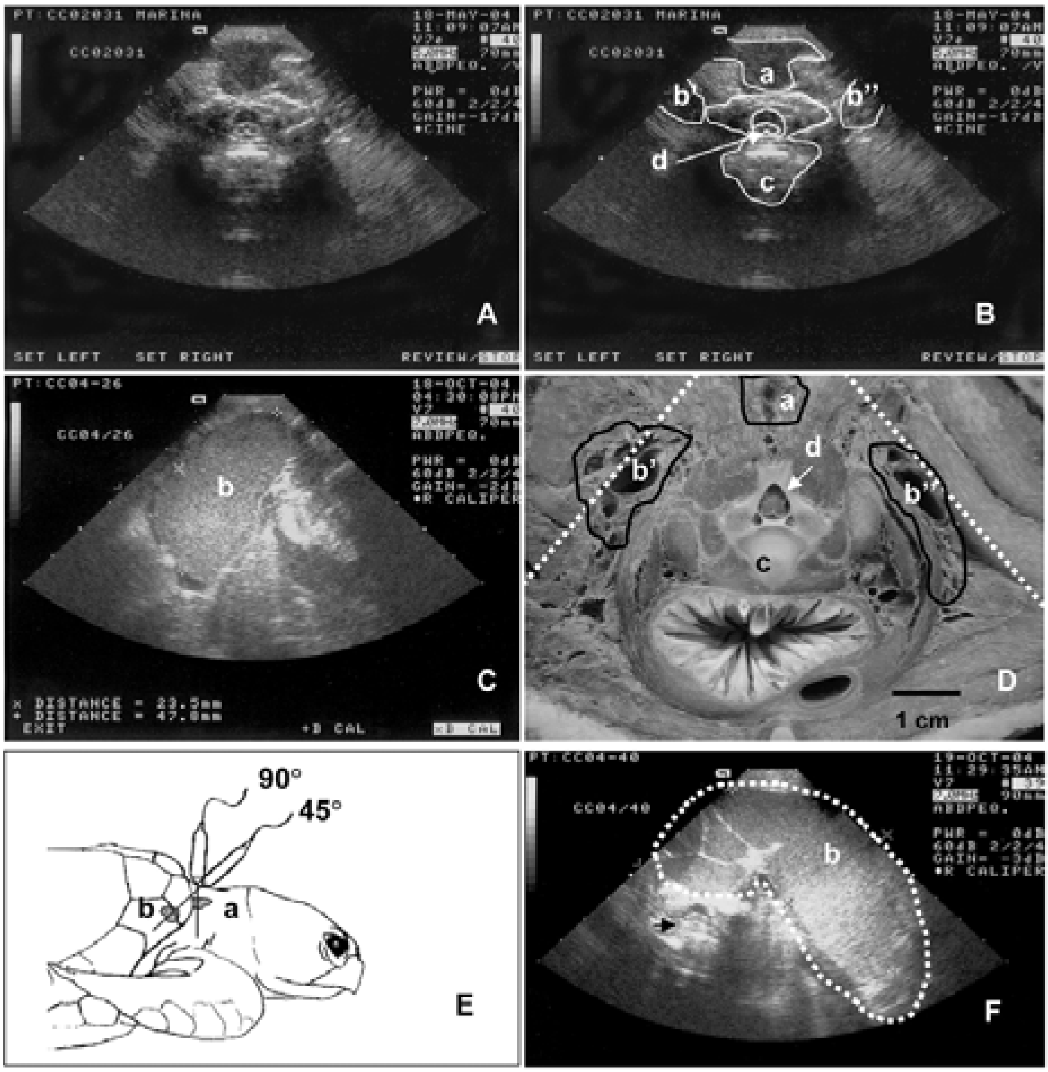

Figure 2: Ultrasound evaluation of the cervical-dorsal structures of the loggerhead sea turtle: a, vertebral vein, anastomosis point to transversal vein; b'-b'', sinuses of external jugular vein, c, vertebral body; d, spinal cord. A and B: Ultrasound images of a transversal scan. C: Ultrasound image of oblique scan of the venous cervical sinus (b) of the jugular vein. D: anatomical transversal cross-section corresponding to transversal scan. E: illustration showing the transversal and transversal oblique planes preferred for imaging of the cervical venous sinuses (a and b, sinues of the jugular vein). F: Ultrasound image of the complex of jugular sinuses seen in a 45° oblique scan, the black arrow indicates the cervical vertebra.

In subadult turtles, the right and left cervicobrachial acoustic windows allowed partial access to the heart and the complete visualisation of the right and left aortic arches and pulmonary arteries, respectively.

The distal end of the oesophagus could be seen through the ventral-cervical and left cervicobrachial acoustic windows as a coarse echogenic structure, identified as the keratinised papillae (Figure 4, A). Although recognised in the necropsies as a lobular structure tissue associated with the fat around the large cardiac vessels, the thymus was not clearly identified in this study due to the similar granular appearance of the esophagus.

The stomach was placed on the left side of the coelomic cavity. Although it could be partially seen in the left cervicobrachial, axillary and prefemoral acoustic windows, it was more frequently imaged through the left axillary acoustic window (Figure 4: B-C). A good landmark to locate this organ was the subscapular muscle seen in a horizontal scan as a hypoechogenic rounded structure followed by a fine echogenic line, the coelomic membrane (Figure 4: B - D). The stomach was usually seen dorsal to this muscle in an oblique dorsal scan (30°-35°).

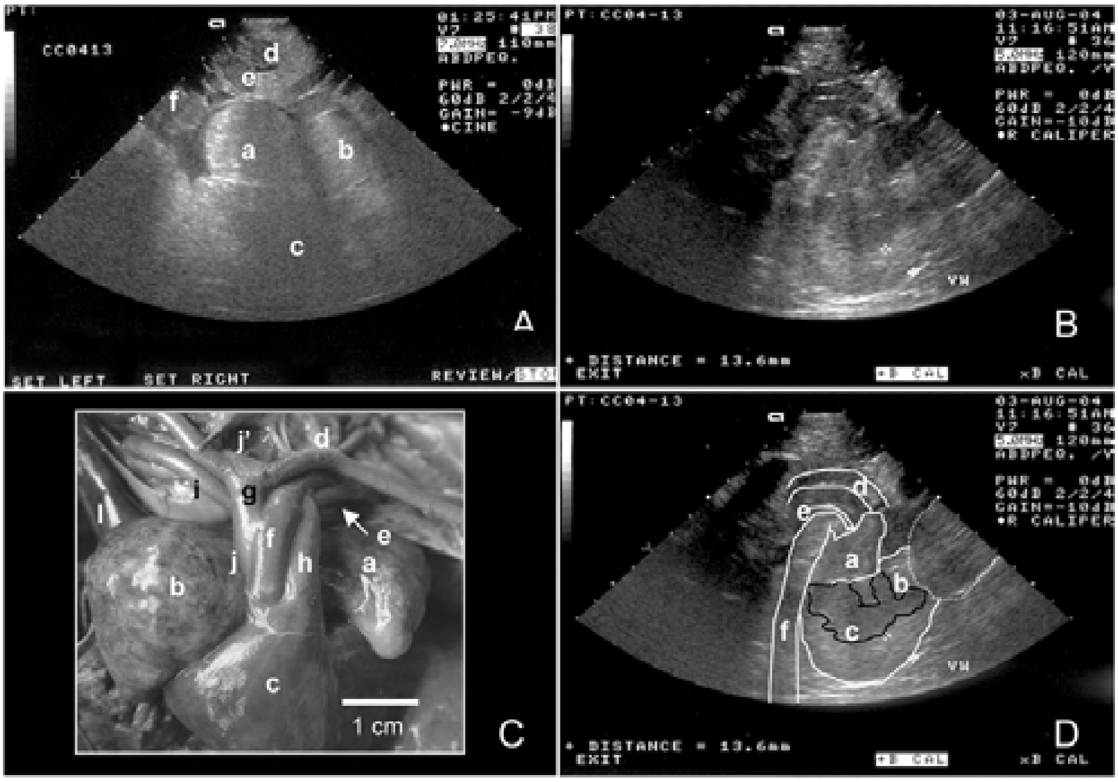

Figure 3: Ultrasonographic images of heart of the loggerhead sea turtle taken from cervical-ventral acoustic window: a, left atrium; b, right atrium; c, ventricle; d, left subclavian artery; e, left pulmonary artery; f, left aorta. A, B and D: Ultrasonographic image taken from cervical-ventral acoustic window. C: Ventral view of anatomical dissection of the heart of juvenile loggerhead sea turtle injected with latex, the right atrium is slighty dilated by the latex. A, left atrium; b, right atrium; c, ventricle; d, left subclavian artery; e, left pulmonary artery; f, left aorta; g, brachicephalic trunk; h, pulmonary trunk; i, right pulmonary artery; j, j', right aorta; l, right precava vein.

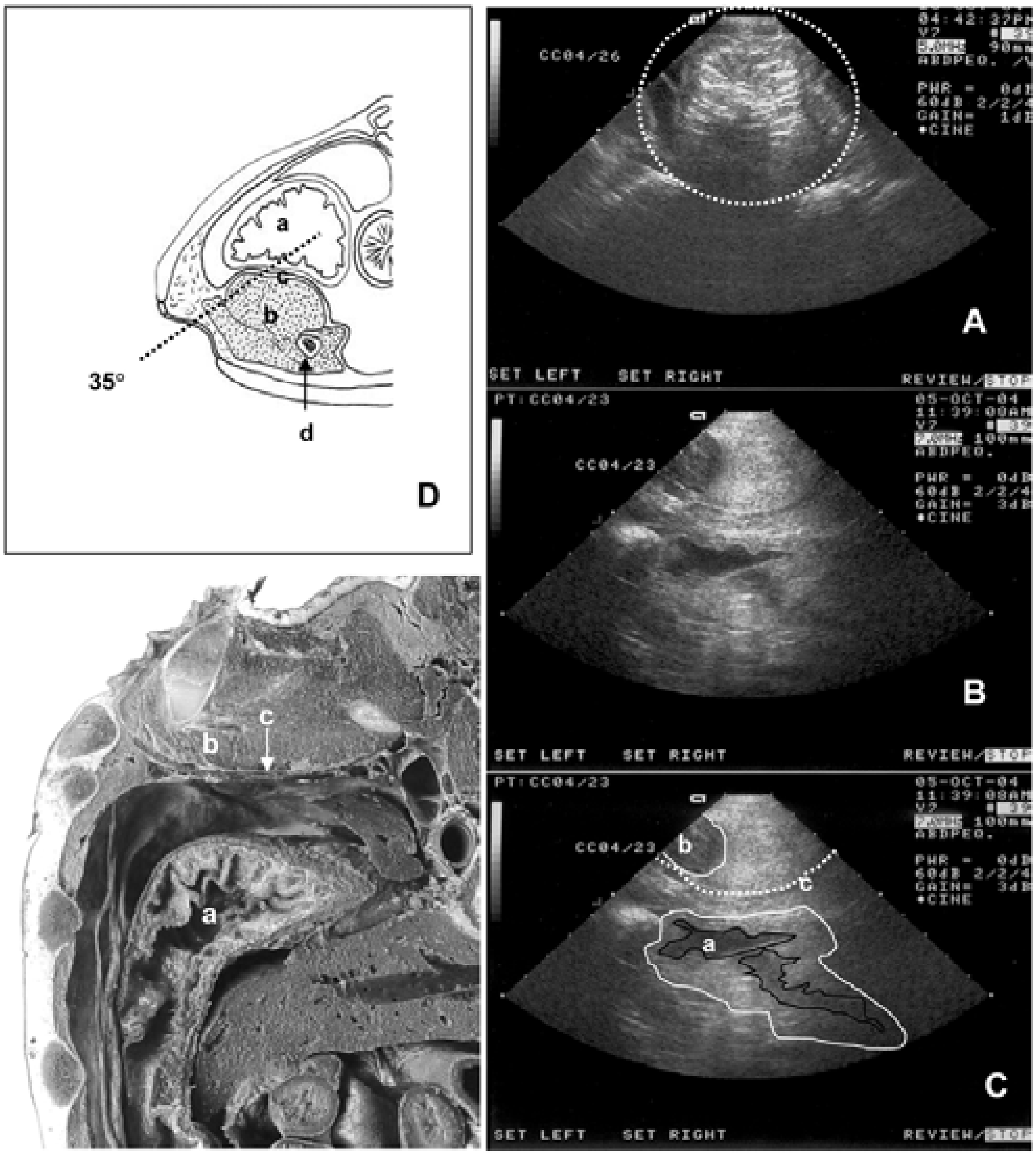

Figure 4: Ultrasound evaluation of the esophagus and stomach of the loggerhead sea turtle. A: Ultrasound image of esophagus, cross-section scan. B-C: Ultrasound image of stomach taken from left axillary acoustic window: a, stomach lumen; b, subscapular muscle; c, coelomic membrane. D: Illustration showing the oblique image plane preferred for imaging the stomach: a, stomach lumen; b, subscapular muscle; c, coelomic membrane; d, coracoid. E: Corresponding frontal gross anatomical seccion.

In general, the stomach showed a thin wall with folds seen as thin hypoechogenic lines, and produced poor images due to the presence of intraluminal gas and contents (Figure 4: B-C).

The liver was visualised as an echogenic structure with granular parenchyma (Figure 5, A). Hepatic vessels were seen as anechogenic tubular structures either in transverse or longitudinal sections (Figure 5, A). The best accesses to this organ were through the left and right axillary acoustic windows (Figure 5, B). The right axillary acoustic window was the one most indicated to see the gallbladder, which had an anechogenic spherical/oval appearance within the right hepatic lobe (Figure 5: A, C). The postcava (also called right hepatic vein) could be identified on entering the right atrium via the sinus venous valve (Figure 5, D) by this acoustic window.

Figure 5: Ultrasound evaluation of liver of the loggerhead sea turtle: A: Ultrasonographic image taken from right axillary acoustic windows: a, branches of right hepatic vein (Postcava); b, hepatic parenchyma; c, subscapular muscle, d, gallbladder. B: Corresponding frontal gross anatomical seccion: a, right hepatic vein; b, hepatic parenchyma; c, subscapular muscle; d, gallbladder; e, area of the right atrium; f, sinuses of jugular vein. C: Ultrasound image of the hepatic parenchyma: d, cross-section of the gallbladder. D: Ultrasound image of the liver and heart: a, right hepatic vein (Postcava); b, hepatic parenchyma; c, subscapular muscle; d, right atrium.

The large and small intestines could be seen in the prefemoral acoustic window from both sides. Loops of small intestine were more frequently imaged on the right side. The ultrasonographic image of the intestine was similar to that of mammals (Mattoon and others 2002), and stratification in five layers could be recognised. The wall of the small intestine was thicker than that of the large intestine (Figure 6, A-B). The serose and submucose layers were easily identified as echogenic lines. The muscular layer, between them, had a hypoechoic to anechoic appearance. The mucosa was the thickest hypoechoic layer (Figure 6, C). On the contrary, the wall of the large intestine did not have clearly distinguishable layers.

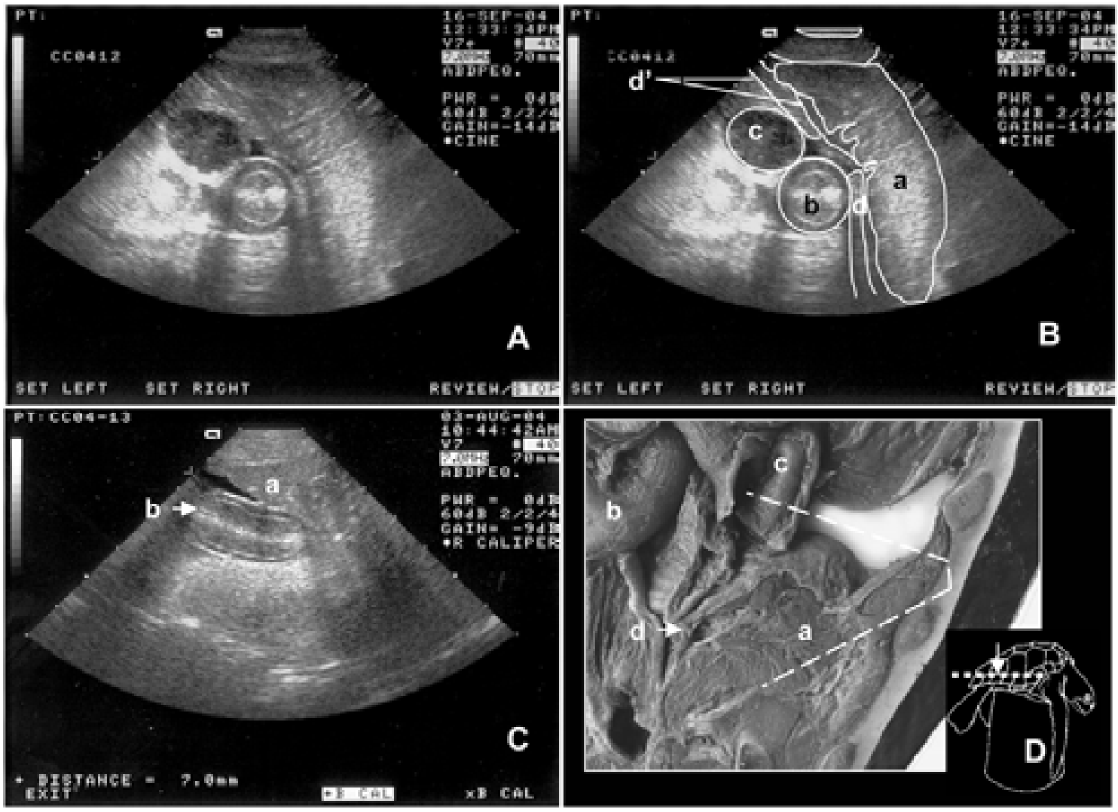

Figure 6: Ultrasound evaluation of the kidney and intestines of the loggerhead sea turtle. A-B: Ultrasonographic images taken from right prefemoral acoustic window: a, right kidney; b, cross-section of small intestine; c, cross-section of large intestine; d and d', blood supply of the kidney. C: Ultrasound image of the kidney (a) and longitudinal section of small intestine (b). D: Illustration showing dorsal view of the imaged area in a frontal anatomical section: a, kidney; b, loop of small intestine; c, section of large intestine; d, renal vein.

The kidneys were easily identified due to the intense renal vasculature, which could be used as a landmark. They could be imaged superficially from the prefemoral acoustic window (Figure 6, D) from the respective side, and showed a uniformly echogenic area, comma like, without a distinct renal pelvis and capsule. The great renal vein was easily seen, cranial to the kidney (Figure 6, A-B).

The urinary bladder could be seen, only when it was completely filled, as an anechoeic globular structure (Figure 7: A, C). It was better identified from the left prefemoral acoustic window (Figure 7, B). Echogenic dots were seen floating within and were considered normal. They could be related not only to the presence of urate crystals but also to parasites or fecal material, which could opportunistically enter as a result of its closed connection with the cloaca (Wyneken 2001). Vesical parasites were found in one of the three dissected turtles (unpublished data).

According to Wyneken (2001), sea turtles have two small, accessory urinary bladders connected to the urinary bladder, each located laterally to the neck of the urinary bladder and dorsal to the pubis. In this study, the neck of the urinary bladder could not be imaged due to the acoustic shadow of the pubic bone. These structures were not found in the gross-anatomy detailed dissections of our work (unpublished data).

The reproductive tract, the spleen, pancreas and adrenal glands could not be identified in this study. The pancreas extends as an irregular strip along the duodenum just past the stomach. The spleen has an oval form located below the pancreas. These organs were not ultrasonographically accessible due to their small size, midline location and the artifacts caused by intestinal loops surrounding them. They were also not documented in a previous study in California desert tortoises (*Xerobates agassizi*) (Penninck and others 1991).

The post-femoral acoustic windows allowed access to the caudal end of the kidney only in a few larger subadult turtles. In juvenile turtles just the femur and muscular mass could be imaged through this point, it was deemed inadequate for the ultrasonographic evaluation of any coelomic structures.

In recent decades ultrasound imaging has been frequently used to evaluate the reproductive status in many reptilian and mammalian species (Küchling 1989, Owens and Kraemer 1990, Casares and others 1997, Rostral and others 1998, Brook and others 2000, Brook and others 2004). Some species of reptiles are not sexually dimorphic, and in these cases the ultrasonographic imaging of the gonads is a reliable and inexpensive method to identify the sex of the animals and select them for reproductive programmes (Morris and Allison 1996). In general, the loggerhead sea turtle do not exhibit differentiated external sexual characteristics until they reach the adult size (SCL>65 cm), which occurs at more than 20 years old (Bjorndal and others 2001). This work reveals that sex identification in subadult turtles can not be performed using ultrasonographic imaging. The small non-developed gonads are mistaken for renal parenchyma, and the tubular structures, such as oviduct and deferent canals, are not visible. The same limitation was found in Kemp's Ridley sea turtles, where only ovarian follicles with sizes greater than 5 mm in diameter, and oviducts with eggs, were ultrasonographically recognised (Rostal and others 1990).

Knowledge of normal anatomy is essential for the interpretation of diagnostic techniques. Chelonians have well-protected internal viscera, and the few body parts not covered by the carapace or plastron are internally limited by the bone of the proximal end of the limbs (scapular and pelvic girdles), which usually limit scanning to one plane. Poor image quality could also be a consequence of the great size of the turtle in relation to the transducer frequency, the amount of fat tissue and the degree of emptiness of the gastrointestinal tract. High-frequency transducers used in this study (7 MHz) were suitable to assess in detail superficial structures like the cervical venous sinuses, stomach, intestines and kidneys. In juvenile turtles, this probe displayed good images of the kidneys and the heart when the latter was seen through the cervical- ventral acoustic window. In subadult animals the transducer of 5MHz was more frequently used, and it allowed a good balance between penetration and resolution. The transducer of 4MHz was used infrequently because of its low resolution. Due to the direct access of the kidneys in the prefemoral acoustic windows, as in other chelonian species, this point could be used to perform ultrasound-guided biopsies of this organ. The hepatic and renal parenchymas were easily imaged and could be evaluated for morphologic alteration in shape and size, as well as for the presence of neoplasia, cysts, abscesses and papillomas.

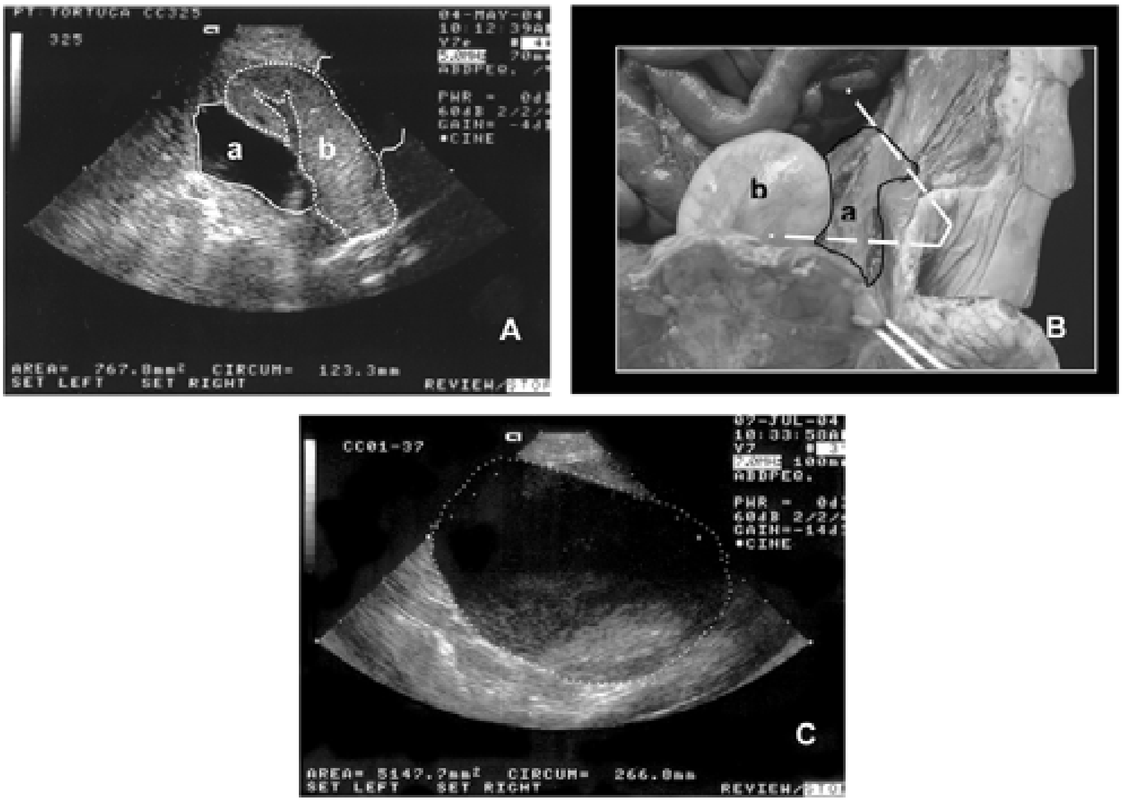

Figure 7: Ultrasound evaluation of the kidney and urinary bladder of the loggerhead sea turtle. A: Ultrasonographic image of urinary bladder (a) and kidney (b). B: Corresponding gross anatomy of the scanned area. C: Full urinary bladder with echogenic dots.

Due to the slow digestive transit time, the presence of food in the gastrointestinal tract in turtles with a fasting period of 24 to 48h produced multiple artifacts and poor images, mainly of the stomach. Concerning the digestive tract, the diagnosis of obstructive processes due to garbage ingestion or severe mucosal damage caused by fishing hooks (accordion effect) could also be possible.

Although it is known in mammals that low-level echoes are returned from fat in certain areas of the body (Nyland and others 2002), low-resolution images are also obtained from some fat turtles, mainly using the cervicobrachial acoustic windows.

This study shows that ultrasonography can be a useful tool for the diagnosis of different internal lesions in juvenile and subadult loggerhead sea turtles. It is inexpensive, safe and easy to use and with practice, most of the internal organs can be located and examined.

Acknowledgements

The authors would like to thank DVM Rosa Novellas and the CRAM volunteers for their help in this work. The English of this manuscript had been corrected by a native English-speaking instructor of English of this University. We also would like to thank the anonymous reviewers.

References

AGUILAR, R. & PASTOR, X. (1995) Impact of Spanish swordfish longline fisheries on the Loggerhead Sea Turtle, *Caretta caretta*, population in the Western Mediterranean. Proceedings of the Twelfth Annual Symposium on Sea Turtle Biology and Conservation. NOAA Technical Memorandum NMFS-SEFSC 361, Georgia, February 25 to 29, 1992. pp. 1-6.

BJORNDAL, K.A., BOLTEN, A.B., KOIKE, B., SCHROEDER, B.A., SHAVER, D.J., TEAS, W.G. & WITZELL, W.W. (2001) Somatic growth function for immature loggerhead sea turtles, *Caretta caretta*, in Southeastern U.S. waters. *Fishery Bulletin* 99: 240-246.

BOLTEN, A. (1999) Techniques for measuring sea turtles. Research and manangement techniques for the conservation of sea turtles. In: IUCN/SSC Marine Specialist Group Publication (4). Eds K. L. Eckert, K. A. Bjorndal, F. A. Abreu-Grobois and M. Donnelly. pp 1-5.
http://www.iucn-mtsg.org/Publications/Tech_Manual/Tech_Manual_en/18-bolten.pdf. Accessed February, 2006.

BROOK, F. M., KINOSHITA, R., BROWN, B. & METREWELI, C. (2000) Ultrasonographic imaging of the testis and epididymis of the bottlenose dolphin, *Tursiops truncatus aduncus*. *Journal of Reproduction and Fertility* 119, 233-240.

BROOK, F, LIM, E.H.T., CHUA, F.H.C. & MACKAY, B. (2004) Assessment of the reproductive cycle of the Indopacific Humpback dolphin, *Sousa chinensis*, using ultrasonography. *Aquatic Mammals* 30, 137-148.

CASARES, M., RÜBEL, A. & HONEGGER, R.E. (1997) Observations on the female reproductive cycle of captive Giant Tortoises (*Geochelone* spp.) using ultrasound scanning. *Journal of Zoo and Wildlife Medicine* 28, 267-273.

GAUDRON, C., LIGNEREUX, Y. & DUCOS DE LAHITTE, J. (2001) Imagerie médicale appliquée à l`anatomie clinique des chéloniens en consultation. Proceedings of the Internacional Congreso on *Testudo* Genus. Toulouse, March 7-10. pp161-182.

HOCHSCHEID, S., BENTIVEGNA, F. & SPEAKMAN, J.R. (2002) Regional Blood Flow in Sea Turtles: Implications for Heat Exchange in an Aquatic Ectotherm. *Physiological and Biochemical Zoology* 75, 66.

IUCN (2004) Red List of Threatened Species.www.iucnredlist.org. Accessed February 22, 2006.

KÜCHLING, G. (1989) Assessment of ovarian follicles and oviductal eggs by ultrasound scanning in live freshwater turtles, *Chelodina oblonga*. *Herpetologica* 45, 89-94.

MARTORELL, J., ESPADA, Y. & RUIZ DE GOPEGUI, R. (2004) Normal echoanatomy of the Red-eared slider terrapin (*Trachemys scripta elegans*). *Veterinary Record* 155, 417-420.

MATTOON, J.S., AULD, D.M. & NYLAND, T.G. (2002) Abdominal ultrasound scanning techniques. In: Small Animal Diagnostic Ultrasound. 2nd edn. Ed. Thomas G. Nyland. Philadelphia, W.B. Saunder Co. pp 49-81.

MORRIS, P. J. & ALLISON, A.C. (1996) Determination of sex in White-throated monitors (*Varanus albigularis*), Gila monsters (*Heloderma suspectum*), and Beaded Lizards (*H. horridum*) using two-dimensional ultrasound imaging. *Journal of Zoo and Wildlife Medicine* 27, 371-377.

NYLAND, T. G., MATTON, J.S., HERRGESELL, E. J. & WISNER, E. R. (2002) Physical principles, instrumentation, and safety of diagnostic ultrasound. *In*: Small Animal Diagnostic Ultrasound. 2nd edn. Ed. T.G. Nyland. Philadelphia, W.B. Saunder Co. pp 1-18.

OWENS, W. & KRAEMER, D.C. (1990) Ultrasound imaging of reproductive organs and eggs in Galapagos tortoises, *Geochelone elephantopus* spp. *Zoo Biology* 9, 349-359.

PENNINCK, D.G., STEWART, J.S., PAUL-MURPHY, J. & PION, P. (1991) Ultrasonography of the California Desert Tortoise (*Xerobates agassizi*): Anatomy and Application. *Veterinary Radiology* 32, 112-116.

PONT, S.G. & ALEGRE, F. N. (2000) Work of the Foundation for the Conservation and Recovery of Marine Life. *Marine Turtle Newsletter* 87, 5-7.

ROSTAL, D., KALB, H., GRUMBLES, J., PLOTKIN, P. & OWENS, D. (1994) Application of ultrasonography to sea turtle reproduction. Proceedings of the Fourteenth Annual Symposium on Sea Turtle Biology and Conservation. NOAA Technical Memorandum NMFS-SEFSC 351, Texas, March 1 to 5, 1994. p181.

ROSTAL, D.C, OWENS, D. W., GLUMBLES, J.S., MACKENZIE, D. & AMOSS JR., M. S. (1998) Seasonal reproductive cycle of the Kemp’s Ridley sea turtle (*Lepidochelys kempi*). *General and Comparative Endocrinology* 109, 232-243.

ROSTAL, D.C., ROBECK, T. R., OWENS, D.W. & KRAEMER, D.C. (1990) Ultrasound imaging of ovaries and eggs in Kemp’s Ridley Sea turtles (*Lepidochelys kempi*). *Journal of Zoo and Wildlife Medicine* 21, 27-35.

ROSTAL, D., ROBECK, T., OWENS, D., LOUIS, E. & KRAEMER, D. (1989) Ultrasonic imaging of ovaries and eggs in sea turtles. Proceedings of the Ninth Annual Symposium on Sea Turtle Biology and Conservation. NOAA Technical Memorandum NMFS-SEFC 232, Georgia, February 7 to 11, 1989. p 257-258.

SAINSBURY, A.W. & GILI, C. (1991) Ultrasonographic anatomy and scanning technique of the coelomic organs of the Bosc monitor (*Varanus exanthermaticus*). *Journal of Zoo and Wildlife Medicine* 22, 421-433.

SCHUMACHER, J. & TOAL, R.L. (2001) Advanced Radiography and Ultrasonography in Reptiles. *Seminars in Avian and Exotic Pet Medicine* 10, 162-168.

SILVERMAN, S. & JANSSEN, D. (1996) Diagnostic Imaging. In: Reptile Medicine and Surgery. Ed. D. R. Mader. Philadelphia, W.B. Saunders Co. pp 258-264

WHITAKER, B.R. & KRUM, H. (1999) Medical Management of sea turtles in aquaria. In: Zoo and Wild Animal Medicine – Currently therapy, 4rd edn. Eds M. E. Fowller, E. Miller. Philadelphia, W. B. Saunders Co. pp 217-231.

WILKINSON, R., HERNANDEZ-DIVERS, S., LAFORTUNE, M., CALVERT, I., GUMPENBERGER, M. & MCARTHUR, S. (2004) Diagnostic Imaging. In: Medicine and Surgery of tortoises and turtles. Eds S. MCarthur, R. Wilkinson and J. Meyer. Victoria, Blackwell Publishing Ltd. pp187-238.

WYNEKEN, J. (2001) The Anatomy of Sea Turtles. NOAA Technical Memorandum NMFS-SEFSC 470. Miami, U.S. Departament of Commerce, 1-172.

4.4. COMPUTED TOMOGRAPHY OF THE VERTEBRAL COLUMN AND COELOMIC STRUCTURES IN THE NORMAL LOGGERHEAD SEA TURTLE (CARETTA CARETTA)

Valente, A.L.; Cuenca, R.; Zamora, M.A.; Parga, M.L.; Lavín, S.; Alegre, F. y Marco, I. (2006). Computed tomography of the vertebral column and coelomic structures in the normal loggerhead sea turtle (*Caretta caretta*). Vet. J. (2006), doi: 10.1016/j.tvjl.2006.08.018.

ARTICLE IN PRESS

Available online at www.sciencedirect.com

ScienceDirect

ELSEVIER

The Veterinary Journal xxx (2006) xxx–xxx

The Veterinary Journal

www.elsevier.com/locate/tvjl

Computed tomography of the vertebral column and coelomic structures in the normal loggerhead sea turtle (*Caretta caretta*)

A.L.S. Valente [a,*], R. Cuenca [a], M. Zamora [b], M.L. Parga [c], S. Lavin [a], F. Alegre [c], I. Marco [a]

[a] *Servei d'Ecopatologia de Fauna Salvatge, Facultat de Veterinària, Universitat Autònoma de Barcelona, 08193 Bellaterra, Barcelona, Spain*
[b] *Diagnosis Mèdica, Còrcega, 345 Barcelona, Spain*
[c] *Centre de Recuperació d'Animals Marins, Camí Ral, 239 08330 Premià de Mar, Barcelona, Spain*

Accepted 31 August 2006

Abstract

The aim of this study was to determine the normal computed tomography (CT) appearance of the vertebral column and coelomic structures of the loggerhead sea turtle (*Caretta caretta*) and to use three-dimensional (3D) and multiplanar reconstructions to indicate the position of each organ in relation to the vertebrae and carapace. Transverse sections of 1 mm thickness were performed in seven clinically healthy and in five dead loggerhead sea turtles using multi-detector CT equipment. A computer workstation was used for multiplanar and 3D reconstructions. Dead turtles were frozen and sectioned in the transverse, dorsal and sagittal planes to compare the anatomical structures' appearance with CT images. Clinically relevant organs including the oesophagus, stomach, trachea, bronchi, lungs, liver, gallbladder, heart, spleen, kidneys and vertebral canal were identified in CT images. Computed tomography provides detailed information on the respiratory system and skeleton; the location of the coelomic structures with respect to the carapace and the vertebrae that is provided in this work will facilitate the use of other ancillary diagnostic techniques such as ultrasound, radiography and biopsy, thereby improving safety of access in surgical procedures.

Keywords: Computed tomography; Diagnostic imaging; Cross-sectional anatomy; Chelonians; Three-dimensional reconstruction

1. Introduction

At marine animal rehabilitation centres, sea turtles are often admitted with traumatic and pulmonary disorders (Pont and Alegre, 2000; Orós et al., 2005). Most traumatic problems affect the flippers or the carapace and are mainly due to entrapment in fishing nets and collision with boat propellers. Due to the dorsal position of the lungs, which are in close contact with the carapace, pulmonary disease often occurs secondary to traumatic injuries of the carapace (Orós et al., 2005).

In sea turtles the axial skeleton is composed of the carapace, plastron bones, vertebrae, ribs and derivatives of the ribs (Wyneken, 2001). The carapace is formed by the scutes which form the outermost layer of the shell and by the bony plates which are the main structural components of the shell. The multiple scutes overlap the bony plates (neural, pleural and peripheral bones) which are fused with the vertebrae or ribs forming a single carapace bone. Neural bones are those that cover the vertebral column. Pleural bones are formed by the ribs and their dermal (ossified) extensions, and the peripheral bones form the margin of the carapace. In most lung disorders and shell or skeletal injuries in the turtle, plain radiographic data do not reveal the extent of complex fractures due to superimposed bone structures (Abou-Madi et al., 2004).

Compared with conventional radiography, computed tomography (CT) allows better distinction of specific tissue densities and discrete changes in organ size, shape, margin

* Corresponding author. Tel.: +34 93 581 19 23; fax: +34 93 581 20 06. *E-mail address:* schifinoval@hotmail.com (A.L.S. Valente).

1090-0233/$ - see front matter © 2006 Elsevier Ltd. All rights reserved.
doi:10.1016/j.tvjl.2006.08.018

Please cite this article in press as: Valente, A.L.S. et al., Computed tomography of the vertebral column and coelomic ..., Vet. J. (2006), doi:10.1016/j.tvjl.2006.08.018

contour and position (Gaudron et al., 2001). Computed tomography is a non-invasive, cross-sectional diagnostic imaging technique that offers significant advantages for detection of pathologies in chelonians, and is ideal for diagnosing skeletal and soft tissue abnormalities (Gumpenberger and Henninger, 2001).

Multi-detector Computed Tomography (MDCT) technology has rapidly and drastically changed the way CT has been used in recent years. By using multiple rows of detector arrays instead of a single detector, MDCT can produce highly accurate three-dimensional (3D) volume data sets allowing reconstruction of the total body, tracheo-bronchial and pulmonary volume rendering, virtual bronchoscopy and colonoscopy, and volumetric reconstruction of the skeleton. In addition, MDCT provides faster and more detailed scanning results, an important consideration in wild animals (ASIH/HL/SSAR, 2001) as it minimizes the deleterious effects of prolonged sedation or physical restraint. Although due to its cost it is not used routinely in veterinary medicine, it is important to recognize that the amount of information it provides in a short-time period may justify its use in endangered species.

Although some publications on CT in other chelonians exist (Gumpenberger and Henninger, 2001; Raiti and Haramati, 1997; Raiti, 1998; Wilkinson et al., 2004; Wyneken et al., 2000), to the authors' knowledge there is only one CT study on the head of the loggerhead sea turtle (Arencibia et al., 2005). No published data concerning the use of CT in the coelomic cavity of this species were found.

Accurate interpretation of multiplanar and 3D CT images of the loggerhead sea turtle requires comparative cross-sectional anatomy images of this species. The purpose of this study was to provide normal CT images of the vertebral column and coelomic structures of the loggerhead sea turtle (*Caretta caretta*), thereby establishing reference standards for organ size and position in this species, and to provide images of virtual tracheo-bronchoscopy and 3D reconstructions of the respiratory tract and bone structures. In the present study we used a combination of CT imaging and gross anatomical sections that allowed accurate identification of the anatomical structures.

2. Materials and methods

Computed tomography was performed in 12 loggerhead sea turtles (seven live: juvenile; and five dead: four juvenile and one subadult). All turtles were accidentally caught in pelagic long line sets and fishing nets off the north-western Mediterranean coast (40°31′–42°26′N and 0°32′–3°10′E) of Spain, and were temporally housed in the rehabilitation facilities of the Rescue Centre for Marine Animals (CRAM), in Premià de Mar, Barcelona, Spain. Only clinically normal animals were included in this study. Dead turtles were kept frozen until the examination and were thawed 24–48 h before the CT procedure, depending on their size.

Live turtles were anaesthetized with a combination of ketamine (15 mg/kg, Imalgene 1000, Merial) and diazepam (0.5 mg/kg, diazepam, Almirall Proderfarma), injected intravenously in the dorsal cervical sinus to avoid head and flipper movement. Cardiac frequency was verified using a mini-doppler (Doppler High Sensitivity Pocket Doppler D900, Huntleigh Healthcare Ltd.) and the animals were carefully kept wet prior to the scan. No intravenously or orally administered contrast material was used, and all animals were positioned in ventral recumbency for the examination.

Computed tomography of the vertebral column and coelomic structures were obtained by a 16-detector row CT scanner (Aquilion 16, Toshiba Medical) using the following parameters: 120 kVp, 250 mA, 16 × 1 mm detector configuration and a 512 × 512 matrix. The field of view ranged from 35 to 52 cm and total examination time was from 10 to 15 s, depending on the size of the turtle. The volumetric reconstruction of image sections with a 1 mm slice width and interval of 0.8 mm were performed. Although the original MDCT sections were taken using 1 mm thickness, better images were obtained after manipulation and adjusting to sections of 4 mm. Multiplanar reformatted images and 3D volume-rendered images were generated on a Vitrea computer workstation (Vitrea version 3.0.1., Vital Images). We used bone and parenchymal filters to improve contrast between the different structures.

In order to carry out the anatomical study and establish a comparison with the MDCT images, the previously scanned dead turtles were placed in individual right-angled polystyrene boxes and these were filled with tap water. The boxes with the cadavers were refrozen at −80 °C for at least 24 h before anatomical sectioning. The turtles were sectioned in a pre-determined plane: transverse, dorsal or sagittal. Serial parallel slices from 18 to 20 mm thickness were obtained using an electric bone saw. Slices were immediately washed with 80% ethanol to eliminate frost build-up and to remove debris, and separated by grids. After labelling, the frozen slices were embedded for 30 min in neutral-buffered 10% formalin solution for thawing. For recording of the fresh surface, a digital high-resolution, 2560 × 1920 pixels camera (Digital Still Camera, Sony DSC-F707, Sony Corporation) was used in daylight. Further transformations of the images such as rotation, scaling, cutting, filtering, and corrections to contrast, brightness and colour were performed with Adobe Photoshop (v 5.5). For each anatomical slice, a corresponding CT image was chosen, and identifiable anatomical structures were labelled on the cadaver sections and on the corresponding CT images. The terminology applied to the anatomical structures corresponded to that of the *Nomina Anatomica Veterinaria*; however, specific terminology for sea turtles (Wyneken, 2001) was also applied.

3. Results

With regard to skeletal structures, multiplanar sagittal reconstruction of the vertebral column permitted evaluation of the vertebrae and the vertebral canal, which was wider in the cervical region than in the other regions of the vertebral column (Fig. 1). The lateral and ventral views of the 3D volume rendering of the vertebral column showed the morphology and arrangement of the vertebrae (Fig. 1). Eight cervical vertebrae were identified (Fig. 1). The ventral part of the atlas was clearly seen in the sagittal multiplanar reconstruction of the vertebral column (Fig. 1).

The intervertebral foramina were easily recognizable in the cervical region being greatest between the seventh and eighth vertebrae (Fig. 1). In the dorsal region, these foramina were not seen between the vertebral arches but rather, as a series of large foramina positioned dorsally and centrally relative to the vertebral bodies, between the vertebral arch and their respective neural bones (Fig. 1) being the exit of the spinal nerve roots from the vertebral canal (Fig. 2). From the ninth dorsal vertebra caudally, the intervertebral foramina reappeared between the vertebral arches (Fig. 2).

The intervertebral space was broad in the cervical region and decreased caudally, becoming almost unrecognizable between the 7th and 10th dorsal vertebrae. Between the 10th dorsal and first sacral vertebra the space was again visible (Figs. 1 and 2). The first dorsal vertebra and the 8–10th dorsal vertebra all had a short body (Fig. 1). The scapula was attached to the first pleural bone immediately cranial to the first pair of ribs, where a non-ossified area was seen in the carapace of a small juvenile turtle (Fig. 2). From the three sacral vertebrae, only the first two were attached to the ileum (Fig. 2). The bodies of the caudal vertebrae showed a thick cartilaginous plug on each end; these vertebrae varied in number, ranging from 13 to 17 vertebrae. The arches and processes also became progressively shorter (Fig. 2).

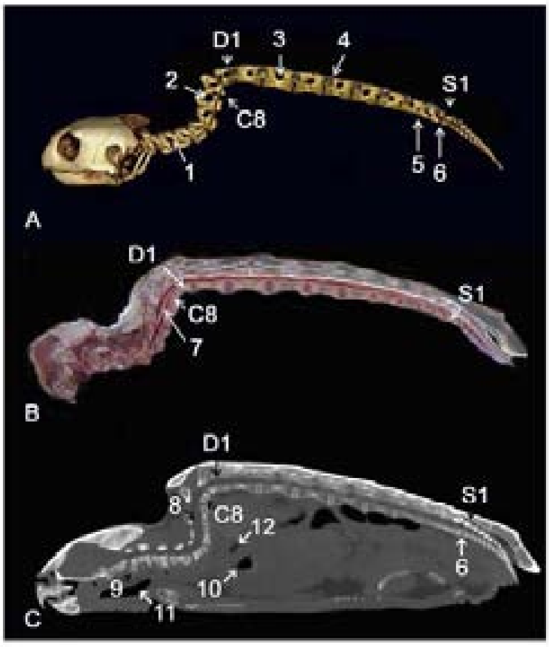

Fig. 1. (A) 3D CT reconstruction, (B) sagittal gross anatomical section and (C) CT multiplanar reconstruction (sagittal plane) of the vertebral column of a juvenile loggerhead sea turtle. A: 1 and 2, intervertebral foramina in the cervical vertebrae; 3, intervertebral foramina in the dorsal vertebrae; 4, costovertebral joint (costocentral joint); 5 and 6, intervertebral spaces. C8: 8th cervical vertebra; D1, 1st dorsal vertebra; S1, 1st sacral vertebra. B: 7, vertebral canal and spinal cord. C: 8, cervical vertebral canal; 9, ventral portion of the atlas; 10, transverse section of the left bronchus; 11, trachea; 12, oesophageallumen.

Clinically relevant organs and anatomical structures including the oesophagus, stomach, trachea, bronchi, lungs, liver, gallbladder, heart, spleen and kidneys were identified in the CT images with the aid of the anatomical sections. The normal appearance and position of the coelomic organs identified on the MDCT images and their relation to the carapace and the vertebral column are indicated in Figs. 3 and 4.

The ventral view of the whole body 3D reconstruction indicating the cranial and caudal border of the heart showed that this organ is located in an area not protected by the plastron bones (Fig. 3).

The liver lobes could be distinguished in the CT images in all sections, but the distinction between the hepatic parenchyma and pectoral musculature was not clear due to lack of contrast (Fig. 3). It was possible to identify the gallbladder in the transverse and dorsal sections (Fig. 3).

The trachea and oesophagus were easily recognizable. The trachea was observed ventral and to the right of the oesophagus and maintained this position from the level of the second to the fourth cervical vertebra (Fig. 5). The carina was seen at the level of the first dorsal vertebra (Fig. 5). When evaluated using virtual bronchoscopy, the tracheal mucosa was seen to have a smooth surface (Fig. 5). The extra and intrapulmonary parts of the bronchi were identified clearly in the 3D pulmonary rendering (Fig. 6). The external part of the left bronchus crossed ventrally to the oesophagus (Fig. 1).

The morphology of the lungs, bronchi and pulmonary blood vessels could be distinguished, and the central intrapulmonary bronchus was clearly seen in the transverse sections (Fig. 6). Each central bronchus extended dorsally and longitudinally into the lung, and had numerous airways extending from it (Fig. 7). The lungs were not lobed (Figs. 6 and 7), and the pulmonary parenchyma was strongly reticulated (Fig. 8). Large vessels such as the aorta and the vena cava could not be identified in the mediastinal space as they are usually seen in mammalian species. Two large pulmonary blood vessels around the central bronchus could be identified in all sections. They extended longitudinally parallel to the bronchus (Fig. 7). The pulmonary artery and vein were identified histologically dorsal and ventral to the central bronchus, respectively (Fig. 6).

Only the external silhouette of the kidneys was identifiable, immediately caudal to the lungs, in the transverse section (Fig. 9).

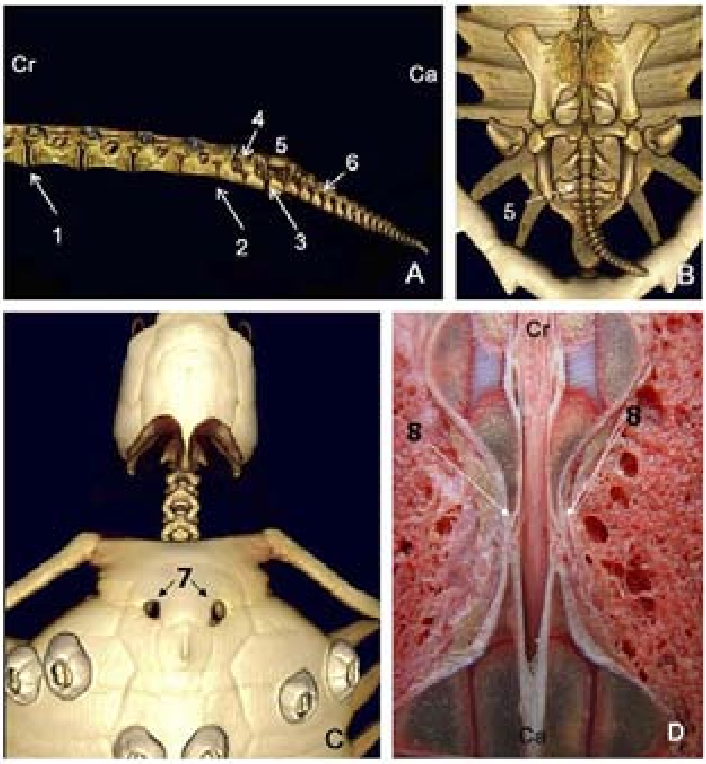

Fig. 2. (A) Lateral and (B) ventral views of 3D CT reconstructions of the vertebral column (sacral and caudal regions), (C) dorsal views of the 3D CT reconstructed carapace and (D) dorsal gross anatomical section of a juvenile loggerhead sea turtle. 1, intervertebral space between the 4th and 5th dorsal vertebrae; 2, intervertebral space between the 8th and 9th dorsal vertebrae; 3, intervertebral space between the 10th dorsal vertebra and 1st sacral vertebra; 4, intervertebral foramen placed between the vertebral arches; 5, 1st sacral vertebra; 6, caudal vertebrae; 7, non-ossified area in the carapace; 8, root of spinal nerves.

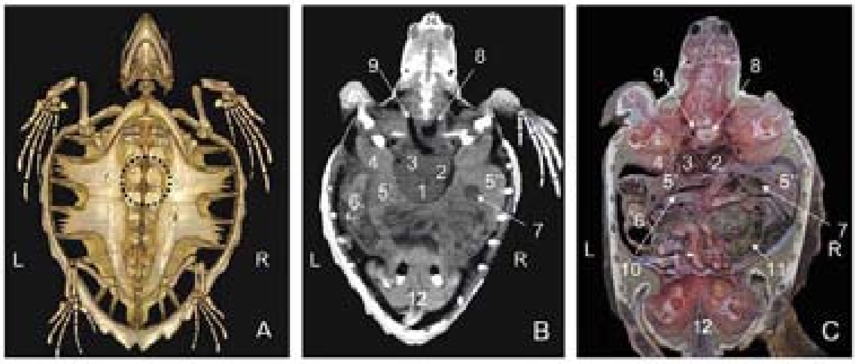

Fig. 3. (A) Ventral view of the skeleton 3D CT reconstruction, (B) multiplanar CT reconstruction (dorsal plane – soft-tissue window) and (C) dorsal gross anatomical section of a juvenile loggerhead sea turtle. A: Indicated area corresponds to the cardiac region. B and C: 1, ventricle; 2, right atrium; 3, left atrium; 4, pectoral musculature; 5′ and 5″ left and right hepatic lobes, respectively; 6, stomach; 7, gallbladder; 8, oesophagus; 9, trachea; 10, small intestine; 11, large intestine; 12, rectum.

4. Discussion

Computed tomography and 3D reconstruction have a role in the diagnosis of a wide range of diseases in a variety of animals (Garland et al., 2002). In our study the 3D volume rendering of the skeleton allowed a clear view of the arrangement of the structures in their natural position. The turtles were sedated because the CT examination was

Please cite this article in press as: Valente, A.L.S. et al., Computed tomography of the vertebral column and coelomic ..., Vet. J. (2006), doi:10.1016/j.tvjl.2006.08.018

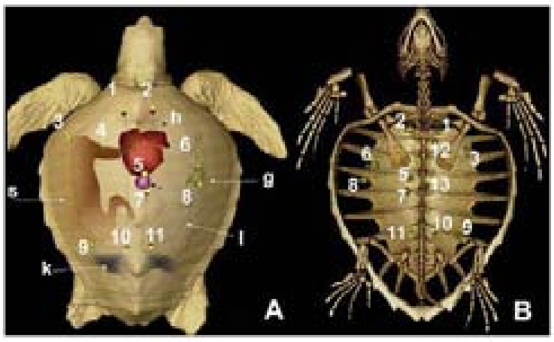

Fig. 4. (A) Dorsal and (B) ventral view of 3D CT reconstructions of the skeleton (plastron bones were removed in B) of a juvenile loggerhead sea turtle. Dots indicate the limits of each organ. 1, 2 cranial borders of the lungs; 3, cranial border of the stomach; 4, position of the cardia (seen only in A); 5, cranial border of the spleen; 6, cranial border of the gallbladder; 7, caudal border of the spleen; 8, caudal border of the gallbladder; 9, caudal border of the stomach; 10 11, caudal border of the lungs; 12, 13 cranial and caudal border of the heart, respectively (seen only in B). Stomach (s), lungs (l), heart (h), spleen (sp), gallbladder (g) and kidneys (k) were illustrated in A.

preceded by another diagnostic imaging procedure. However, considering the short time (10–15 s) required for a turtle examination we believe that this procedure could be carried out without chemical restraint.

The presence of an "intervertebral foramen" located dorsal to each vertebral body, from the 1st to the 8th dorsal vertebra instead of between the neural arches of adjacent vertebra seems a peculiarity of chelonians, since in this group of reptiles the neural arches are directly fused and the nerve roots do not exit via the intercentral joints (between the vertebral bodies) as they do in mammals. Differences in width of the intervertebral space seemed to be related to the shape of the vertebral centra and how they are joined to each other. The shapes of articulating surfaces at the ends of the vertebral centra of reptiles are of evolutionary and functional importance (Gaffney, 1990). We have found cervical vertebra of the loggerhead sea turtle to be predominately *procoelus* (the front of the *centrum* is concave and the rear of the *centrum* is convex) whereas the dorsal ones seemed to be weakly *amphicoelus*. In *amphicoelous* vertebrae the cranial and caudal ends of the cen-

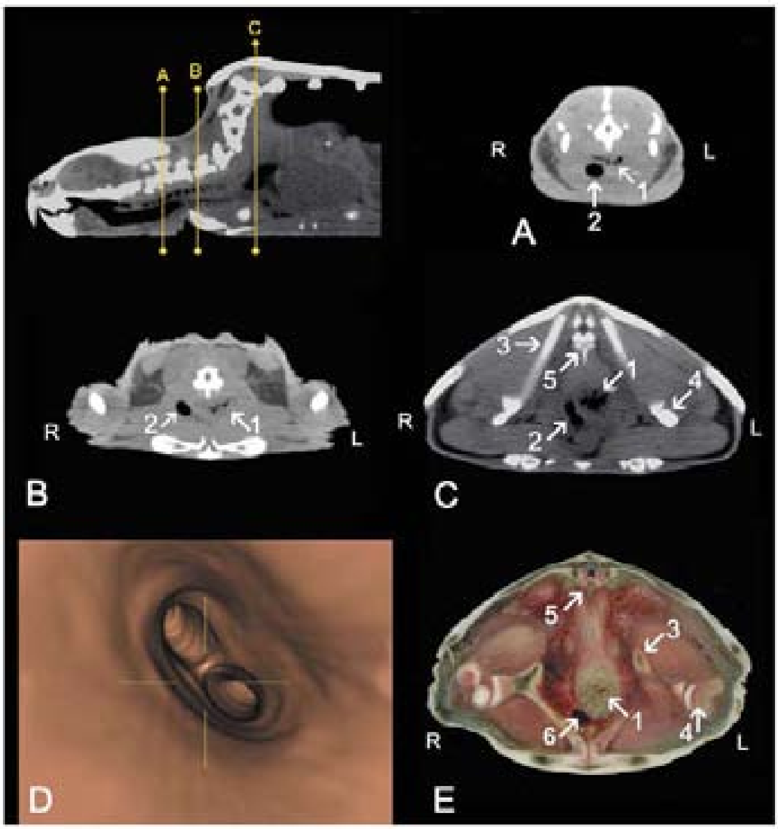

Fig. 5. (A C) Computed tomography images, transverse plane soft-tissue window, (D) virtual bronchoscopy image and (E) corresponding gross anatomical section of a juvenile loggerhead sea turtle. 1, oesophagus; 2, trachea; 3, scapula; 4, humerus head; 5, 1st dorsal vertebra; 6, carina. D, internal view of the tracheal bifurcation (carina).

Please cite this article in press as: Valente, A.L.S. et al., Computed tomography of the vertebral column and coelomic ..., Vet. J. (2006), doi:10.1016/j.tvjl.2006.08.018

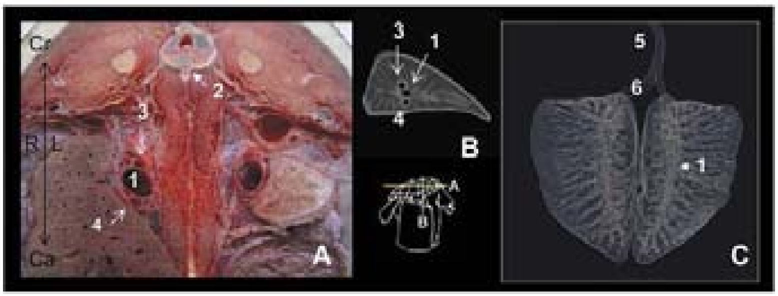

Fig. 6. (A) Dorsal gross anatomical section, (B) multiplanar CT (transverse plane – soft-tissue window) and (C) 3D CT reconstructions of the respiratory tract of the loggerhead sea turtle. 1, bronchus; 2, 6th cervical vertebra; 3, pulmonary artery; 4, pulmonary vein; 5, trachea; 6, extrapulmonary bronchus.

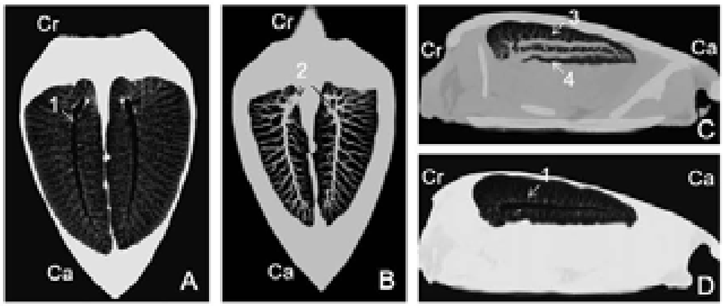

Fig. 7. Multiplanar CT reconstructions, (A, B – dorsal plane, C, D – sagittal plane; both with CT lung window) of the lungs of a juvenile loggerhead sea turtle. 1, central bronchus; 2, pulmonary vasculature; 3, pulmonary artery; 4, pulmonary vein.

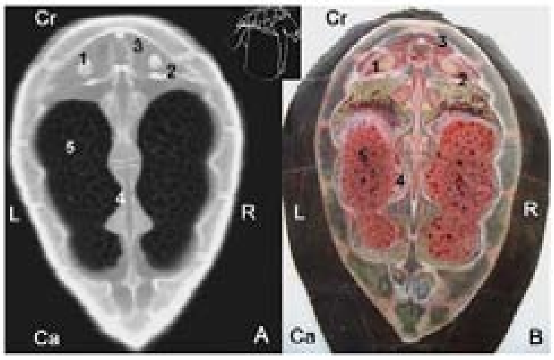

Fig. 8. (A) Multiplanar reconstruction (dorsal plane – soft-tissue window) and (B) corresponding gross anatomical section of a small juvenile loggerhead sea turtle. 1, scapula; 2, 1st pair of ribs; 3, 8th cervical vertebra, 4, 3rd dorsal vertebra; 5, pulmonary parenchyma.

trum are concave, and instead of a typical intervertebral disc with *nucleus pulposus* as occurs in mammals (*acoelous*), a cartilage plug is present in the intervertebral spaces. This kind of centrum is a feature of early reptiles' vertebrae that did not apparently move very much relative to one another (Williston, 1914), as is the case with the turtles' dorsal vertebrae. Information concerning the vertebral column of the loggerhead sea turtle is scarce. Wyneken (2001) described the general vertebral gross anatomy of the sea turtle. However, detailed information focusing on vertebral morphology and its arrangement was not provided.

Knowledge of the intervertebral foramina position and the morphology of each vertebra obtained with MDCT could also potentially improve the evaluation of the spinal cord and nerve roots in magnetic resonance images of turtles with carapace injuries associated with neurological signs. These may result from propeller or hull impact, shark-bite wounds, and the action of fishermen who may deliberately cause head trauma to turtles presumed to have reduced catches or damaged equipment (Panagopoulos et al., 2001; McArthur, 2004; Parga et al., 2005).

Although CT is not the most suitable diagnostic technique to evaluate soft tissues we have obtained good images of the heart, stomach, liver, gallbladder, kidneys and some parts of the intestine. Due to the flattened shape of the turtle's body in the dorsoventral direction and the unusual dorsal position of the lungs, CT images of the turtles' coelomic cavity differ from those observed in domestic animals such as the dog and cat (De Rycke et al., 2005; Samii et al., 1998). In transverse CT images of the thoracic cavity of dogs and cats using the lung setting it is possible to identify the heart, large vessels and anatomical structures in the mediastinal region because of the contrast formed by the lungs, which almost totally fill the thoracic cavity. The position of the heart of the loggerhead sea

Please cite this article in press as: Valente, A.L.S. et al., Computed tomography of the vertebral column and coelomic ..., Vet. J. (2006), doi:10.1016/j.tvjl.2006.08.018

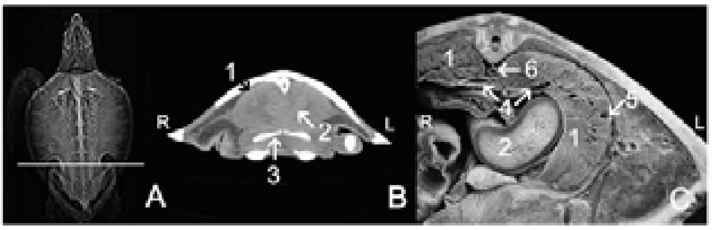

Fig. 9. Transverse CT image (soft-tissue window) of the renal region and corresponding anatomical section of a juvenile loggerhead sea turtle. A, section location; B: 1, kidneys; 2, intestinal loop; 3, pubic bones. C: 4, renal veins; 5, branch of the external iliac vein. 6, aorta artery.

turtle, with the atria limited cranially by the pectoral muscles and the ventricle limited laterally by the hepatic lobes, does not provide the air–tissue interface contrast usually observed in CT images of the mammalian thorax. On the other hand, the normal difference in density of these organs made it possible to distinguish them. In juvenile loggerhead sea turtles a wide window between the left and right hyoplastron was observed in our study, which coincided with the cardiac area. The position of the heart was similar to that found in the tortoise and other turtles. However in these species, the hyoplastron bones and endoplastron are joined close together forming an unique bony plate covering the whole ventral surface of the coelomic cavity (McArthur et al., 2004). The bone gap in the plastron of young loggerhead sea turtles may make them more vulnerable to compressive injury when accidentally captured in trawling nets.

In this study, we have verified that MDCT is a useful tool to identify the position of the oesophagus and its relationship with the trachea and bronchia. This could help clinicians to evaluate the extent of damage produced by an accidentally swallowed fishhook caught in the digestive tract and determine the best way to access it in a surgical procedure. Since perforating oesophageal lesions could secondarily affect the larynx (Orós et al., 2005), and therefore the upper airways, virtual bronchoscopy could be used to evaluate airway integrity.

One of the most important clinical contributions of CT examination is in relation to the pulmonary system. Craniocaudal and lateral radiographic views are normally used for detecting pulmonary diseases in chelonians (Hernandez-Divers and Hernandez-Divers, 2001). However, when associated with fracture of the carapace, local inflammatory response and bone fragment superimposition usually impede an accurate evaluation of the pulmonary parenchyma. Multi-detector computed tomography provides accurate information on the lungs and airways because the slow respiratory rate of chelonians associated with the lung-air contrast permits high quality visualization of the lungs and the airways. The general morphology of the respiratory tract of loggerhead sea turtles described in our work is consistent with that of a previous histological work performed in hatchings of this species (Fleetwood and Munnell, 1996). The position of the carina found in our study appear to be slightly more caudal than in land tortoises, in which the trachea bifurcates after coursing a relatively short distance down the neck (Murray, 2006). The difference in the position of carina in this case seems to be related with the morpho-functional characteristic of the neck observed in different groups of the Testudines. In tortoises and most turtles (Cryptodira) the neck vertebrae flex vertically, allowing the head to be drawn straight back within the shell. In these species the most cranial position of the carina allows breathing even when the head and neck are withdrawn. As in sea turtles the ability to retract the head has been lost (Pecor, 2003), the relatively caudal position of the bronchial bifurcation does not cause any breathing impediment.

In chelonians in particular, the anatomy of the lower respiratory tract is of clinical importance. Inflammatory exudates particularly those associated with infectious diseases tend to accumulate in the dependent portion of the lung. This location precludes timely elimination through the bronchi and trachea as one would expect in mammalian patients (Murray, 1996). Pneumonia in the red-eared slider (*Trachemys scripta*) has been detected in slightly paramedian sagittal CT scans in which the normal reticular lung pattern is found to be missing (Wilkinson et al., 2004).

The kidneys of sea turtles are located retroperitoneally between the peritoneum and the shell and differ in the morphology and angio-architecture from those found in mammalians (Wyneken, 2001). They are metanephric and lack a distinct cortex, medulla and renal pelvis. The kidneys were seen as a homogeneous parenchyma in CT images contrasting only with the peripheral fat present between them and the carapace.

The general anatomy of loggerhead sea turtles is comparable to that found in other chelonian species but with differences in the relative size of some organs. For instance, the lungs of tortoises seem to have much more volume than those of the loggerhead sea turtle. In transverse section at level of the heart base, in a tortoise the lungs occupy about two-thirds of the height of the coelomic cavity (Wilkinson et al., 2004), whereas in loggerhead sea turtles they are only in the dorsal third of this cavity. In the former, this organ has a pyramidal shape tapering in its caudal end, and in the latter the lungs are more flattened. In addition, the pectoral

Please cite this article in press as: Valente, A.L.S. et al., Computed tomography of the vertebral column and coelomic ..., Vet. J. (2006), doi:10.1016/j.tvjl.2006.08.018

musculature in loggerhead sea turtles observed in this study was more developed than that of tortoises (Wilkinson et al., 2004).

The use of MDCT allowed a fast examination, multiplanar reconstructions and an excellent 3D volume rendering which provided assessment of the skeleton and lung morphology in great detail. Comparison with the anatomical sections was indispensable in our study to recognize the parenchymatous organs in the CT images, although it was difficult to distinguish abdominal soft-tissue structures such as intestine portions, pancreas and reproductive organs because of their small size and/or a lack of contrast between them and the surrounding tissues.

5. Conclusions

Computed tomography solves problems of superimposed skeletal structures seen in plain radiographs and can be used to evaluate fractures, luxations, bone demineralization, neoplasia and visceral calcifications.

The slow respiratory rate of reptiles associated with the lung-air contrast allowed the lungs to be visualized in detail, suggesting that this may be a technique potentially suitable for diagnosing a great variety of pulmonary pathologies. The morphology of the lung of juvenile loggerhead sea turtles seen using MDCT is consistent with the morphology reported in a previous histological study performed in hatchlings of the same species. Compared to other diagnostic imaging modalities, MDCT provides excellent information about the respiratory system and skeleton in a short examination time, thereby minimizing the risks of anaesthesia. The location of the coelomic structures with respect to the carapace and the vertebrae that is provided in this work will facilitate the examination and interpretation of other ancillary diagnostic techniques such as ultrasound and X-rays, improving safety of access in biopsies and surgical procedures as a result.

Acknowledgements

The authors thank Professor Dr. Francisco Reina and technician Isabel Delgado Calvarro, Facultat de Medicina, UAB, for their help with the anatomical sections, and the radio-diagnostic technician Montse March for technical support with the MDCT.

References

Abou-Madi, N., Scrivani, P., Kollias, G.V., Hernandez-Divers, S.M., 2004. Diagnosis of skeletal injuries in chelonians using computed tomography. Journal of Zoo and Wildlife Medicine 35, 226–231.

Arencibia, A., Rivero, M.A., Casal, A.B., González-Romano, N., Orós, J., 2005. CT and Cross-sectional Anatomy of the Normal Head of the Loggerhead Sea Turtle (*Caretta caretta*). Anatomia, Histologia, Embryologia 34, 3.

ASIH/HL/SSAR., 2001. Guidelines for use of live amphibians and reptiles in field research. American Society of Ichthyologists and Herpetologists (ASIH), The Herpetologists' League (HL) and Society for the Study of Amphibians and Reptiles (SSAR), pp. 1–20. Available from: http://www.asih.org/pubs/herpcoll.html. Accessed 4 July 2006.

De Rycke, L., Gielen, I.M., Simoens, P.J., Bree, H.V., 2005. Computed tomography and cross-sectional anatomy of the thorax in clinically normal dogs. American Journal of Veterinary Research 66, 512–524.

Fleetwood, J.N., Munnell, J.F., 1996. Morphology of the airways and lung parenchyma in hatchlings of the loggerhead sea turtle, *Caretta caretta*. Journal of Morphology 227, 289–304.

Gaffney, E.S., 1990. The comparative osteology of the Triassic turtle Proganochelys. Bulletin of the American Museum of Natural History 194, 1–263.

Garland, M.R., Lawler, L.P., Whitaker, B.R., Walker, I.D.F., Corl, F.M., Fishman, E.K., 2002. Modern CT applications in veterinary medicine. Radiographics 22, 55–62.

Gaudron, C., Lignereux, Y., Ducos de Lahitte, J., 2001. Imagerie médicale appliquée a l'anatomie clinique des chéloniens en consultation. In: Proceedings of the International Congress on Testudo Genus, pp. 161–179.

Gumpenberger, M., Henninger, W., 2001. The use of computed tomography in avian and reptile medicine. Seminars in Avian and Exotic Pet Medicine 10, 174–180.

Hernandez-Divers, S., Hernandez-Divers, S., 2001. Diagnostic imaging of reptiles. In Practice July/August, 370–391.

McArthur, S., 2004. Problem-solving approach to conditions of marine turtles. In: McArthur, S., Wilkinson, R., Jean, M. (Eds.), Medicine and Surgery of Tortoises and Turtles. Blackwell Publishing Ltd., Victoria, Australia, pp. 301–307.

McArthur, S., Meyer, J., Innis, C., 2004. Anatomy and physiology. In: McArthur, S., Wilkinson, R., Jean, M. (Eds.), Medicine and Surgery of Tortoises and Turtles. Blackwell Publishing Ltd., Victoria, Australia, pp. 35–72.

Murray, M.J., 1996. Pneumonia and normal respiratory function. In: Mader, Douglas R. (Ed.), Reptile Medicine and Surgery. WB Saunders Co., Philadelphia, pp. 396–405.

Murray, M.J., 2006. Cardiopulmonary anatomy and physiology. In: Mader, Douglas R. (Ed.), Reptile Medicine and Surgery. Elsevier Inc., Philadelphia, pp. 124–134.

Orós, J., Torrent, A., Calabuig, P., Déniz, S., 2005. Diseases and causes of mortality among sea turtles stranded in the Canary Islands, Spain (1998–2001). Diseases of Aquatic Organisms 63, 13–24.

Panagopoulos, D., Sofouli, E., Teneketzis, K., Margaritoulis, D., 2001. Stranding data as an Indicator of fisheries induced mortality of sea turtles in Greece. In: Proceedings of the 1st Mediterranean Conference on Marine Turtles, Rome, Italy.

Parga, M., Valente, A.L., Zamora, M.A., Lavin, S., Alegre, F., Cuenca, R., Marco, I., 2005. Carapace trauma associated with hind limb paralysis in a loggerhead sea turtle. In: Proceedings of the Spring Meeting of the British Veterinary Zoological Society 200, p. 41.

Pecor, K., 2003. "Testudines" (On-line), Animal Diversity Web. Available from: http://animaldiversity.ummz.umich.edu/site/accounts/information/Testudines.html. Accessed 5 July 2006.

Pont, S.G., Alegre, F.N., 2000. Work of the foundation for the conservation and recovery of marine life. Marine Turtle Newsletter 87, 5–7.

Raiti, P. 1998. The use of computerized tomography and magnetic resonance imaging in chelonian medicine. In: Proceedings of the Association of Reptilian and Amphibian Veterinarians, pp. 51–53.

Raiti, P., Haramati, N., 1997. Magnetic resonance imaging and computerized tomography of a gravid leopard tortoise (*Geochelone pardalis pardalis*) with metabolic bone disease. Journal of Zoo and Wildlife Medicine 28, 189–197.

Samii, V.F., Biller, D.S., Koblik, P.D., 1998. Normal cross-sectional anatomy of the feline thorax and abdomen: comparison of computed tomography and cadaver anatomy. Veterinary Radiology and Ultrasound 39, 504–511.

Wilkinson, R., Hernandez-Divers, S., Lafortune, M., Calvert, I., Gumpenberger, M., MCarthur, S., 2004. Diagnostic imaging. In: McArthur, S., Wilkinson, R., Jean, M. (Eds.), Medicine and Surgery of Tortoises and Turtles. Blackwell Publishing Ltd., Victoria, Australia, pp. 187–238.

Williston, S.W., 1914. Water reptiles of the past and present. Arment Biological Press, Landisville, PA, p. 156.

Wyneken, J., Wilke, W.D., Steinberg, F., 2000. Looking at turtles in three dimensions. In: Proceedings of the 20th Annual Sea Turtle Symposium, Orlando, Florida, pp. 106–107.

Wyneken, J. 2001. The Anatomy of Sea Turtles. U.S. Department of Commerce NOAA Technical Memorandum NMFS-SEFSC 470, pp. 1–172.

Please cite this article in press as: Valente, A.L.S. et al., Computed tomography of the vertebral column and coelomic ..., Vet. J. (2006), doi:10.1016/j.tvjl.2006.08.018

4.5. SECTIONAL ANATOMIC AND MAGNETIC RESONANCE IMAGING FEATURES OF COELOMIC STRUCTURES OF LOGGERHEAD SEA TURTLES

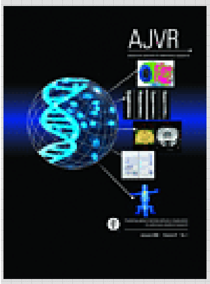

Valente, A.L.; Cuenca, R.; Zamora, M.A.; Parga, M.L.; Lavín, S.; Alegre, F. y Marco, I. (2006). Sectional anatomic and magnetic resonance imaging features of coelomic structures of loggerhead sea turtles. Am. J. Vet. Res., 67: 1347-1353.

Sectional anatomic and magnetic resonance imaging features of coelomic structures of loggerhead sea turtles

Ana Luisa S. Valente, DVM, MSc; Rafaela Cuenca, DVM, PhD; Maria Angeles Zamora, DM; Maria Luz Parga, DVM, MSc; Santiago Lavin, DVM, PhD; Ferrán Alegre, DVM; and Ignasi Marco, DVM, PhD

Objective—To compare cross-sectional anatomic specimens with images obtained via magnetic resonance imaging (MRI) of the coelomic structures of loggerhead sea turtles (*Caretta caretta*).

Animals—5 clinically normal live turtles and 5 dead turtles.

Procedures—MRI was used to produce T1- and T2-weighted images of the turtles, which were compared with gross anatomic sections of 3 of the 5 dead turtles. The other 2 dead turtles received injection with latex and were dissected to provide additional cardiovascular anatomic data.

Results—The general view on the 3 oriented planes provided good understanding of cross-sectional anatomic features. Likewise, major anatomic structures such as the esophagus, stomach, lungs, intestine (duodenum and colon), liver, gallbladder, spleen, kidneys, urinary bladder, heart, bronchi, and vessels could be clearly imaged. It was not possible to recognize the ureters or reproductive tract.

Conclusions and Clinical Relevance—By providing reference information for clinical use, MRI may be valuable for detailed assessment of the internal anatomic structures of loggerhead sea turtles. Drawbacks exist in association with anesthesia and the cost and availability of MRI, but the technique does provide excellent images of most internal organs. Information concerning structures such as the pancreas, ureters, intestinal segments (jejunum and ileum), and the reproductive tract is limited because of inconsistent visualization. (*Am J Vet Res* 2006;67:1347–1353)

Abbreviation

MRI	Magnetic resonance imaging

Magnetic resonance imaging is a sophisticated computerized imaging technique used as a clinical diagnostic tool in human medicine since 1971.[1] Compared with other diagnostic imaging tools, MRI has advantages and disadvantages. Magnetic resonance imaging does not use ionizing radiation and is not dangerous to patients or technical personnel.[2] It is a powerful technique for obtaining images of soft tissues in various planes without repositioning of the animal,[3] and it allows visualization of blood vessels without the use of contrast medium.[4] However, more time is required for data analysis when MRI is used, compared with other techniques, and sedation or anesthesia is usually needed. Ferromagnetic objects such as microchips, projectiles, or fishing hooks can cause tissue damage and artifact spots on the image because the static magnetic field and spatial gradient field induce torque and translational forces on an object, which can be displaced or heated.[5] The use of MRI is expensive, compared with other imaging techniques, but its use in wildlife is justified in endangered species because of the amount of diagnostic information that can be gathered in a short period of time and with little risk to the animal.[6-8]

Because chelonians have internal viscera entirely covered by osseous structures (carapace and plastron bones), the use of MRI to visualize and evaluate the coelomic structures has several advantages over other conventional techniques that use radiographs, including a representation of detailed cross-sectional anatomic features without distraction from superimposed structures, variations in gray scale formats, enhanced contrast resolution, and computer reconstruction of multiplane images.[4] However, its true potential will only be realized when sufficient clinicians have used the technique on enough turtles to provide accurate interpretation of the resulting images.[10]

Some authors have reported the MRI appearance of the internal structures in other species of chelonians such as the spur-thighed tortoise (*Testudo graeca*), Aldabra giant tortoise (*Dipsochelys elephantine*), Hermann's tortoise (*Testudo hermani*), central Asian tortoise (*Testudo horsfieldii*), leopard tortoise (*Geochelone pardalis pardalis*), *Kinixys* spp, and the red-eared slider terrapin (*Trachemys scripta elegans*).[9-12] To the authors' knowledge, the literature contains only 1 article that includes a description of gross cross-sectional anatomic features correlated with the use of MRI to detect internal tumors in green turtles (*Chelonia mydas*) with cutaneous fibropapillomatosis,[13] in which the authors describe the normal MRI appearance of this species on the basis of 1 healthy turtle and 3 dead turtles.

The loggerhead sea turtle is an endangered species[14] in the Mediterranean Sea mainly because of high mortality rates caused by fishing activity.[15] As a result, this species is also the most commonly seen in

Received October 25, 2005.
Accepted March 1, 2006.
From the Servei d'Ecopatologia de Fauna Salvatge, Facultat de Veterinària, Universitat Autònoma de Barcelona, 08193 Bellaterra, Barcelona, Spain (Valente, Cuenca, Lavin, Marco); the Diagnosis Médica, Córcega 345, 08037 Barcelona, Spain (Zamora); and the Centre de Recuperació d'Turtles Marins, Camí Ral 239, 08330 Premià de Mar, Barcelona, Spain (Parga, Alegre).
The authors thank Dr. Francisco Reina, Isabel Delgado Calvarro, and Angeles Lafuente for technical support.
Address correspondence to Dr. Valente.

rescue centers on the northwestern Mediterranean coast.[16] Most of those turtles have internal damage from hooks, traumatic injuries, or digestive disorders caused by ingestion of garbage.[16] In most cases, complementary diagnostic imaging methods are necessary to establish a diagnosis.

The purpose of the study reported here was to compare cross-sectional anatomic specimens with images obtained via MRI of the coelomic structures of loggerhead sea turtles.

Materials and Methods

Magnetic resonance imaging was performed on 5 live juvenile loggerhead sea turtles, 4 dead juvenile turtles, and 1 dead subadult turtle. Dead turtles were imaged only to correlate the images with corresponding frozen sections to permit description of sectional anatomic features. Description of the MRI findings in clinically normal turtles was based on the 5 healthy turtles. Sex of the turtles could not be identified because they were sexually immature and were classified as juvenile or subadult according to carapace length.[17] The turtles had a minimum straight carapace length[18] of 29.5 to 49.8 cm and were accidentally caught in pelagic longline sets and fishing nets along the northwestern Mediterranean coast (40°31' to 42°26 N' and 0°32' to 3°10' E) of Spain. For purposes of the present study, only those turtles in which the hook was superficially attached in or near the mouth and easily removed through the oral cavity were included. Live turtles were temporarily housed in the rehabilitation facilities of the Rescue Centre for Marine Turtles, Premià de Mar, Barcelona, Spain, and were fed mainly sardines. Only turtles in good health, as determined on the basis of results of physical, radiographic, and hematologic examinations, were scanned. Dead turtles were kept frozen until the MRI procedure and were thawed 24 to 48 hours before the MRI procedure, depending on size.

The MRI was performed by use of a 1.5-Tesla superconducting magnet.[a] The imaging protocol consisted of sagittal, transverse, and dorsal spin-echo T1-weighted images (600 to 920/15/2; TR/TE/NEX) and fast spin-echo T2-weighted images (4,050 to 10,000/100/2; TR/TE/NEX), with 4- to 6.6-mm slice thickness without slice interval and a 288 × 192/320 × 224 matrix. Depending on the turtle's size, the sequence variables, mainly the TR and TE, had to be changed. No contrast medium was used.

An initial attempt was made to restrain the head and flippers of the turtles by means of a large self-adhesive band; however, it became necessary to immobilize turtles via IV injection in the dorsal cervical sinus with a combination of ketamine[b] (15 mg/kg) and diazepam[c] (0.5 mg/kg). Prior to the scan, heart rate was checked with a mini-Doppler instrument and the turtles were carefully kept wet. Images were obtained beginning at 180 to 300 seconds after the turtles were adequately sedated.

After the MRI images were obtained, 3 of the 5 scanned dead turtles were placed in individual right-angled polystyrene boxes filled with tap water for the anatomic cross-sectioning study. The boxes with the cadavers were frozen at −80°C for at least 24 hours before anatomic sectioning. Each of the 3 cadavers was sectioned in an oriented plane (sagittal, dorsal, and transverse) to approximate the MRI sections. Serial parallel sections from 18 to 20 mm thick were obtained by use of an electric bone saw. The anatomic sections were thicker than those of the MRI to maintain integrity and position of the anatomic structures in the slices for consultation during the study. It was expected to fit 4 or 5 MRI sections to each anatomic section, considering loss of material from the saw. Slices were immediately washed with 80% ethanol to eliminate frost buildup and remove debris and were then separated by grids. After labeling, the frozen slices were immersed for 30 minutes in neutral-buffered 10% formalin solution for thawing. A digital high-resolution, 2,560 × 1,920- pixel camera[d] and daylight was used to record the image of the fresh surface. Further image processing such as rotation, scaling, cutting, filtering, and corrections for contrast, brightness and color were performed with software.[e] In 2 other dead turtles, latex was injected through the jugular vein and the dorsal aorta. Large heart vessels and renal vasculature were dissected for additional morphologic data. The anatomic terminology applied was that of the *Nomina Anatomica Veterinaria*. Specific terminology for sea turtles[19] was also applied. To map the organs in the coelomic cavity in relation to the turtle's exterior, a digital grid was composed that was superimposed virtually on each MRI dorsal image, with initial adjustment of the anterior and posterior lines of the grid to the cranial and caudal tips of the carapace. For each turtle, the grid was adjusted to carapace size and the quadrants were automatically and proportionally adjusted (**Figure 1**).

Results

In live and dead turtles, better tissue differentiation, and, by extension, easier identification of morphologic structures and organs, was achieved via examination in T2-weighted images. In general, organ contours were not so well defined in the images taken in T1-weighted sequence.

Anatomic structures seen on T2-weighted images of the cadaver specimens matched with structures identified in the corresponding anatomic sections (**Figures 2 and 3**). Compared with the live turtles, the vessels and some parenchymatous organs, such as the liver and the kidney, of the dead specimens had hyperintense signals in T2-weighted images.

In the T1- and T2-weighted images of live and dead turtles, some areas of the carapace and plastron had a different kind of signal (Figures 2 and **4**). Three layers could be visualized in the transverse T2-weighted sections of the carapace: a hypointense external layer; a central, slightly hyperintense layer; and a thinner, internal hypointense layer. The inner portion of the carapace was lined by a hyperintense layer that corresponded to the coelomic membrane and fluid. Areas of carapace with an absence of signal in T2-weighted scans were observed in the fontanelles (the nonossified intercostal space in the distal third of the ribs[19]). For the plastron, the connective tissue could be identified in T1-weighted images and only the bones could be visualized in T2-weighted images.

The esophagus was seen as a tubular structure joining the stomach dorsally from the first to the second central quadrant (**Figures 1, 2, and 4–8**) of the coelomic cavity. The esophageal lumen and its conical keratinized papillae were well visualized in transverse and sagittal scans, whereas the S-shaped curve before the cardiac sphincter was better imaged in the dorsal plane. In general, the layers of the wall of the digestive tract were seen and the submucosal layer of the esophagus was more visible because of the hyperintensity of the papillae in the T2-weighted image.

The stomach was on the left side of the coelomic cavity, occupying the second and third left quadrants (Figures 1–3). This organ was directly in contact laterally with the coelomic membrane, medially with the first part of the duodenum and liver, and ventrally with the left lobe of the liver; dorsally it was separated from the left lung by the coelomic membrane (Figure 7). In T2-weighted images, this organ was easily identified and the volume and intensity of the signal observed in the lumen was inconsistent.

The first part of the duodenum coursed parallel to the caudal border of the liver transversely in the coelomic cavity (Figures 3 and 6) from the second left to the second right quadrants (Figures 1 and 2). Dorsally, in the second right quadrant, the first part of the duodenum received discharge from the gallbladder via a common bile duct that was seen in the anatomic sections but could not be clearly identified on MRI images (Figures 3, 6, and 7). In live turtles, the signal in this part of the small intestine was hyperintense, compared with the liver. The cranial duodenal flexure could be identified when the image was compared with the anatomic sections. In 3 live turtles, it was possible to see points of narrowing of the large intestine (Figure 8) that were interpreted as physiologic, irregular, peristaltic movements. The pancreas, identified in the anatomic sections as a flat structure attached in this region of the coelomic cavity, was difficult to recognize in live turtles because of its isointensity, compared with the liver. In dead specimens, this organ could be identified because of the changes of the liver signal. Dorsally, in the second central quadrant, close to the liver and first part of duodenum, was the spleen, which had an oval to elongated form and yielded a slightly hypointense signal, compared with the liver, in T1-weighted images and a hyperintense signal in T2-weighted images.

The descending colon was better visualized in the dorsal plane scans. It was located craniocaudally on the left side in the third left quadrant (Figures 1 and 3) and was adjoined to the rectum in the fourth central quadrant (Figures 1, 4, and 8).

The liver had 2 lobes that were imaged in the second left and right quadrants (Figures 1 and 2), respectively. In this area, the organ was easily recognized in all planes of the MRI sections (Figures 3 and 6–8). Compared with muscle, the hepatic parenchyma was hyperintense in T1-weighted images and slightly hypointense in T2-weighted images (Figures 7 and 8). The gallbladder had an elliptical form with the major axis oriented almost vertically in the second right quadrant. It was located on the right hepatic lobe and easily recognized in all 3 planes because of its hypointense and hyperintense signals in T1- and T2-weighted images, respectively (Figures 6 and 7). The great left and right hepatic veins coursed transversely in the left and right lobes, respectively, and were visible in both sequences in live turtles and clearly seen in T2-weighted images of dead turtles (Figure 3). Only in 1 turtle could the left hepatic vein be easily recognized in T2-weighted images.

The heart was located ventrally in the coelomic cavity between the first and second central quadrants (Figures 1 and 2) and adjacent to the plastron. The ventricle extended caudally to the hepatic lobes and cranial duodenal flexure (Figure 3). The myocardium

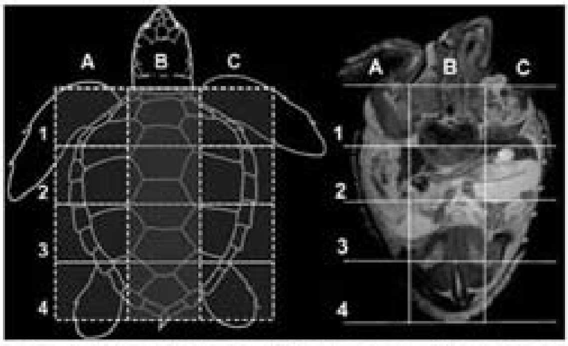

Figure 1—Schematic drawing of the dorsal view of a loggerhead sea turtle, results of corresponding dorsal T2-weighted MRI, and matrix used to describe anatomic structures. 1A = First left quadrant. 1B = First central quadrant. 1C = First right quadrant. 2A = Second left quadrant. 2B = Second central quadrant. 2C = Second right quadrant. 3A = Third left quadrant. 3B = Third central quadrant. 3C = Third right quadrant. 4A = Fourth left quadrant. 4B = Fourth central quadrant. 4C = Fourth right quadrant.

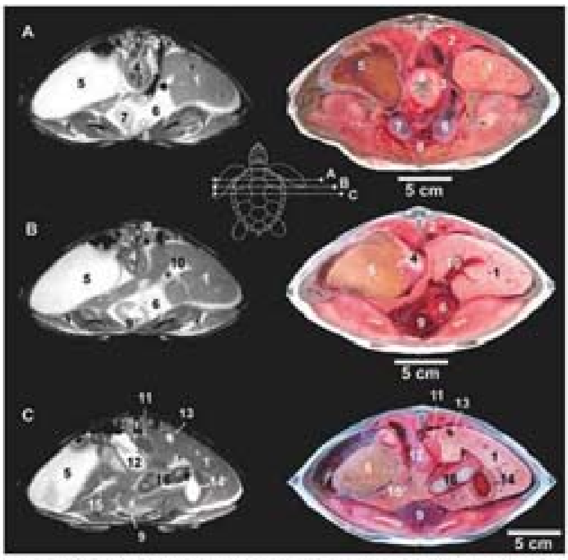

Figure 2—Results of transverse T2-weighted MRI (left column) and corresponding anatomic sections (right column) of a dead loggerhead sea turtle (caudal view) at different levels of the carapace (A, B, and C). Schematic drawing indicates section level. 1 = Liver. 2 = Right lung. 3 = Right bronchus. 4 = Esophagus. 5 = Stomach. 6 = Right atrium. 7 = Left atrium. 8 = Transverse section of large vessels of cardiac base. 9 = Ventricle. 10 = Right hepatic vein. 11 = Spleen. 12 = Large intestine. 13 = Postcava vein. 14 = Gallbladder. 15 = Left hepatic vein. 16 = Duodenum.

had similar signal intensity to pectoral muscles in both sequences, and in the T2-weighted images, the shape of the heart could be identified because of the hyperintense signal of the pericardial fluid in the cardiac sheath (Figure 6). In the transverse MRI section immediately caudal to the junction of the first and second vertebral scutes,[19] it was possible to recognize the transverse section of the great vessels, such as the left and right aorta, pulmonary arteries, and brachiocephalic trunk (Figure 8).

The plastron bones covered most of the ventral surface of the coelomic cavity. However, a large area

Figure 3—Results of dorsal T2-weighted MRI (A and B) and corresponding anatomic sections (C and D) of a dead loggerhead sea turtle. 1 = Stomach. 2 = Liver. 3 = Duodenum. 4 = Gallbladder. 5 = Ventricle. 6 = Kidney. 7 = Spleen. 8 = Right hepatic vein. 9 = Pancreas.

not protected by bone was identified in the images of the cardiac region of the juvenile specimens (Figure 8) and confirmed on the basis of osteologic preparations (Figure 4).

The junctions between the right and left cranial vena cavae and the left hepatic vein and the caudal vena cava could be imaged in a dorsal scan immediately ventral to the caudal end of the esophagus, revealing a typical flow void signal (Figure 8). The short, thick, right and left renal veins joined and formed the caudal vena cava that coursed cranially, on the right side of the coelomic cavity, toward the heart.

The lungs were located dorsally in the coelomic cavity (Figure 2) and extended approximately three quarters of the carapace length. Because of the great amount of air present, no signal was observed except the discrete thin septa, which resembled a honeycomb structure (Figures 4, 7, and 8). The cranial part of the left and right bronchi was external to the pulmonary parenchyma, and their longitudinal sections were seen in transverse scans of the caudal third of the first central quadrant.

The kidneys were located dorsally in the third left and right quadrants (Figures 1 and 3) and partially in the third central quadrant and were better observed in transverse and sagittal sections. In the latter, the kidneys' shape resembled that of a boomerang with the great curvature inserted in the internal concavity of the carapace. The kidneys were hyperintense in relation to the adjacent muscles in T2-weighted images (Figure 8) and fairly hyperintense in T1-weighted images. Transverse sections of the renal veins and external iliac veins were seen in a transverse scan. Ureters and reproductive structures could not be recognized. In live turtles, the urinary bladder was identified as a result of its fluid content, which was hypointense and hyperintense in T1- and T2-weighted images, respectively. However, the entire contour of the urinary bladder was not well outlined. Signal intensity of some coelomic structures seen in T1- and T2-weighted images was compared with muscle (Appendix).

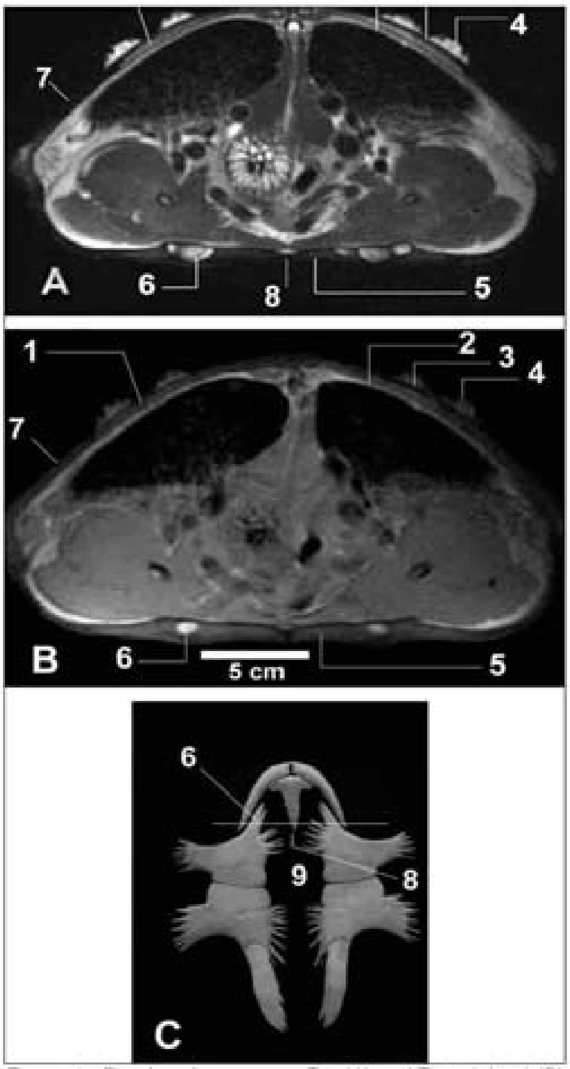

Figure 4—Results of transverse T2- (A) and T1-weighted (B) MRI of a live loggerhead sea turtle and photograph of an osteologic preparation of plastron bones of a loggerhead sea turtle (C). 1 = Flat bone. 2 = Coelomic membrane (coelomic fluid). 3 = Keratinized epidermal layer. 4 = Cirripeds (external parasites). 5 = Connective tissue. 6 = Hyoplastron (plastron bone). 7 = Fontanelles. 8 = Endoplastron (plastron bone). 9 = Cardiac area.

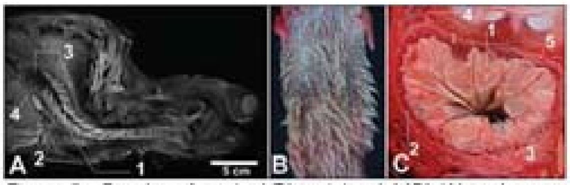

Figure 5—Results of sagittal T2-weighted MRI (A) and gross photographs of the esophagus (B and C) of a loggerhead sea turtle. 1 = Esophageal papillae (projections of submucosal). 2 = Muscular layer. 3 = Lumen (cardiac sphincter). 4 = Serosa. 5 = Keratinized layer.

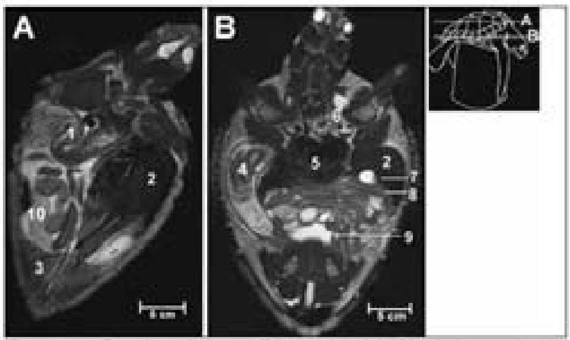

Figure 6—Results of dorsal T2-weighted MRI of the coelomic cavity of a live loggerhead sea turtle at different levels of the carapace (A and B). 1 = Cardiac sphincter. 2 = Liver. 3 = Kidney. 4 = Stomach. 5 = Heart. 6 = Esophagus. 7 = Gallbladder. 8 = Duodenum. 9 = Urinary bladder or coelomic fluid. 10 = Descending colon.

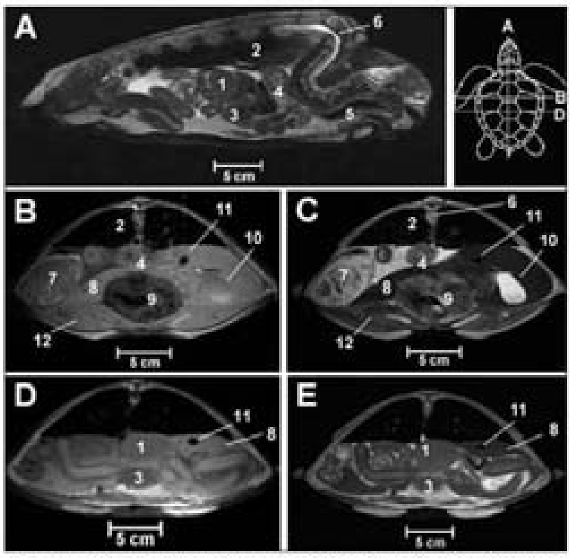

Figure 7—Sagittal T2-weighted image (A) and transverse T1- (left) and T2-weighted (right) images (B–E) from MRI of the coelomic cavity of a live loggerhead sea turtle. 1 = Spleen. 2 = Lung. 3 = Ventricle. 4 = Esophagus. 5 = Trachea. 6 = Spinal cord. 7 = Stomach. 8 = Liver. 9 = Right atrium. 10 = Gallbladder. 11 = Postcava vein. 12 = Pectoral musculature.

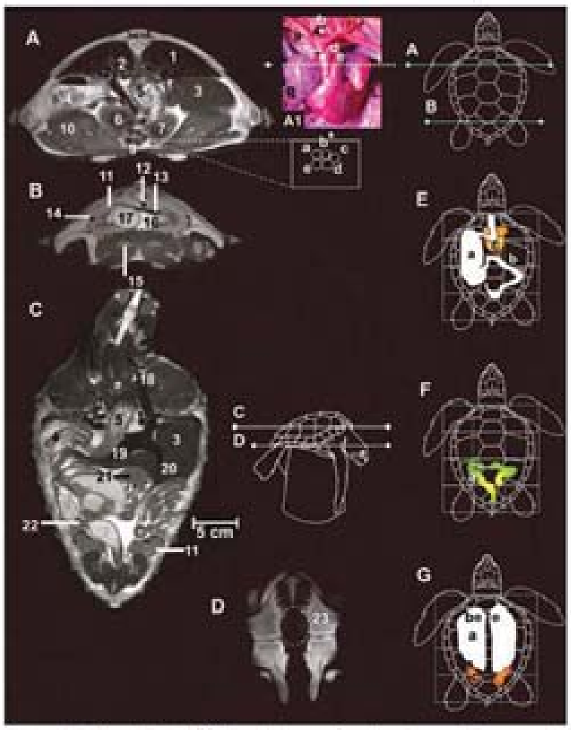

Figure 8—Results of MRI and schematic drawings of topographic anatomic features of a live loggerhead sea turtle. Views A and B—Caudal transverse T2-weighted images. View A1 is a ventral view of an anatomic dissection of the heart injected with latex; notice the right pulmonary artery (a), right aorta (b), brachiocephalic trunk (c), left aorta (d), and the left pulmonary artery (e). Views C and D—Dorsal T2-weighted images; the circular area on View D indicates the cardiac region. View E—Schematic drawing of the stomach (a), duodenum (b), and heart (c). View F—Schematic drawing of the large intestine (a). View G—Schematic drawing of the lungs (a), bronchi (b), and kidneys (c). 1 = Right lung. 2 = Left bronchus. 3 = Liver. 4 = Stomach. 5 = Esophagus. 6 = Left atrium. 7 = Right atrium. 8 = Left aorta. 9 = Transverse section of large vessel of cardiac base. 10 = Pectoral musculature. 11 = Left kidney. 12 = Dorsal aorta. 13 = Renal vein. 14 = External iliac vein. 15 = Pubis and pelvic muscles. 16 = Urinary bladder. 17 = Descending colon. 18 = Right cranial vena cava. 19 = Left hepatic vein. 20 = Caudal vena cava. 21 = Spleen. 22 = Narrowing of large intestine. 23 = Hyoplastron bone.

Discussion

In previous reports[10,12] of MRI in reptilian species, it is stated that most chelonians do not develop major problems during the time required for examination via MRI and may not even require sedation. In the present study, chemical restraint was necessary in addition to the immobilization of the turtle's head and flippers with a large self-adhesive band. Although all live turtles were subjected to the same procedure under similar conditions (ie, similar anesthetic dose, external temperature, body surface humidity, and physical restraint), wide variation in anesthetic effect was observed during the approximately 40 minutes of examination. Immobilization had to be maintained by administering higher doses of anesthesia (up to 3 times the recommended dose), which was still insufficient to prevent slight movements of the flippers and head. Because most studies that used MRI in chelonians were performed on tortoises, we deduced that physical restraint of sea turtles was hampered by the fact that, unlike tortoises, they cannot retract their limbs and head inside the shell. Conversely, the unpredictable response to anesthesia may have been caused by inability of the ketamine-diazepan combination to block reaction to the loud noise made by the magnetic pulses, as has been observed in dogs.[20] In green turtles subjected to MRI examination for detection of internal tumors, a ketamine-medetomidine combination injected 20 minutes before the scan provided adequate sedation.[13] Nevertheless, the unknown individual responses of loggerhead sea turtles to the powerful magnetic field used in MRI (30,000 times greater than the Earth's) need further research, in view of the sea turtle's known ability to orient and navigate by use of electromagnetic fields.[21,22]

Sea turtles may feed on garbage and floating plastic bags, which become hooked on the esophageal digestive papillae.[23] Macroscopically, the sharp papillae resemble those found on the buccal mucosa of cattle and sheep. By use of the anatomic sections as reference points it was verified that the papillae were formed by projections of the submucosa and had an outer surface covered by a thin keratinized epithelium that was not imaged because of lack of signal. The hyperintense signal observed in the T2-weighted images indicated water in the submucosa, which had a shiny appearance in the anatomic sections. The exact function of these papillae is unknown, but they are presumed to trap food while excess water is expelled prior to swallowing.[19] Magnetic resonance imaging of the esophagus could be important as a complementary method to diagnose esophageal lesions and partial obstructions caused by foreign bodies lodged between or on papillae. The esophageal mucosa is not clearly visualized by use of endoscopy in loggerhead sea turtles because of the large size of the papillae (as long as 2.5 cm), which prevents examination of the underlying mucosa and may obscure small foreign bodies.[24] Lumen narrowing often develops because of the inflammatory reaction and fibrosis at the point where fishhooks are lodged (not only the mucosa but also the submucosa and muscular layers)[25]; therefore, the duration of the healing process in sea turtles is lengthy. By permitting evaluation of the regression of tissue inflammation after removal of the hook is performed surgically or endoscopically, MRI could be recommended as part of a release protocol and would aid in decreasing long stays in the rescue center.

The low-frequency cardiac movements did not create artifacts that compromised image interpretation. Although most internal viscera are protected by rigid tissue (dermal bones), the cardiac region was surprisingly unprotected as seen by use of MRI. The information obtained via MRI concurred with observations made by the authors on osteologic preparations of juvenile turtles. We believe that these findings have not been reported because previous studies lacked evaluation of the cross-sectional relationship between the skeleton and the internal viscera. The scant ossification of the medial edges of the hyoplastron bones in juvenile turtles could make them more susceptible to compression in trawling nets.

Although better images were obtained by use of T2-weighted images, it is clinically important to perform the 2 sequence types because T1-weighted images could reveal changes in the water or fat concentrations in organs, indicating the possibility of infiltrative inflammatory processes, edema, liver fat degeneration, splenitis, or hydronephrosis. Likewise, T1-weighted images could be useful in sea turtle rehabilitation for detecting crude oil ingestion, a frequent finding in dead turtles.[25]

Topographic anatomic features and their correlation with MRI are well documented in various mammalian species.[26-30] Although we could not find reports of studies that used methodology comparable to that of the present study, comparison of the internal organs of turtles with those of dogs scanned at 1 Tesla unit revealed the same difficulties in visualizing the pancreas caused by the small amount of contrast with the intestine.[30] The spleen of loggerhead sea turtles had the best contrast in T2-weighted images, compared with dogs, in which T1-weighted sequences provided the best contrast. The alimentary canal of dogs is best evaluated by use of moderated T1-weighted images because they provide good contrast between the intestine wall and the surrounding fatty tissue.[30] In the present study, T2-weighted images provided the best visualization of the alimentary canal. This difference could be related to the nutritional status of the free-ranging turtles used in this study, which did not have the large fat deposits in the mesentery that typically occur in domestic and captive animals.

In dogs, the kidneys are best delineated by T1-weighted sequences, which provide good contrast between the medulla and the cortex. Because turtles do not have 2 distinct renal layers, the layers observed in dogs are not seen in loggerhead sea turtles.[30] Unlike dogs, the turtle kidneys were best recognized in T2-weighted images and had a heterogeneous parenchyma with high blood supply.

The morphologic characteristics of chelonians cause difficulties in applying conventional techniques for location and examination of the coelomic organs. The carapace has 2 main layers, the inner bony dermal layer and the outer scaly epidermal layer.[31] Differentiation of these layers observed in the transverse MRI sections was attributable to the presence or absence of osseous structures and connective tissues at specific points of the carapace. The thin layer formed by compact bone and the outer keratinized epidermal layer account for the lower signal observed along the external periosteal surface of the bone. These layers could be identified only in those turtles with cirripeds encrusted in their shell because cirripeds act as hyperintense landmarks that permit identification of the thickness of the hypointense outer layer. Cancellous bone found in the flat bones of the carapace and plastron had a hyperintense signal, compared with the cortical bone; this is attributable to the presence of bone marrow, as in dogs and cats.[32] The fontanelles were quite wide in all turtles studied and, therefore, provided a hypointense signal in the T2-weighted image.

Although the gross anatomic features of the loggerhead sea turtles were similar to other sea turtles,[19] differences in the signal intensity of some tissues were observed. In T2-weighted images of spur-thighed tortoises and Aldabran tortoises, blood vessels had a hyperintense signal and the liver and heart were more hyperintense than the pectoral musculature.[10] Also, in green turtles, the branching pulmonary vasculature was easily seen in the dorsal plane because of the contrast between its hyperintense signal and the hypointensity of the pulmonary parenchyma.[13] In healthy loggerhead sea turtles, the blood and, consequently, vascular structures had a typical void signal. Likewise, the signal intensity of the myocardium, compared with the skeletal muscle, in T2-weighted images was isointense in loggerhead sea turtles, whereas it was slightly hyperintense in green turtles.[13] The same appearance of the blood vessels and liver observed in those chelonian species was seen in dead loggerhead sea turtles in the present study. This change in signal intensity, observed mainly in the blood vessels and high blood supply structures of dead turtles, was also observed in MRI of dead turtles and was related to the absence of blood flow.[f] Caution is therefore recommended for future descriptions of MRI studies because dead turtles yield different signals than live turtles and should not be included indiscriminately in such studies.

Detailed images of small chelonians may be obtained when the whole body is scanned. In large chelonians such as sea turtles, the size of field of view (50 × 50 cm) and the gantry limits the single-scan whole-body examination. In this study, most of the turtles were juvenile, so they were placed into the gantry sideways to image the whole body in a single examination. However, a dead subadult sea turtle scan requires 2 steps, which requires examination time of 95 minutes and makes it unsuitable for a live turtle because of the risks involved with prolonged anesthesia.

a. Excelart, Medical Systems, Toshiba Co, Tokyo, Japan.
b. Imalgene 1000, Merial, Saint Priest, France.
c. Diazepam prodes injectable, Almirall Prodesfarma, Barcelona, Spain.
d. Digital still camera, Sony DSC-F707, Sony Corp, Tokyo, Japan.
e. Photoshop, version 5.5, Adobe Systems Inc, San Jose, Calif.
f. Snellman M. *Magnetic resonance imaging in canine spontaneous neurological disorders: an evaluation of equipment and methods.* Academic dissertation, Section of Veterinary Diagnostic Imaging, Department of Clinical Veterinary Sciences, Faculty of Veterinary Medicine, University of Helsinki, Helsinki, Finland, 2000.

Appendix—T1- and T2-weighted MRI signals of coelomic structures of loggerhead sea turtles, compared with signals from muscle.

Organ or structure	T1-weighted	T2-weighted
Myocardium	Isointense	Isointense
Liver	Hyperintense	Hypointense
Spleen	Isointense	Hyperintense
Kidneys	Hyperintense	Hyperintense
Fat tissue	Hyperintense	Hyperintense
Compact bone	Hypointense	Hypointense
Cancellous bone (carapace and plastron)	Hyperintense	Hypointense

References

1. Damadian RV. Tumor detection by nuclear magnetic resonance. *Science* 1971;171:1151–1553.
2. Schreiber WG, Teichmann EM, Schiffer I, et al. Lack of mutagenic and co-mutagenic effects of magnetic fields during magnetic resonance imaging. *J Magn Reson Imaging* 2001;14:779–788.
3. Dennis R. Estudio por imágenes de resonancia magnética, perspectiva general de su uso actual en medicina veterinaria. *Vet Int* 1995;2:52–61.
4. Tucker RL, Gavin PR. Brain imaging. *Vet Clin North Am Small Anim Pract* 1996;26:735–758.
5. Nicholas Joseph Jr RT. Protection and safety from energies used in: x-ray, CT, nuclear medicine and PET, and MRI part VI MRI safety for health care personnel. Radiographic Imaging CEU Source LLC Web site. Available at: www.radiographicceu.com/article12.html. Accessed Feb 6, 2006.
6. Walzer C, Url A, Robert N, et al. Idiopathic acute onset myelopathy in cheetah (*Acinonyx Jubatus*) cubs. *J Zoo Wildl Med* 2002;34:36–46.
7. Jandial R, Greenberg MS, Aryan HE et al. Lumbar diskectomy in a human-habituated western lowland gorilla. *Internet J Neurosurg* [serial online]. 2005;2:1–11. Available at: www.ispub.com/ostia/index.php?xmlFilePath=journals/ijns/front.xml. Accessed Jul 25, 2005.
8. Thornton SJ, Hochachka PW, Crocker DE, et al. Stroke volume and cardiac output in juvenile elephant seals during forced dives. *J Exp Biol* 2005,208:3637–3643.
9. Röbel A, Kuoni W, Augustiny N. Emerging techniques: CT scan and MRI in reptile medicine. *Semin Avian Exot Pet Med* 1994;3:156–160.
10. Wilkinson R, Hernandez-Divers S, Lafortune M, et al. Diagnostic imaging. In: McArthur S, Wilkinson R, Jean M, eds. *Medicine and surgery of tortoises and turtles*. Victoria, Australia: Blackwell Publishing Ltd, 2004;187–238.
11. Raiti P, Haramati N. Magnetic resonance imaging and computerized tomography of a gravid leopard tortoise (*Geochelone pardalis pardalis*) with metabolic bone disease. *J Zoo Wildl Med* 1997;28:189–197.
12. Straub J, Jurina K. Magnetic resonance imaging in chelonians. *Semin Avian Exot Pet Med* 2001;10:181–186.
13. Croft LA, Graham JP, Schaf SA, et al. Evaluation of magnetic resonance imaging for detection of internal tumors in green turtles with cutaneous fibropapillomatosis. *J Am Vet Med Assoc* 2004;225:1428–1435.
14. Convention on international trade in endangered species of wild fauna and flora Web site. Appendices I, II and III. Availaible at: www.cites.org/eng/app/appendices.shtml Accessed Apr 6, 2005.
15. Aguilar R, Pastor X. Impact of Spanish swordfish longline fisheries on the loggerhead sea turtle, *Caretta caretta*, population in the western Mediterranean, in *Proceedings*. 12th Annu Symp Sea Turtle Biol Conserv 1992;FSC 361, 1–6.
16. Pont SG, Alegre FN. Work of the Foundation for the Conservation and Recovery of Marine Life. *Marine Turtle Newsletter* 2000;87:5–7.
17. Dodd CK Jr. *Synopsis of the biological data on the loggerhead sea turtle* Caretta caretta *(Linnaeus 1758). US Fish and Wildlife Service biological report 88(14).* Washington, DC: US Fish and Wildlife Service, 1988;35–82.
18. Bolten A. Techniques for measuring sea turtles. In: Eckert KL, Bjorndal KA, Abreu-Grobois FA, et al, eds. *Research and management techniques for the conservation of sea turtles. IUCN/SSC marine specialist group publication No. 4.* Washington, DC: IUCN Species Survival Commission, 1999;110–115.
19. Wyneken J. *The anatomy of sea turtles. US Department of Commerce NOAA Technical Memorandum NMFS-SEFSC-470.* Washington, DC: US Department of Commerce, 2001.
20. Shore A. Magnetic resonance imaging. *Vet Clin North Am Small Anim Pract* 1993;23:437–459.
21. Irwin WP, Lohmann KJ. Magnet-induced disorientation in hatchling loggerhead sea turtles. *J Exp Biol* 2003;206:497–501.
22. Avens L, Lohmann KJ. Navigation and seasonal migratory orientation in juvenile sea turtles. *J Exp Biol* 2004;207:1771–1778.
23. McArthur S. Problem-solving approach to conditions of marine turtles. In: McArthur S, Wilkinson R, Jean M, eds. *Medicine and surgery of tortoises and turtles.* Victoria, Australia: Blackwell Publishing Ltd, 2004;301–307.
24. Pressler BM, Goodman RA, Harms CA, et al. Endoscopic evaluation of the esophagus and stomach in three loggerhead sea turtles (*Caretta caretta*) and a malaysian giant turtle (*Orlitia borneensis*). *J Zoo Wildl Med* 2003;34:88–92.
25. Orós J, Torrent A, Calabuig P, et al. Diseases and causes of mortality among sea turtles stranded in the Canary Islands, Spain (1998–2001). *Dis Aquat Organ* 2005;63:13–24.
26. Colaço B, Ferreira D, Gonzalo-Ordén M, et al. The use of magnetic resonance imaging in the study of canine brain anatomy. *Rev Port Cienc Vet* 2003;548:159–165.
27. Marino L, Sudheimer K, Pabst DA, et al. Magnetic resonance images of the brain of a dwarf sperm whale (*Kogia simus*). *J Anat* 2003;203:57–76.
28. Glyde M, Doyle R, McAllister H, et al. Magnetic resonance imaging in the diagnosis and surgical management of sacral osteochondrosis in a mastiff dog. *Vet Rec* 2004;155:83–86.
29. Murray R, Tim M. Use of magnetic resonance imaging in lameness diagnosis in the horse. *In Pract* 2005;27:138–146.
30. Assheuer J, Sager M. *MRI and CT atlas of the dog.* Berlin: Blackwell Science Ltd, 1997;347–403.
31. Burke AC. The development and evolution of the turtle body plan: inferring intrinsic aspects of the evolutionary process from experimental embryology. *Am Zool* 1991;31:616–627.
32. Armbrust LJ, Hoskinson JJ, Biller D, et al. Low-field magnetic resonance imaging of bone marrow in the lumbar spine, pelvis and femur in the adult dog. *Vet Radiol Ultrasound* 2004;5:393–401.

Annexes – Additional Papers

5. ANNEXES – ADDITIONAL PAPERS

5.1. EVALUATION OF DOPPLER ULTRASONOGRAPHY FOR THE MEASUREMENT OF BLOOD FLOW IN YOUNG LOGGERHEAD SEA TURTLES (CARETTA CARETTA) *(IN PRESS)*

Valente, A.L.; Parga, M.L.; Espada, Y., Lavin, S.; Alegre, F.; Marco, I. and Cuenca, R. (2007). Evaluation of Doppler ultrasonography for the measurement of blood flow in young loggerhead sea turtles (*Caretta caretta*). Vet. J. Aceptado para publicación. Doi: 10.1016/j.rvj..2007.03.006

Available online at www.sciencedirect.com
ScienceDirect
ELSEVIER
The Veterinary Journal xxx (2007) xxx–xxx
The Veterinary Journal
www.elsevier.com/locate/tvjl

Evaluation of Doppler ultrasonography for the measurement of blood flow in young loggerhead sea turtles (*Caretta caretta*)

Ana Luisa Valente [a,*], Maria Luz Parga [b], Yvonne Espada [c], Santiago Lavin [a], Ferrán Alegre [b], Ignasi Marco [a], Rafaela Cuenca [a]

[a] Servei d'Ecopatologia de Fauna Salvatge, Facultat de Veterinària, Universitat Autònoma de Barcelona, 08193 Bellaterra, Barcelona, Spain
[b] Centre de Recuperació d'Animals Marins, Camí Ral, 239, 08330 Premià de Mar, Barcelona, Spain
[c] Departament de Medicina i Cirurgia Animal, Facultat de Veterinària, Universitat Autònoma de Barcelona, 08193 Bellaterra, Barcelona, Spain

Accepted 9 March 2007

Abstract

The aim of this study was to identify ultrasound accessible blood vessels in the loggerhead sea turtle (*Caretta caretta*) and describe their Doppler waveform patterns, peak systolic velocity, mean velocity, systolic/diastolic ratio as well as pulsatility and resistive indices. B-mode, colour and pulsed-wave Doppler examinations were performed on 10 turtles. Flow measurements were recorded for the left and right aorta, epigastric and internal iliac arteries, and right hepatic vein. Additionally, the large blood vessels of three dead turtles were injected with latex and dissected for anatomical support. A parabolic flow velocity profile was observed in all arteries. The waveforms of the right and left aortic arteries showed an unusual pattern when compared with mammals. The hepatic vein flow velocity waveform of the loggerhead sea turtle was found to be similar to that in the dog, although the flow velocity in the C-wave was higher than that in the A-wave. The low resistance flow pattern observed suggests that the loggerhead sea turtle's organs require a continuous blood supply.

Keywords: Loggerhead sea turtle; Blood flow; Doppler wave patterns; Ultrasonography; Reptiles

Introduction

The loggerhead sea turtle (*Caretta caretta*) is an endangered species often admitted to marine rescue centres in the Mediterranean region. As is the case with other species of chelonians, health assessment poses a formidable challenge for reptilian veterinarians due to the animals' specific morphology and physiology (Murray, 2006a), and ancillary methods are usually required to obtain an accurate diagnosis. Turtles in a state of shock or with no external reaction to mechanical stimuli are frequently admitted to rehabilitation centres (Balazs, 1986; Stabenau et al., 2001). Loggerhead sea turtles captured in fishing nets usually display, on first appraisal, signs of drowning and/or shock (Balazs, 1986; Stabenau et al., 2001), and it is frequently difficult to distinguish between a live and a recently deceased turtle.

Doppler ultrasonography represents a non-invasive technique that is useful for the routine examination of blood flow in the vessels of many domestic species (Szatmári et al., 2001; Fernández del Palacio et al., 2003). It is an inexpensive technique suitable for repeated measurements and with a wide field of applications. In sea turtles, previous ultrasound studies have focused the reproductive physiology (Rostal et al., 1990) and the normal ultrasonographic B-mode appearance of cervical structures and coelomic organs (Valente et al., in press). Information concerning the use of Doppler ultrasound in sea turtles has not however been found in the literature. Accurate measurements of blood flow are essential in haemodynamic studies and could be useful in establishing a diagnosis in injured sea turtles, help in resuscitation procedures (Stabe-

* Corresponding author. Tel.: +34 93 581 19 23; fax: +34 93 581 20 06.
E-mail address: schifinoval@hotmail.com (A.L. Valente).

1090-0233/$ - see front matter © 2007 Published by Elsevier Ltd.
doi:10.1016/j.tvjl.2007.03.006

Please cite this article in press as: Valente, A.L. et al., Evaluation of Doppler ultrasonography for the measurement ..., The Veterinary Journal (2007), doi:10.1016/j.tvjl.2007.03.006

u et al., 2001) and to monitor anaesthetized patients Iurray, 2006b).

Reptiles have a complex cardiovascular system, quite fferent from that of mammals. They have many venous nuses, ventricles incompletely subdivided into two chamrs, aortic arteries and a renal portal system (Wyneken, 01; Murray, 2006a; Holz, 2006). Data on cardiovascular ysiology in chelonians are widely scattered in the literare and are characterized by significant gaps. To the thors' knowledge, a description of haemodynamic mearements for clinical application in sea turtles has not en published.

The purpose of this study was to identify blood vessels sily accessed by ultrasound in this species and describe eir Doppler waveform patterns, peak systolic velocity, ean velocity, systolic/diastolic ratio and pulsatility (PI) d resistive (RI) indices. Gross anatomical information the circulatory system (including the portal renal sysn) is provided to support the identification of the vessels amined.

aterials and methods

B-Mode, colour and pulsed-wave Doppler examinations were permed in 10 loggerhead sea turtles (four juveniles and six sub-adults), ng an Acuson ultrasound machine (Computed Sonography Siemens XP/10), in conjunction with 5.0, 6.0 and 7.0 MHz sector phased array nsducers. The turtles showed a minimum straight carapace length of 0–58.5 cm, a weight range of 3.5–26.8 kg, and were accidentally caught pelagic long-line sets and fishing nets along the North-western Mediranean coast (40°31′–42°26′N and 0°32′–3°10′E) of Spain.

During the study the turtles were temporarily housed in the rehabiliion facilities of the Rescue Centre for Marine Animals (CRAM), Preá de Mar, Barcelona, Spain. Only turtles in good condition, based on ysical, radiographic and haematological parameters, were used in this dy.

The animals were manually restrained in ventral recumbancy without lation. The Doppler evaluation was performed in a standard tempera-e-controlled room at an ambient temperature of 21–25 °C. Ultrasound s performed in 10 acoustic windows (cervical-dorsal and cervical-ven-l, left and right cervicobrachial, left and right axillary, left and right femoral and left and right postfemoral) (Valente et al., in press). upling gel (Polaris II, GE Medical Systems) was placed on the surface the transducer, which was oriented mainly on the horizontal plane. B-ode imaging was used to examine the heart (seen in the cervical-ventral oustic window) and large vessels and to guide the Doppler cursor cement in it. The same investigator performed all Doppler ultrasound aminations.

Following the orientation of the electronic callipers, Doppler tracings re recorded when an angle of 45° or less between the ultrasound beam d the direction of blood flow was achieved. Freeze trace and electronic sors were used to make the measurements. The flow parameters istive index (RI) and pulsatility index (PI) from each waveform specm were measured and calculated using the internal callipers and the alytic software of the ultrasound unit following the formulae: $= (S - D)/S$; $PI = (S - D)/A$ and S/D ratio (systolic/diastolic), where s the systolic peak (max velocity), D is the minimum diastolic velocity d A is the temporal mean velocity over one cardiac cycle (mean veloc-). Schematic drawings indicating the acoustic windows and the vessels luated are shown in Fig. 1. Three dead turtles were injected with latex ough the jugular vein, left and right aortic arteries and femoral vein. e large heart vessels and renal vasculature were dissected for additional rphological data. Specific anatomical terminology for sea turtles was opted (Wyneken, 2001).

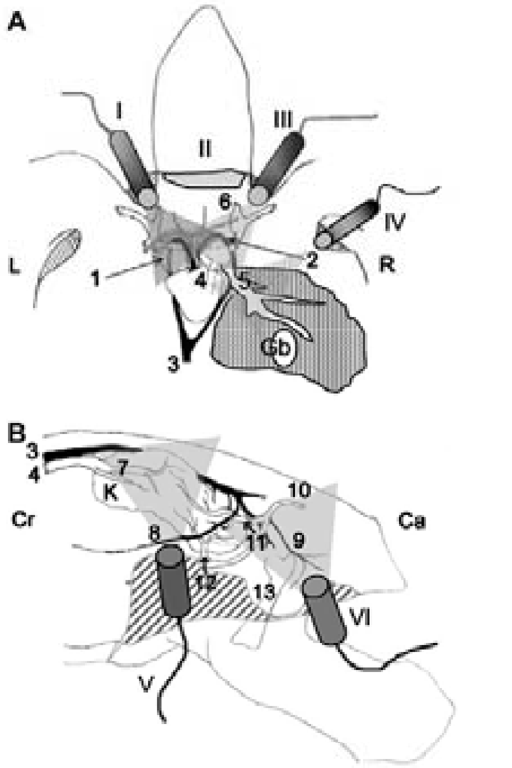

Fig. 1. Schematic drawings of the large vessels in the cardiac, hepatic and renal areas (some seen in the ultrasound examination) of loggerhead sea turtles. Arteries are represented in black and veins in white. (A) dorsal view of the area of the heart and (B) lateral view of the renal area: 1, left aorta; 2, right aorta; 3, abdominal aorta; 4, caudal vena cava; 5, right hepatic vein, Gb: gallbladder; 6, venous sinus at junction between jugular and brachial veins; 7, renal vein; 8, epigastric artery; 9, internal iliac artery; 10, iliac vein; 11, hypogastric vein (caudal portal renal vein); 12, epigastric vein (lateral portal renal vein); 13, femur. k, kidney; I, left cervicobrachial acoustic window; II, cervical-ventral acoustic window; III, right cervicobrachial acoustic window; IV, right axillary acoustic window; V, left prefemoral acoustic window; VI, left postfemoral acoustic window.

The data were analyzed statistically with STATISTICA for Windows (Stat Soft, Inc.) software. The data were tested for normality with the Shapiro–Wilk test. Paired t tests were used to compare flow measurements in paired vessels (left and right side) and differences were considered to be significant at $P < 0.05$.

Results

The mean heart rate was 29.1 beat/min (range 23–36). The highest rates (30–36 beat/min) were found in the juvenile turtles whereas values ranged between 23 and 32 beat/min in the sub-adults. Two sub-adult turtles with heart rates of 30 and 32 beat/min, respectively, were above the mean value for this group. In the juvenile turtles, the heart was entirely seen using a dorsal scan through the ventral cervical acoustic windows. An echocardiographic appearance of hyperkinetic ventricular motion with an exaggerated ventricular wall movement was observed. The left and right aortic arteries, epigastric and internal iliac arteries, and right hepatic vein were identified via ultrasonography but the iliac veins could not be visualised. The 7.0 MHz transducer was better for visualising the renal area and the postfemoral acoustic window. To assess the heart, aortic arteries and the right hepatic vein the 5.0 and 6.0 MHz transducers were used.

The left and right aortic arteries could be seen through the left and right cervicobrachial acoustic windows, respectively. From these windows, a complex image crossing many vessels was frequently observed at the cardiac base. Identification of the aortic arteries was based on their position, shape (a pronounced arch), large diameter (0.8–14.8 mm) and caudal blood flow direction (Fig. 2A and C). The vessel walls appeared as parallel, hyperechoic, thin lines. A cross-section of the left and right aortic arches was also seen when the cervical-dorsal window was examined. They were medial to the venous sinus formed by the junction of the external and internal jugular veins and the axillary vein on each side (Fig. 2B). However, in this acoustic window, the angle between the ultrasound beam and the vessels was in most cases almost perpendicular, generating unsuitable images for blood flow measurements. The visualisation of the aortic arteries through the ventral cervical acoustic window was inconsistent.

The waveforms of the right and left aortic arteries were similar. A parabolic flow profile without a spectral window was observed in eight turtles (Fig. 3A) and a discrete (mild) spectral window was present only in two turtles. Values of flow measurements and indices are showed in Table 1. No statistical differences were found between the flow parameters from the left and right aortic arteries. Compared with other arteries measured in this study, the aortic arteries showed the highest pulsatility and resistive indices.

The right hepatic vein and its junction with the caudal vena cava were clearly seen through the right axillary acoustic window, its echogenic wall enabling clear identification in the hepatic parenchyma. Close by, and positioned medially, the venous sinus of the right atrium was seen, and used as a landmark. Flow coming toward the transducer (above the baseline) and a triphasic pattern in the blood flow velocity profile was observed with A and C waves being identified. The C wave was higher than the A-wave (Fig. 3B).

Positioning the probe parallel to the carapace at the prefemoral acoustic windows enabled us to assess the left and right epigastric arteries, which crossed caudal to the kidneys and their gross anatomy indicated that they were not involved in blood supply to this organ (Fig. 4A). A parabolic flow velocity profile was observed (Fig. 3C; Table 1).

Anatomical dissections showed that most of the renal blood supply was provided by the renal portal system comprising two large renal afferent portal veins: the hypogastric vein, penetrating the kidney caudally, and the epigastric vein that enters this organ laterally in its cranial half (Fig. 5B). These veins and the renal arteries could not be

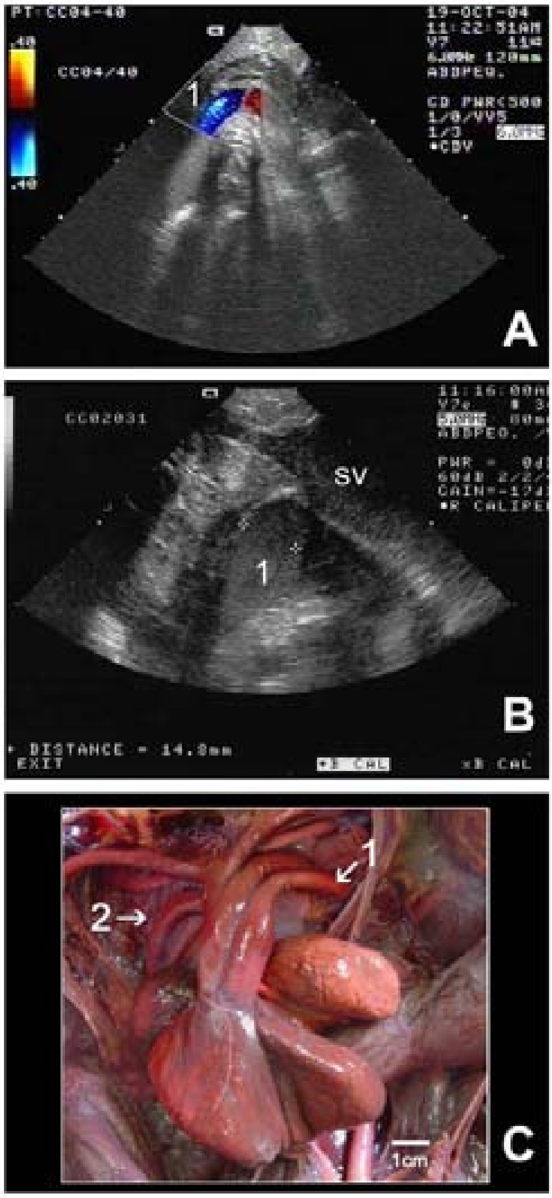

Fig. 2. (A) B-mode and colour flow Doppler ultrasound image of larg vessels of loggerhead sea turtles seen through the left cervicobrachia acoustic window (red for Doppler shifts towards the ultrasound beam an blue for shifts away from it). (B) B-mode ultrasound image of the sam arch seen through dorsal cervical acoustic window. Cursors measure th diameter. (C) Ventral view of dissected heart: 1, left aortic arch; 2, righ aorta (or right aortic arch); sv, sinus venous. (For interpretation of th references to colour in this figure legend, the reader is referred to the wel version of this article.)

clearly identified in the ultrasound examination. Only the renal vein (a single large efferent renal vein as shown in Fig. 5A) could be observed consistently in the ultrasound

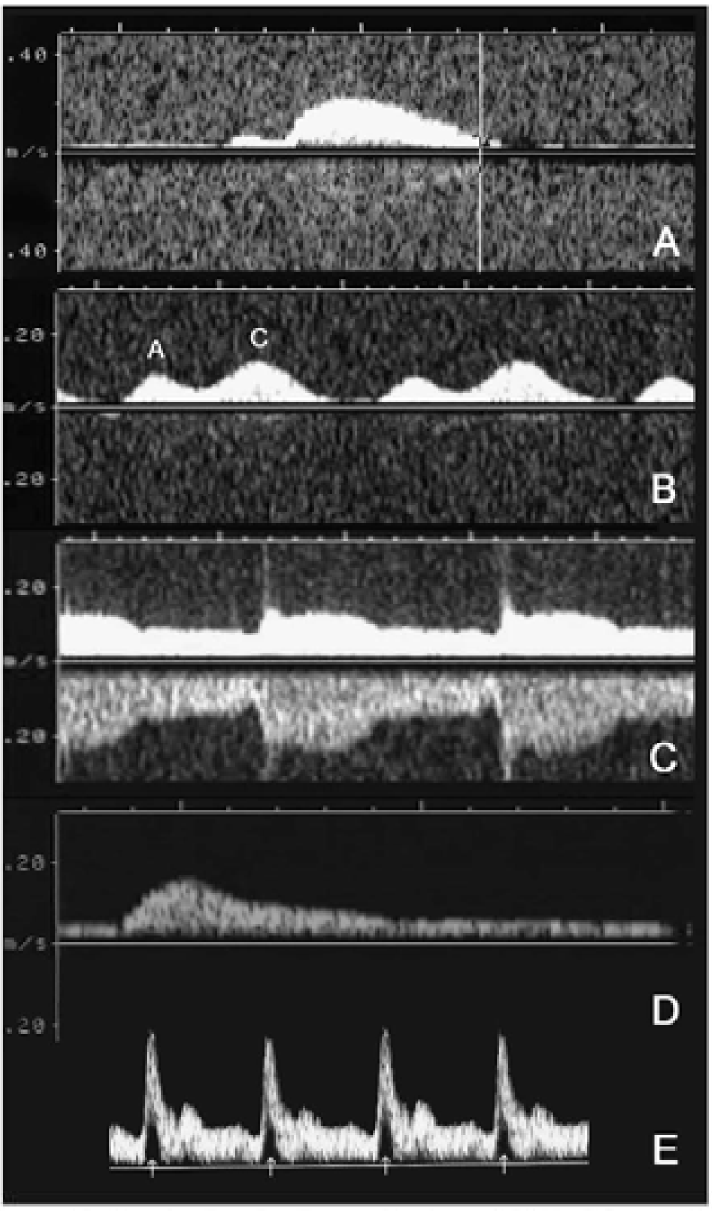

Fig. 3. Doppler waveforms of large vessels of loggerhead sea turtles. (A) aorta, (B) right hepatic vein (A and C-waves are indicated), (C) epigastric artery, (D) internal iliac artery and (E) normal pattern profile of the aorta of a mammal (arrows on the baseline indicate spectral windows).

examination, and was positioned cranial to the kidney (Fig. 4B and C).

The internal iliac arteries were identified in the postfemoral acoustic windows. The ultrasound beam was directed cranio-dorsally, dorsal to the hip joint. The arteries were consistently seen in the pelvic musculature passing dorso-caudally to the ilium (Fig. 6) and showed an unpronounced systolic peak followed by decreased continuous flow. Blood flow measurements are presented in Table 1.

Discussion

In humans and domestic animals it is known that endothelial dysfunction is present in individuals with arteriosclerosis and other causes of chronic heart failure, which could be diagnosed by abnormal responses in blood flow (Glagov et al., 1988; Kagawa et al., 1998). In the case of reptilians, there is scant information for clinicians concerning functional anatomy, circulatory physiology and pathology

Please cite this article in press as: Valente, A.L. et al., Evaluation of Doppler ultrasonography for the measurement ..., The Veterinary Journal (2007), doi:10.1016/j.tvjl.2007.03.006

Table 1
Peak systolic velocity (V_{max}), mean velocity (V_{mean}), pulsatility (PI) and resistive (RI) indices, and systolic/diastolic ratio in juvenile and sub-adul loggerhead sea turtles

Arteries	V_{max} (m/s)	V_{mean} (m/s)	PI	RI	Systole/diastoli
Left aorta	0.22 ± 0.08	0.12 ± 0.05	1.37 ± 0.44	0.71 ± 0.10	3.81 ± 1.27
Right aorta	0.19 ± 0.07	0.10 ± 0.04	1.30 ± 0,36	0.70 ± 0.12	3.76 ± 1.30
Left epigastric	0.14 ± 0.04	0.08 ± 0.02	0.86 ± 0.30	0.52 ± 0.11	2.2 ± 0.57
Right epigastric	0.19 ± 0.05	0.11 ± 0.04	1.04 ± 0.41	0.58 ± 0.12	2.6 ± 0.84
Left internal iliac	0.13 ± 0.05	0.08 ± 0.04	0.65 ± 0.45	0.46 ± 0.13	1.95 ± 0.54
Right internal iliac	0.13 ± 0.05	0.08 ± 0.04	0.83 ± 0.61	0.48 ± 0.16	2.16 ± 0.86

Mean ± standard deviation are presented.

(Dangerfield et al., 1976; Cucu, 1977). The absence of physiological parameters could be a principal obstacle to reaching a diagnosis of circulatory failure in this animal group.

The heart rate observed in our study and its negative correlation with body mass agrees with data cited by previous authors for the species (Chittick et al., 2002; Hochscheid et al., 2002). Physical distress due to manual restraint and some room temperature oscillation during examination could be responsible for the beat increase observed in two sub-adult turtles.

The small acoustic window created by the scapular girdle bones, carapace and plastron bones limited access to the aortic arteries and did not allow transducer rotation to obtain different views as is possible in dogs, where the left caudal (apical) parasternal location is commonly used to measure left ventricular outflow tract and aortic root blood flow velocities (Kienle and Thomas, 2002).

The atypical aortic waveform observed in this study seems to reflect the differences in the cardiovascular anatomy and physiology between mammals and reptiles. For example, in sea turtles there are two aortic arteries, the shunted ventricle is partially divided into three chambers (*cavum pulmonare, cavum venosum and cavum arteriosum*) and the animals have low blood viscosity (Wells and Baldwin, 1994). In sea turtles, the blood flow can be altered to shunt either deoxygenated blood to the lungs or oxygenated blood to the body, providing the animal with greater control over its blood flow, allowing long diving times (Hicks, 2002).

When the lungs are being ventilated and pulmonary resistance is low, as much as 60% of the cardiac output goes to the lungs (Murray, 2006a). In this case, during normal respiration, atrial systole causes blood to flow into the single ventricle filling the *cavum pulmonare* and *venosum*. Concurrently, pulmonary blood runs from the left atrium into the *cavum arteriosum*. During the ventricular systole, blood from the *cavum venosum* and *pulmonare* flows to the low-pressure pulmonary circuit and blood from the *cavum arteriosum* is forced through the partially contracted *cavum venosum* to exit the heart via the left and right aortic arches (Murray, 2006a).

According to one hypothetical analysis illustrated by Hicks (2002), in this kind of circulation, the ratio of peak systolic blood pressure in the systemic and pulmonary flows is close to 1:1. The heart functions as a single pressure

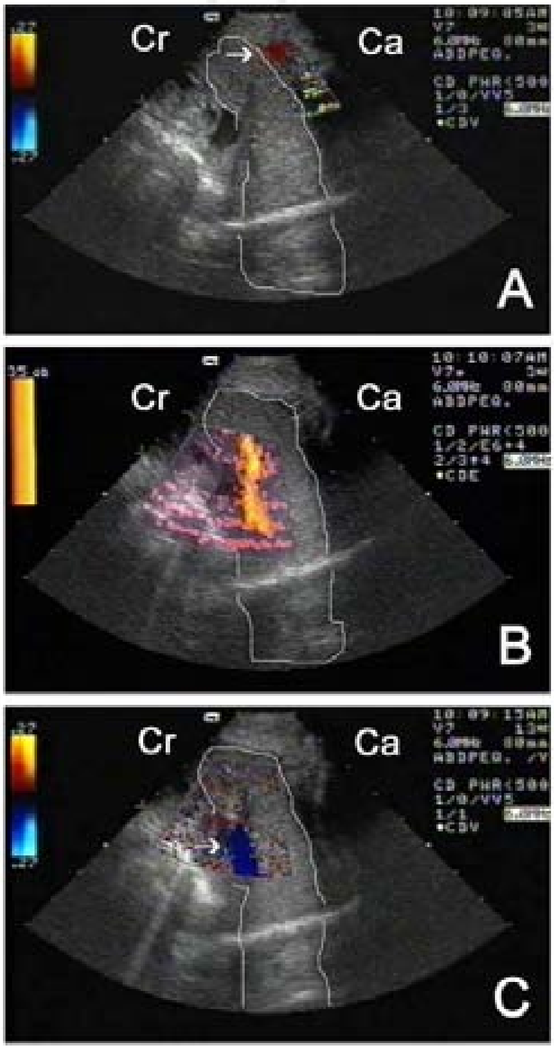

Fig. 4. Ultrasound colour Doppler view of loggerhead sea turtle kidney. (A) Arrow indicates the left epigastric artery. (B) Presence of blood flow (seen in yellow, energy Doppler amplitude flow) in the cranio-ventral par of the kidney. (C) Renal vein. Cr, cranial; Ca, caudal. (For interpretation of the references to colour in this figure legend, the reader is referred to th web version of this article.)

Please cite this article in press as: Valente, A.L. et al., Evaluation of Doppler ultrasonography for the measurement ..., The Veterinary Journal (2007), doi:10.1016/j.tvjl.2007.03.006

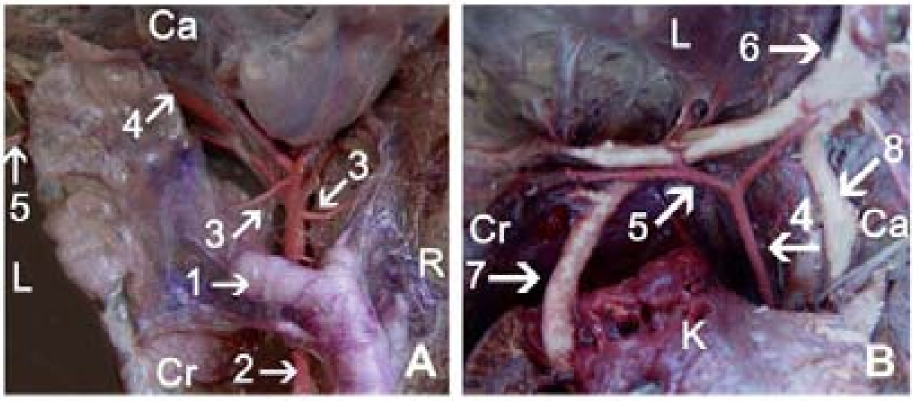

Fig. 5. Gross anatomical dissection of a loggerhead sea turtle kidney. (A) Ventral view. (B) Dorso-lateral view (kidney partially removed). K, dorsal face of kidney; 1, renal vein; 2, abdominal aorta artery; 3, renal arteries; 4, external iliac artery; 5, epigastric artery; 6, iliac vein; 7, epigastric vein (lateral renal portal vein); 8, hypogastric vein (caudal renal portal vein).

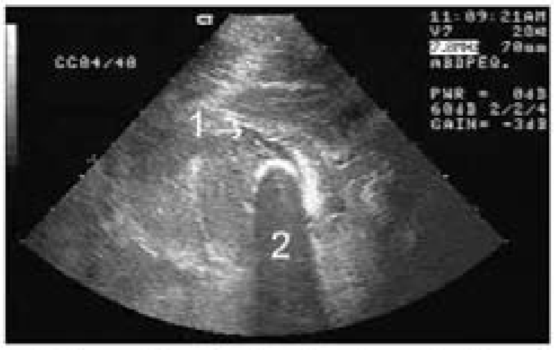

Fig. 6. Ultrasound view through postfemoral acoustic window of a loggerhead sea turtle. 1, internal iliac artery; 2, ilium.

pump, with shunt direction and magnitude varying by changes in pulmonary and systemic vascular resistances. The mammalian ratio of systemic to pulmonary vascular resistance is between 7.0 and 10.0 (Van den Bos et al., 1982). Since differences in flow wave shapes can be explained by the amount of reflection in the vascular bed (Van den Bos et al., 1982), the phylogenetic development of a double circulation with systemic and pulmonary vascular circuits (high-pressure and low-pressure circulations, respectively) in mammals could be the principal cause of the differences found in the aortic profiles, PI and RI of the loggerhead sea turtle compared with dogs (Miño et al., 2004).

Ventricular contraction tends to bring the heart apex to the muscular ridge separating the *cavum pulmonare* from the *cavum arteriosum* and *venosum*, thereby creating a barrier against the flow of blood from the *cavum arteriosum* into the *cavum pulmonare*. The exaggerated (hyperdynamic) ventricular wall motion observed in our study is considered normal for chelonians (Murray, 2006a) and is also present in dogs with left-to-right shunts or valvular regurgitation when end-diastolic volume is increased and end-systolic volume is normal to slightly increased (Kienle and Thomas, 2002).

The hepatic flow velocity waveform found in our study resembles those known for the dog and the ball python with A, C and V-waves being identified (Finn-Bodner and Hudson, 1998; Starck and Wimmer, 2005). However, unlike those findings, the spectrum was observed above the baseline in our study. Interpretation of the flow direction is related to transducer positioning and anatomical features of the species examined. In dogs, ultrasonographic examination of the hepatic vein is performed by placing the transducer on the ventral midline directly caudal to the xiphoid process of the sternum, with caudal-cranial orientation of the ultrasound beam (Mattoon et al., 2002). In the ball python, the images were obtained by placing the transducer on the left side of the large ventral scales, with the caudal part of the gallbladder being used as a landmark (Starck and Wimmer, 2005). In both species the ultrasound beam crosses the liver caudo-cranially, in the same direction as the blood flow in the hepatic veins. A positive Doppler shift is obtained if the beam is aligned in the direction of the flow whereas a negative signal (below the baseline) is present when the flow is away from the beam (Nicolaides et al., 2002). In the loggerhead sea turtle the right hepatic vein was assessed at its most cranial point, through the axillary acoustic window, therefore the flow was observed coming up to the transducer which could explain the above baseline pattern observed.

Another difference with the dog is the A and C-wave flow velocity. The A-wave represents the blood flow velocity in the hepatic vein during atrial diastole and the C-wave represents the blood flow velocity in the vein during the ventricular diastole (Pozniak, 2002). Flow velocity peak in the C-wave was higher than that in the A-wave in the loggerhead sea turtle in the present study. This pattern has also been observed in ball pythons (Starck and Wimmer, 2005) and could be related to the hyperkinetic motion of the ventricle during ventricular diastole when the ventricle presses against the filled atria at the same time as the atrioventricular monocusp valve is opened, causing a more rapid expulsion of the blood from the atria. Additionally, the right atrium fills two of the three compartments of the single ventricle, the *cavum venosum* and *cavum pulmonale*, while blood from the left atrium passes directly to the *cavum arteriosum* (Murray, 2006a). During the atrial systole the flow nearly stops and a slight reverse flow was observed, as occurs in dogs (Finn-Bodner and Hudson, 1998).

There is a great paucity of interpretative studies of the Doppler spectrum in reptiles. The low resistance flow pattern observed in the arteries studied here, indicated by broad systolic peaks and continuous, high velocity flow in diastole with gradually decreasing velocity (Pozniak, 2002), has also been seen in the ball python in a postprandial condition (Starck and Wimmer, 2005) and suggests that the loggerhead sea turtle's organs need a continuous blood supply. Normal peak flow velocities in systole in the outflow tract regions and proximal large vessels in dogs and cats are usually around 1 m/s with some patients having velocities approaching 2 m/s (Kienle and Thomas, 2002). In sea turtles we found flow velocities 10 times less than those described. The pulsatility (PI) and resistive (RI) indices in the aortic arteries were lower than those described for dogs, where PI and RI in the abdominal aorta artery were 3.09 and 0.91, respectively (Miño et al., 2004). PI and RI values from other reptilian species were not found in the literature.

Anatomical studies on the renal portal system have been carried out in various chelonian species, and anatomical terminology applied to the vessels has been confusing. Wyneken (2001) stated that in sea turtles the hypogastric vein enters the kidneys posteriorly and ventrally. The renal portal veins drain from the dorsal kidney capillaries into the external iliacs at the level of the epigastric veins, or into the posterior extent of the abdominal vein. However, in this work the schematic drawing presented does not permit clear identification of the hypogastric vein. Other authors (Holz et al., 1997; Holz, 2006) have described the afferent renal portal veins in the red-eared slider as being the iliac and hypogastric veins or generically renal portal veins.

We have assumed that the hypogastric vein is a branch of the external iliac vein referred to as the circumflex iliac vein by Holz et al. (1997). The iliac vein described by these authors as entering approximately two-thirds of the way caudal to the cranial pole of the kidney is the same as that observed in the anatomical dissections of turtles in the current study which been termed the epigastric vein. These important renal veins could not be visualised and measured in the ultrasonographic examination due to the small acoustic windows. For example, the epigastric vein runs close to the carapace bone along its lateral curvature, passing just dorsal to the prefemoral fossa, in an area inaccessible to the ultrasound beam.

To measure heart rate in chelonians, Murray (2006b) indicated the usefulness of the Doppler flow detector placed directly over the carotid artery. In sea turtles thi artery would seem not to be as accessible as in others spe cies of chelonians because of its deep position and the larg muscular neck. The internal iliac arteries could therefore b used as an alternative way to check the heart rate in larg turtles, when access to the carotid and aortic arches, eithe through the neck or cervicobrachial acoustic windows, i difficult.

Conclusion

The Doppler waveform of the aortic arteries of logger head sea turtle differs from that known in mammals in tha the plug flow pattern and the clear spectral window are no consistently observed. The low resistance flow pattern found in these large arteries reflects peculiarities in the car diovascular anatomy and physiology of the reptiles, such a the presence of two aortas and the shunted ventricle. Con sequently, peak systolic velocity, mean velocity, pulsatilit and resistive indices of the both right and left aortic arterie of the loggerhead sea turtle are smaller than those recordec for the abdominal aorta of the dog. The hepatic vein flow velocity waveform of the loggerhead sea turtle is similar to that of the dog, although the flow velocity of the C-wave i higher than that of the A-wave. The vessels (hypogastric and epigastric veins) that form the renal portal system in the loggerhead sea turtle are similar to those found in the red-eared slider, although with differing nomenclature usec by previous authors.

Based on the results of this study, we conclude tha Doppler ultrasonography could be an important tool in detecting quantitative changes in blood flow in the logger head sea turtle. Normal patterns and flow values providec in this study could help in the future assessment or evalua tion of cardiovascular disorders in injured turtles. Addi tional studies using similar Doppler parameters including an increased number of turtles and adult individuals are needed in order to complement the database on loggerheac sea turtle blood flow.

Acknowledgements

The authors would like to thank DVM Rosa Novellas DVM Encarna Casas Diáz and DVM Gregorio Mentab erre Garcia for their help in this work.

References

Balazs, G.H., 1986. Resuscitation of a comatose green turtle. Herpeto logical Review 17, 79–80.

Chittick, E.J., Stamper, M.A., Beasley, J.F., Lewbart, G.A., Horne, W.A. 2002. Medetomidine, ketamine, and sevoflurane for anesthesia o injured loggerhead sea turtles: 13 cases (1996–2000). Journal of th American Veterinary Medical Association 221, 1019–1025.

Fernández del Palacio, M.J., Fuentes, V.L., Bonagura, J.D., Schober K.E., Hatfiel, D.G., Laughlin, M.H., 2003. Evaluation of transcuta neous Doppler ultrasonography for measurement of blood flow in th femoral artery of pigs. American Journal of Veterinary Research 64 43–50.

Finn-Bodner, S.T., Hudson, J.A., 1998. Abdominal vascular sonography. Veterinary Clinics of North America: Small Animal Practice 28, 887–942.

Glagov, S., Zarins, C., Giddens, D.P., Ku, D.N., 1988. Hemodynamics and atherosclerosis. Insights and perspectives gained from studies of human arteries. Archives of Pathology and Laboratory Medicine. 112, 1018–1031.

Hicks, J.W., 2002. The physiological and evolutionary significance of cardiovascular shunting patterns in reptiles. News in Physiological Science 17, 241–245.

Hochscheid, S., Bentivegna, F., Speakma, J.R., 2002. Regional blood flow in sea turtles: implications for heat exchange in an aquatic ectotherm. Physiological and Biochemical Zoology 75, 66–76.

Holz, P., 2006. Renal anatomy and physiology. In: Mader, D.R. (Ed.), Reptile Medicine and Surgery. Elsevier Inc., Philadelphia, pp. 135–144.

Holz, P., Barker, I.K., Crawshaw, G.J., Dobson, H., 1997. The anatomy and perfusion of the renal portal system in the red-eared slider (*Trachemys scripta elegans*). Journal of Zoo and Wildlife Medicine 28, 378–385.

Kagawa, Y., Hirayama, K., Uchida, E., Izumisawa, Y., Yamaguchi, M., Kotani, T., Niiyama, M., Yoshino, T., Taniyama, H., 1998. Systemic atherosclerosis in dogs: histopathological and Immunohistochemical studies of atherosclerotic lesions. Journal of Comparative Pathology 118, 195–206.

Kienle, R.D., Thomas, W.P., 2002. Echocardiography. In: Nyland, T.G., Mattoon, J.S. (Eds.), Small Animal Diagnostic Ultrasound. W.B. Saunders Co., Philadelphia, pp. 354–423.

Mattoon, J.S., Auld, D.M., Nyland, T.G., 2002. Abdominal ultrasound scanning techniques. In: Nyland, T.G., Mattoon, J.S. (Eds.), Small Animal Diagnostic Ultrasound. W.B. Saunders Co., Philadelphia, pp. 49–81.

Miño, N., Espino, L., Suárez, M., Santamarina, G., Barriero, A., 2004. Estudio de la aorta abdominal mediante Doppler spectral pulsado en perros. Archivos de Medicina Veterinaria 36, 87–92.

Murray, M.J., 2006a. Cardiopulmonary anatomy and physiology. In: Mader, D.R. (Ed.), Reptile Medicine and Surgery. Elsevier Inc., Philadelphia, pp. 124–134.

Murray, M.J., 2006b. Cardiology. In: Mader, D.R. (Ed.), Reptile Medicine and Surgery. Elsevier Inc., Philadelphia, pp. 181–195.

Nicolaides, K., Rizzo, G., Hecker, K., Ximenes, R., 2002. Doppler in Obstetrics – Basic Principles. www.centrus.com.br (Consulted in December 1, 2006).

Pozniak, M.A., 2002. Ecografía Doppler del hígado. In: Allan, P.L., Dubbins, P.A., Pozniak, M.A., McDicken, W.N. (Eds.), Ecografía Doppler clínica. Ediciones Harcourt S.A., Madrid, pp. 123–168.

Rostal, D.C., Robeck, T.R., Owens, D.W., Kraemer, D.C., 1990. Ultrasound imaging of ovaries and eggs in Kemp's Ridley sea turtles (*Lepidochelys kempi*). Journal of Zoo and Wildlife Medicine 21, 27–35.

Stabenau, E.K., Moon, P.F., Heming, T.A., 2001. Resuscitation of sea turtles. Marine Turtle Newsletter 62, 3–5.

Starck, J.M., Wimmer, C., 2005. Patterns of blood flow during the postprandial response in ball pythons, *Python regius*. The Journal of Experimental Biology 208, 881–889.

Szatmári, V., Sótonyi, P., Vörös, K., 2001. Normal duplex Doppler waveforms of major abdominal blood vessels in dogs: a review. Veterinary Radiology & Ultrasound 42, 93–107.

Valente, A.L., Parga M.L., Espada, Y., Lavin, S., Alegre, F., Marco, I. and Cuenca, R., in press. Normal ultrasonographic imaging of the loggerhead sea turtle (*Caretta caretta*). Veterinary Record.

Van den Bos, G.C., Westerhof, N., Randall, O.S., 1982. Pulse wave reflection: can it explain the differences between systemic and pulmonary pressure and flow waves? Circulation Research 51, 479–485.

Wells, R.M.G., Baldwin, J., 1994. Oxygen transport in marine green turtle (*Chelonia mydas*) hatchlings: blood viscosity and control of haemoglobin oxygen-affinity. Journal of Experimental Biology 188, 103–114.

Wyneken J, 2001. The Anatomy of Sea Turtles. U.S. Departament of Commerce NOAA Technical Memorandum NMFS-SEFSC 470, pp. 1–172.

Please cite this article in press as: Valente, A.L. et al., Evaluation of Doppler ultrasonography for the measurement ..., The Veterinary Journal (2007), doi:10.1016/j.tvjl.2007.03.006

5.2. INGESTA PASSAGE AND GASTRIC EMPTYING TIMES IN LOGGERHEAD SEA TURTLES (CARETTA CARETTA) *(IN PRESS)*

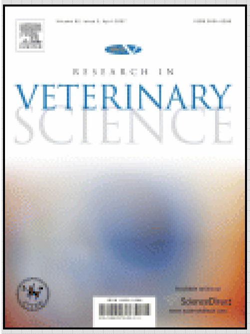

Valente, A.L.; Marco, I.; Parga, M.L.; Lavin, S.; Alegre, F. and Cuenca, R. (2007). Ingesta passage and gastric emptying times in loggerhead sea turtles (*Caretta caretta*). Res Vet Sci. Aceptado para publicación.

INGESTA PASSAGE AND GASTRIC EMPTYING TIMES IN LOGGERHEAD SEA TURTLES (*Caretta caretta*)

A. L.Valente, I. Marco, M. L. Parga, S. Lavin, Alegre F. and R. Cuenca

Address of authors:
Servei d'Ecopatologia de Fauna Salvatge. Facultat de Veterinària, Universitat Autònoma de Barcelona; 08193-Bellaterra, Barcelona, Spain (Valente, Cuenca, Lavin, Marco).
Centre de Recuperació d'Animals Marins; Camí Ral 239, 08330 - Premià de Mar, Barcelona, Spain (Parga, Alegre)

Corresponding author: Ana Luisa Valente.
Servei d'Ecopatologia de Fauna Salvatge, Facultat de Veterinària, Universitat Autònoma de Barcelona; 08193-Bellaterra, Barcelona, Spain.
Telephone: +34 93 581 19 23;

Abstract

Ingesta passage times of soft flat foam dishes and gastric emptying time of barium-impregnated polyethylene spheres (BIPS®) were measured in 22 and 8 loggerhead sea turtles (*Caretta caretta*), respectively. Transit time (T_1) was considered as the time between ingestion and first elimination, and retention time (T_{50}) and total transit time (T_{85}) the expulsion time of 50% and 85% of the markers, respectively. The experiments were carried out at different times of the year and water temperature was recorded. A set of dorso-ventral radiographs was taken to locate the BIPS®, and the gastrointestinal anatomy of 5 dead turtles was studied to help with interpretation of the radiographs. No significant correlation was observed between T_1, T_{50},T_{85} and minimum straight carapace length (SCLmin) or body mass and no statistical difference was found in ingesta passage transit times between juvenile (n=6) and sub-adult turtles (n=16). Mean passage times of the dishes (in days) were: T_1=9.05, T_{50} =12.00 and T_{85}=13.19. Gastric emptying time using BIPS® was 24 to 48h. . The transit time (T_1) for the BIPS® was longer (13.25±4.86 days) than the foam markers (8.5±2.73 days) in 8 turtles studied simultaneously. Although the total transit time tended to be faster in turtles submitted to water temperatures between 20° and 23.6°C no significant correlation was observed between T_1, T_{50} and T_{85} and the temperature.

Keywords: loggerhead sea turtle, *Caretta caretta*, BIPS®, ingesta passage time, transit time, gastrointestinal tract morphology.

Introduction

The loggerhead sea turtle (*Caretta caretta*) is a world-wide endangered species which is highly susceptible to human activity. The accidental ingestion of waste products from oil operations, plastic bags and other kinds of debris is one cause of mortality of this species throughout its distribution (Balazs, 1985; Bjorndal *et al.* 1994; Tomás *et al.* 2002; Milton and Lutz, 2003).

In some areas, such as the Mediterranean Sea, gastrointestinal disorders are common due to the ingestion of fishhooks, which cause traumatic injuries to the gastrointestinal tract leading to death (Pont and Alegre, 2000). Most turtles accidentally captured by fishing activities are released without removal of the hook. On admitttance to the marine rescue centres, diagnosis of gastrointestinal disorders in these turtles is very difficult; necropsy findings frequentely reveal severe gastrointestinal injuries such as enteritis followed by necrosis, bowel obstruction and intussusceptions produced by the folding effect of the line pulling through the intestine (Orós *et al*. 2005, Di Bello *et al*. 2006 a,b).

In domestic animals, knowledge of the ingesta passage and the normal gastric emptying times are useful in detecting gastrointestinal motility disorders and partial obstructions of the pylorus or small intestine (Manfred and Camilleri, 1992; Guilford, 2001). The digestive passage time of inert and indigestible markers, normally plastic pieces, or their simultaneous use with another type of marker have been used in many species, including chelonians (Lanyon and Marsh 1995; Spencer *et al.* 1998; Hernot *et al*. 2006; Hailey, 1997).

Barium sulphate suspension is the most frequently-used technique thanks to its inexpensiveness. However, it is not quantitative and evaluates the gastric emptying rate of the liquid but not the solid fraction of the ingesta (Guilford, 2001). When compared with a scintigram, the latter provides more accurate information (Goggin *et al.* 1998). Alternatively, barium-impregnated polyethylene spheres (BIPS®) have provided a range of diagnostic options which reduce the need to undertake exploratory surgery on cats and dogs (Nelson *et al.* 2001; Weber *et al.* 2002). The BIPS® are inert, white and have a density similar to food, but are sufficiently radiodense to show up clearly on abdominal radiographs.

In reptiles, mainly in herbivorous species, such as the iguana (*Iguana iguana*), Leopard tortoise (*Testudo pardalis*), desert tortoise (*Xerobates agassizii*), Galapagos Giant tortoise (*Geochelone nigra*), Greek tortoise (*Testudo hermanii*) and the short-necked turtle (*Emydura macquarii*), digestive studies have been performed to assess the normal transit and retention times and functional anatomy of the digestive tract (Barboza, 1995; Taylor *et al.*, 1996; Meyer, 1998; Spencer *et al.*, 1998; Smith *et al.*, 2001; Hatt *et al.*, 2002). The retention time in the aforementioned chelonians have varied from 7.5 to 14.8 days and were strongly influenced by both temperature and diet. Mean transit time of herbivorous species such as the Greek and Leopard tortoises were 2.6-17.3h and 6-6.91 days, respectively (Taylor *et al.*, 1996; Meyer, 1998). Hailey (1997) compared the digestive efficiency and gut morphology of omnivorous and herbivorous African tortoises (*Kinixys spekii* and *Geochelone pardalis*, respectively). The author found the transit time was lower in *K. spekki* (2.2 days) than in *G. pardalis* (3.8 days).

As to loggerhead sea turtles, Di Bello *et al.* (2006b) evaluated the post-enterotomy transit time of barium sulphate in the intestinal tract of six animals. Gastric emptying times and total digestive transit times were 34-264 h and

192-960 h, respectively. The authors stated that although often adequate for the diagnosis of obstruction, the procedures were not easily performed on some turtles.

The aim of the current study is to report on ingesta passage times in the healthy loggerhead sea turtles using specific indices such as the transit and retention times. Further, we have added the index T_{85} as 'total transit time' considering the long time of ingesta passage in chelonians. This work aimed to generate baseline data on digestive physiology, and to determine whether the established method of transit time assessment used in dogs and cats using BIPS® could be applied.

Materials and Methods

Twenty-two loggerhead sea turtles (6 juvenile and 16 subadult specimens) accidentally caught in pelagic long line sets and fishing nets off the north-western Mediterranean coast of Spain were used in this study. Only those turtles in which the hook was superficially attached in or near the mouth and easily removed through the oral cavity were included in the study. Turtles showed minimum straight carapace length (SCLmin) of 31.5-54.5 cm and body weight of 4.4-22.2 kg. Juvenile turtles (n=6) were considered to be those with a SCLmin of 21 to 40 cm and sub-adults (n=16) those with a SCLmin of 41 to 65 cm (Dodd, 1988). The turtles were temporarily housed in the rehabilitation facilities of the Rescue Centre for Marine Animals (CRAM), in Premià de Mar, Barcelona, Spain. Complete blood count and serum chemistry values fell within normal limits. Only clinically normal animals were included in this study.

Turtles were accommodated in individual outdoor tanks measuring 100 x 100 x 50 (deep) cm and were kept at the acclimatisation centre for a minimum of 2 weeks prior the study. The photoperiod ranged between 11h/13h and 13h light/11h dark according to season of the year. During the study, all turtles were fed at 48 h intervals with a diet based on hake (*Merluccius merluccius*) and sardines (*Sardina pilchardus sardina*) (1:1) in a quantity equivalent to 1.5 – 2.5% of the turtle body mass. No difference in the food intake was observed in the different seasons. Water temperature in the different tanks ranged according to the ambient temperature, and was measured twice daily (morning and afternoon), the mean values for each tank being used in the analyses.

Colour-marker experiments were carried out in 3 periods: early autumn, summer and winter, using 12 (8 subadults and 4 juveniles; mean body mass=11.5kg, mean SCLmin= 41.8cm), 8 (6 subadults and 2 juveniles; mean body mass=14.38kg, mean SCLmin= 45.25cm) and 2 turtles (2 subadults; mean body mass=21.35kg, mean SCLmin= 52.75cm) respectively. We used different animals in each season. Each turtle, depending on its size, was given 10-20 coloured markers made with 5mm of diameter dishes of soft flat foam (Evaland, Evapal®- Palencia, Spain) placed inside the fish at first feeding. The presence of the coloured markers in the faeces or floating in the water was recorded daily.

In the 8 turtles used in the study during the summer, BIPS® (Medical I.D. Systems, Inc.- Michigan, USA) were used simultaneously with the colour markers in the same animals to assess gastric emptying and digesta intestinal transit times. BIPS® capsules with two sphere sizes - 1.5mm (30 units) and 5 mm (10 units) - were used. BIPS® and the colour markers were put inside of a mouth of one sardine that was swallowed by the turtle. Dorso-ventral radiographs were taken 2h after the test meal to verify that all BIPS® were really swallowed. In the first week, radiographic monitoring was performed each 24h. As no great changes in the position of the BIPS® were observed within the first 24h, we decided to use a 48h interval for subsequent radiographs for the remainder of the 21-day experiment. Lateral radiographs were extremely difficult to interpret because of the displacement and overlapping of the gastrointestinal tract with other soft tissue organs and carapace bony structure. Thus, all results reported are based on dorso-ventral radiographs only.

To determine the arrangement of the intestine and to identify the position of the BIPS® in the radiographs taken during the study, a preliminary anatomical study was performed in 5 dead juvenile turtles. Two cadavers were dissected, the arrangement of the intestines recorded *in situ,* and intestine length measured. The transition from ileum to colon was identified due to the presence of an iliocecal valve followed by a great enlargement of the colon, macroscopical changes in the colour and texture of the mucosa and a visible decrease in intestinal wall thickness (Wyneken, 2001). Three cadavers were frozen at -80° C and sectioned with an electric bone saw in serial parallel sections between 18 and 20 mm thick, each one in an oriented plane (sagittal, dorsal and transverse).

Ingesta transit times are defined as follows: Transit time (T_1) the time between the ingestion of the coloured markers and the first defecation containing experimental material; Retention time (T_{50}) and Total transit time (T_{85}) as the time required to excrete a minimum of 50% and 85% of ingested markers, respectively. Concerning BIPS®, T_1 was assumed once the first large size sphere (5mm) was missing on the radiographs. We have added the index T_{85} instead T_{100} as 'total transit time' considering the long time of ingesta passage in chelonians. Gastric emptying time was defined as the time between first and last radiograph with BIPS® in the stomach area and was measured when all ten large BIPS® were out of the stomach.

Results - given as means ± sd, n= number of individuals - were analyzed with STATISTICA for Windows (Stat Soft, Inc.). A Shapiro-Wilk test was used to verify the normality of data distribution. Linear regressions and Pearson's Correlation were calculated between the T_1, T_{50} and T_{85} and temperature data, body mass and SCLmin. Graphics were done with Microsoft® Office Excel 2003. The best-fitting tendency line was used. Statistical differences for factors of variation such as kind of markers (colour markers *versus* BIPS®) and season (early autumn, summer and winter) were analyzed by a one-way ANOVA, a Levene Test for the homogeneity of variances, and a Scheffe test.

Results

The turtle dataset used in this study included some heterogeneous data because different juvenile and subadult turtles were examined in different seasons. Additionally, to evaluate the transit of the BIPS®, 8 turtles experimented in the summer must to be handled each 48h for radiographic examination which might influence in the results. The stress level produced by this handling and how much it influenced the results could not be ascertained.

The data showed normal distribution. Coloured markers were expelled in several defecations and were easily visualized and recovered. In the study (using the foam dishes) with the 22 turtles, T_1 was 9.05 ±3.05 (5 -16) days, T_{50} 12.00±4.53 (5-20) days and T_{85} 13.19±4.64 (5-21) days. Low and no significant correlation was observed between ingesta passage times (T_1, T_{50}, T_{85}) and SCLmin or body mass ($p>0.05$). No differences were observed between juveniles and subadults (Table 1).

The mean tank water temperature ranged between 16.27° C (winter) and 23.86° C (summer), with a range variation of as much as 3° C in a same tank on a single day during summer. No significant correlation was observed between water temperature and T_1, T_{50} and T_{85} (T1, r=-0.24 p=0.27; T50, r=-0.16 p=0.5; T85, r=-0.26 p=0.25). No significant difference was observed among T_1, T_{50} and T_{85} of turtles studied in the three seasons ($p>0.05$) (Table 2).

The quadratic regression curve was best fitted to the temperature data and ingesta passage times distribution. Total transit time tended to be faster in turtles submitted to water temperatures between 20°C and 23.6°C. The highest determination coefficient was observed when the total transit time (T_{85}) was plotted (Fig. 1).

Table 1. Pearson's Correlation between of the passage times (T_1, T_{50} and T_{85}) of coloured markers *versus* body mass (BM) and SCLmin and their comparison between aging groups of loggerhead sea turtles.

Passage times (days)	Person's Correlations				Aging grouping		t	df	p	n-juv	n-sub
	BM	p	SCLmin	p	juveniles	subadults					
T_1	-0.20	0.38	-0.17	0.46	10.33	8.56	-1.23	20	0.23	6	16
T_{50}	-0.17	0.46	-0.12	0.60	12.83	11.67	-0.52	19	0.61	6	15
T_{85}	0.08	0.72	0.13	0.56	13.00	13.27	0.12	19	0.91	6	15

n-juv, n-sub: number of juveniles and subadults, respectively.

Table 2. Passages times (T_1, T_{50} and T_{85}) of coloured markers in the digestive tract of loggerhead sea turtles in different year seasons.

Passage time (days)	**Seasons**			**Variance**			**Scheffe Test (p values)**		
	winter	autumn	summer	F-value	df	p	winter x autumn	winter x summer	summer x autumn
T_1	13±4.24	8.75±2.86	8.5±2.73	2.06	2	0.15	0.19	0.17	0.98
T_{50}	16±5.66	11.91±4.70	11.13±4.12	0.93	2	0.41	0.52	0.42	0.93
T_{85}	20.5±0.71	12.55±4.84	12.25±3.33	3.41	2	0.06	0.07	0.07	0.99
mT°C	16.31±0.06	19.60±1.74	23.86±0.76	-	-	-	-	-	-

mT°C = Mean temperature of the water in the pools

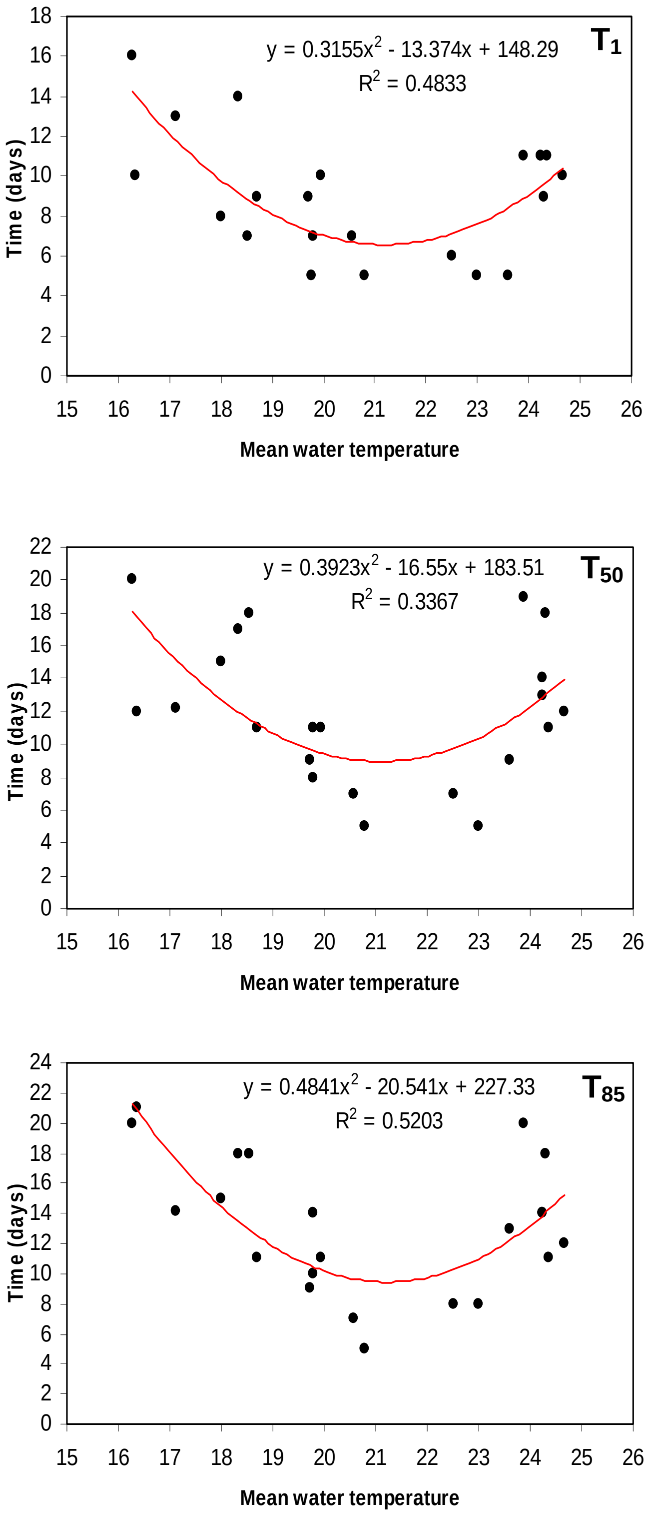

Figure 1. Quadratic regression between ingesta passage times (T_1, T_{50} and T_{85}) using colour markers and mean tank water temperature of turtles studied.

All turtles showed the BIPS® in the stomach 2h after ingestion. In this period, in 6 of the 8 tested turtles, the BIPS® were seen in the most caudal part of this organ (pyloric part). Gastric emptying time was 24 to 48h. Large and small BIPS® moved in groups in the intestine (Fig. 2). However, in 2 turtles we observed that the BIPS® were retained for 48 h in specific parts of the digestive tract. In the radiographs, the exact positioning of the BIPS® in the intestine could not be identified and the orocolic transit time (usually calculated in dogs) could not be calculated. The superimposition of the carapace and pelvis with the small BIPS® made quantitative monitoring difficult.

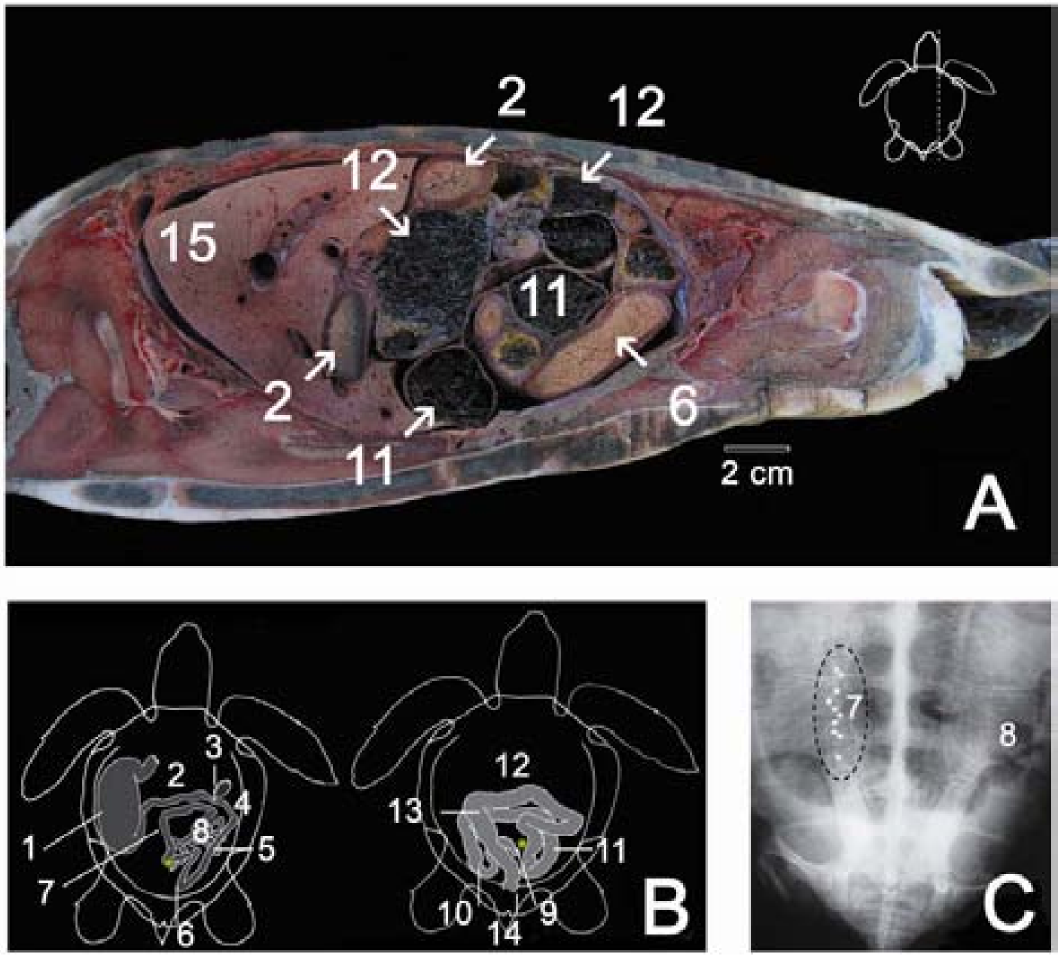

Figure 2. Anatomical sagittal section of the juvenile loggerhead sea turtles (A) and drawing of the arrangement of the gastrointestinal tract (B): 1. stomach, 2. cranial part of duodenum, 3. gallbladder, 4. cranial flexure of duodenum, 5. descending duodenum, 6. caudal flexure of duodenum, 7. jejunum, 8. ileum, 9. ileo-colic junction, 10. ascending colon, 11. ventral transverse colon, 12. dorsal transverse colon, 13. descending colon, 14. cloaca, 15. liver. Dorso-ventral radiograph of juvenile loggerhead sea turtle studied with BIPS® (C): 7. Big and small BIPS® travelling in intestine, 8. Loops of ileum

.

In eight turtles, the BIPS® were expelled all together in T_1. In turtles tested simultaneously with BIPS® and colour markers, T_1 of the BIPS® was slower (13.25±4.86 days) than the coloured markers (8.5±2.73 days) ($p<0.01$, t=-3.56, df=7). Eight of the twenty-five turtles retained some coloured markers and/or small BIPS® in their digestive tract at the end of the 23-day study period.

The anatomical study of the gastrointestinal tract in juveniles revealed that the small and large intestine were quite equal in length (turtle 1: SLCmin 31cm, small intestine length 164cm, large intestine length 148cm; turtle 2: SLCmin 32 cm, small intestine length 135cm, large intestine length 120cm), with no apendicular cecal dilatation or structure. The large intestine (transverse colon) was
divided into a dorsal and ventral part, resembling that of the equine large intestine (Fig. 2).

Discussion

An ideal marker is one that travels at the same rate as the food ingested. However, markers do not always move with the food or nutrients, making choice of marker one of the most important considerations in ingesta passage time studies (Robbins, 1993). Colour markers made from soft flat foam proved to be of great practical use in the sea turtle tanks. The major advantage observed in our study was ease of collection in faeces or in water due to floatability, which made accurate recovery and counting very easy. Sheets of ethyl vinyl acetate are inexpensive and are available in a wide variety of colours, being used widely in children’s games thanks to low toxicity. The material did not lose colour in salt water and the markers could be manufactured using a standard hole punch.

In dogs, age affects T_{50} and orocecal transit time (OCTT). However, body size does not affect these parameters (Weber *et al.* 2003). Also, in Gopher and Galapagos Giant tortoises, retention time did not depend significantly on weight or age (Bjorndal, 1987; Hatt *et al.* 2002). Nevertheless in Galapagos Giant tortoises, it is interesting to note that the solid fraction of the digesta was retained differently in adult and juvenile tortoises (Hatt *et al.* 2002). In the current study, body mass and size of the turtle showed no significant correlation with the ingesta passage transit times and no differences in T_1, T_{50} and T_{85} were observed between juvenile and subadult specimens. In the live wild sea turtle, age (aging class) is usually estimated on carapace size and might not represent the real age.

Although described by the manufacturer as being ‘low density’, BIPS® were developed in view of the specific gravity of dry dog food, higher than the food of turtles. This was verified on expulsion in the defecation - the BIPS® sank to the bottom while the colour markers stayed on the water surface together with the faeces. Due to their specific gravity, in sea turtles the BIPS® might travel together with the solid phase of the digesta whereas the very-low-density colour markers might travel with the liquid phase, thus accounting for the difference in evacuation time. In dogs, one set of dorso-ventral and lateral radiographs 6-24 hours after BIPS® administration on an empty stomach is required to establish their position in the gastrointestinal tract. In our study we took radiographs after 2h (to check that all markers were ingested) and after 24 h. As most of the turtles showed no changes in the BIPS® position in the first 24h, we decided to increase radiographic monitoring to every 48h thereafter. The ingesta transit times in the loggerhead sea turtle is longer than those reported for dogs and cats for which BIPS® are recommended (Weber *et al.*, 2003). Therefore, in this species this method involves a high number of radiographs for each animal. This fact along with the limitations of the lateral radiographs and difficulties to address the right position of the BIPS® in the intestines don't justify its use in this species.

In our study, in a concurrent experiment, the transit time of the BIPS® was found to be longer than that of the colour markers. Previous studies comparing methods to evaluate retention time of digesta in lizards and tortoises have highlighted the importance of taking into account differences in the ingesta passage time and phase separation (solid and liquid), especially where transit time is long - an important digestive strategy in reptiles (Hatch and Afik, 1999; Hatt *et al.*, 2002). A substantial difference in transit time using liquid phase markers has been observed in congeneric species of tortoises such as the *Testudo hermanni* and *T. pardalis* studied with gastrofin® and barium sulphate suspension respectively. A very fast transit time (2.6 h at 30.6°C) was observed in Greek tortoises and a relatively slower transit time (about 6 days at 29°C) in Leopard tortoises (Taylor *et al.* 1996; Meyer, 1998). The slow transit time in the Leopard tortoises could be associated with chemical immobilization carried out before the oral administration of barium.

The total transit time presented by Di Bello et al. (2006b) in six loggerhead sea turtles examined with barium sulphate administration three weeks after surgical procedure varied from 8 to 40 days. The gastric emptying time observed by these authors was much longer than that found in our study with healthy turtles.

The gut passage time is a reflection of gastric motility, in turn a reflection of health status, kind of food and ambient temperature of a reptile (Skoczylas, 1978; Spencer *et al.* 1998). Kind and frequency of feeding and water temperature of tanks were not mentioned by Di Bello *et al*. (2006b). The postoperative condition of the turtles in the study mentioned could imply gastric dysrhythmias, accounting for delay in gastric emptying time, as observed in mongrel dogs after undergoing abdominal surgery (Hotokezaka *et al.*, 1997).

Compared with the mean total transit time (mean T_{85}=13.23 days), the gastric emptying time (2 days) found in the loggerhead sea turtle seems to be relatively short. Radiographical and sectional studies in reptilians have shown that in omnivorous and carnivorous species the stomach is where the hold-up is longest, whereas in herbivorous species this appears to be in the caecum and proximal colon (Guard, 1980). Retention times observed in the loggerhead sea turtles in the current study were as long as those found in herbivorous chelonian species, such as the desert and Galapagos tortoises that experienced similar or even higher ambient temperatures (Bjorndal, 1987; Barboza, 1995; Hailey, 1997; Hatt *et al.*, 2002). In reptiles, generally the herbivore intestine is longer than the omnivore intestine, and the omnivore intestine is longer than the carnivore intestine (Diaz-Figueroa and Mitchell, 2006). The ratio of large intestine to small intestine lengths is significantly related to gut retention in omnivorous and herbivorous African tortoises (Hailey, 1997). The high ratio between large and small intestines observed in this study resembles those of tortoises, in which the large intestine is the section of the digestive tract with a great apparent area (Barboza, 1995). This finding could justify the relatively long retention time observed in the loggerhead sea turtles. Further studies concerning on morphology and digestive physiology are need in order to explain the function of the large intestine in this species.

The digesta transit times of turtles studied in different seasons did not show significant differences. These results disagree with those found in other chelonians (Meyer, 1998; Spencer *et al.* 1998). Concerning sea turtles, green turtles exposed to a laboratory simulation of subtropical winter and summer conditions showed relatively low thermal dependence of metabolic rate over the range of temperatures from 17 to 26ºC (Southwood *et al.*, 2003). As to loggerhead sea turtles, a previous study performed in the Mid-Atlantic indicated that this species prefers to remain in areas with sea surface temperatures ranging from an average of 19.38 to 25.7 ºC (Thomas and Dabo, 2005). The temperature range at which the turtles of our study tended to show fastest total transit time is placed just in the median of the preferred temperature range for the loggerhead sea turtles and could suggest the optimum or "comfort temperature" for this species.

Since in our study important factors such as acclimatisation, kind, amount and frequency of feeding were standardized, it is important to consider to what extent other captivity conditions could affect metabolism, breaking the positive correlation between temperature and metabolism known in reptiles (Gillolly *et al.* 2001). The ingesta passage times are proportionally related to the ambient temperature in reptiles (Skoczylas, 1978). Therefore we would expect to find shorter ingesta passage times in turtles experimented in summer than those studied in autumn and winter which was not found in our study. On the one hand, results from winter could be influenced by the little number of animals studied which compromises the statistical results. On the other hand, the absence of differences in the ingesta passage times between summer and autumn could indicate that the water temperature range experimented in these seasons did not affect significantly the turtles' metabolism. The stress caused by the handling the turtles at much more frequent intervals to perform the radiographs and the rapid water overheating in the summer should be also considered to explain the tendency to increase T_{85} at higher water temperatures (Fig 1). In this season, wide temperature range was observed in the tanks due to the small volume of water and the major effect of sunlight. The effect of intense heat as a potential stressor in juvenile and subadult sea turtles has not been studied. However, Gregory *et al.* (1996) found that small loggerhead turtles captured in the summer showed markedly higher corticosterone concentrations than those of large turtles captured in the same season and of all turtles captured during the winter, suggesting that a higher metabolic rate in this aging class due to higher water temperatures may be the basis for the variability of corticosterone between seasons. Sato *et al.* (1995) found that loggerhead sea turtles maintain body temperature higher than the ambient water temperature while swimming at sea, the difference being about 0.7 – 1.7 ºC. In crocodilians, efficient temperatures for ingestion and digestion are between 25 ºC and 35 ºC; temperatures higher than 35 ºC cause an undue amount of stress and inappetence (Lane, 2006). Like most reptiles, free-ranging sea turtles use behavioural means, such as postural adjustments or movements between different thermal microclimates, to maintain body temperature within a preferred range (Avery, 1982) which in our experiment was restricted by captivity conditions.

We believe that the new information provided in this study of ingesta passage time, the use of coloured ethyl vinyl acetate markers instead of BIPS® and knowledge regarding the effect of a excessive handling and comfort temperature of the loggerhead sea turtle may help rehabilitation centers and aquariums establish better conservation and management strategies, mainly in those turtles with digestive disorders or where there is a suspicion of the digestion of foreign bodies such as fishhooks.

Acknowledgments

The authors would like to thank the CRAM volunteers for their help in management of the turtles, and Dr. Jesus Piedrafita, Facultat de Veterinaria, UAB, for statistical support. Thanks also go to the anonymous reviewers.

References

Avery, R.A. 1982. Field studies of body temperatures and thermoregulation. In: C. Gans and F.H. Pough, eds. Biology of the Reptilia. Vol 12. Academic Press, London. Pp 93-166.

Balazs, G.H. 1985. Impact of ocean debris on marine turtles: entanglement and ingestion.. *In*: R.S. Shomura and H.O. Yoshida (eds.), Proceedings of the Workshop on the Fate and Impact of Marine Debris. November 27-29, 1984. Honolulu, Hawaii. US Dep. of Comm., NOAA Tech. Memo. NMFS, NOAA-TM-NMFS-SWFC-54. Pp. 387-429.

Barboza, P.S. 1995. Digesta passage and functional anatomy of the digestive tract in the desert tortoise (*Xerobates agassizii*). Journal of Comparative Physiology B 165, 193-202.

Bjorndal, K.A. 1987. Digestive efficiency in a temperate herbivorous reptile, *Gopherus polyphemus*. Copeia 3, 714-720.

Bjorndal, K.A., Bolton, A.B., Lagueux, C.J. 1994. Ingestion of marine debris by juvenile sea turtles in coastal Florida habitats. Marine Pollution Bulletin 28, 154-158.

Diaz-figueroa, O. and Mitchell, M.A. 2006. Gastrointestinal Anatomy and Physiology. In: D.R. Mader (Ed.). Reptile Medicine and Surgery.. Elsevier Inc. Philadelphia. Pp 145-162.

Di Bello, A., Valastro, C. and Staffieri, F. 2006a. Surgical approach to the coelomic cavity through the axillary and inguinal regions in sea turtles. Journal of American Veterinary Medical Association 228, 922-5.

Di Bello, A., Valastro, C., Staffieri, F. and Crovace, A. 2006b. Contrast radiography of the gastrointestinal tract in sea turtles. Veterinary Radiology & Ultrasound 47, 351-354.

Dodd, CK Jr. 1988. Synopsis of the biological data on the loggerhead sea turtle *Caretta* (Linnaeus 1758). U.S. Fish and Wildlife Service Biological Report 88, 35-82

Gillooly, J.F., Brown, J.H., West, G.B, Savage, V.M. and Charnov, E.L. 2001. Effects of Size and Temperature on Metabolic Rate. Science 293, 2248-2251

Goggin, J.M., Hoskinson, J.J., Butine, M.D., Foster, L.A. and Myers, N.C.1998. Scintigraphic assessment of gastric emptying of canned and dry diets in healthy cats. American Journal of Veterinary Research 159, 388-392.

Gregory L.F., Gross, T.S., Bolten, A.B. and Bjorndal, K.A. 1996. Plasma corticosterone concentrations associated with acute captivity stress in wild loggerhead sea turtles (*Caretta caretta*). General and Comparative Endocrinology 104, 312-320.

Guard, C.L. 1980. The reptilian digestive system: general characteristics. In: Schmidt-Nielsen K *et al.* (eds). Comparative physiology: primitive mammals. Cambridge University Press, Cambridge. Pp 43-51.

Guilford, G. 2001. Pros and cons of radiopaque markers for GI diagnosis. Proceedings of the World Small Animal Veterinary Association, World Congress, Vancouver 2001.

Available:http://www.vin.com/VINDBPub/SearchPB/Proceedings/PR05000/PR00129.htm

Hailey, A. 1997. Digestive efficiency and gut morphology of omnivorous and herbivorous African tortoises. Canadian Journal of Zoology 75, 787-794.

Hatch KA and Afik D. 1999. Retention time of digesta in insectivorous lizards – a comparison of methods and species. Comparative Biochemistry and Physiology Part A 124, 89-92.

Hatt, J.M, Gisler R., Mayes, R.W., Lechner-Doll, M., Clauss, M., Liesegang, A. and Wanner, M. 2002. The use of dosed and herbage n-alkanes as markers for the determination of intake, digestibility, mean retention time and diet selection in Galapagos tortoises (*Geochelone nigra*). The Herpetological Journal 12, 45-54.

Hernot, D.C., Biourge, V.C., Martin, L.J., Dumon, H.J. and Nguyen, P.G. 2005 Relationship between total transit time and faecal quality in adult dogs differing in body size. Journal of Animal Physiology and Animal Nutrition 89,189-193.

Hernot D.C., Dumon, H.J., Biourge, V.C., Martin, L.J., Nguyen, P.G. 2006. Evaluation of association between body size and large intestinal transit time in healthy dogs. American Journal of Veterinary Research 67, 342-347.

Hotokezaka, M., Mentis, E.P., Patel, S.P., Combs, M.J., Teates, C.D. and Schirmer, B.D. 1997. Recovery of gastrointestinal tract motility and myoelectric activity change after abdominal surgery. Archives of Surgery 132, 410- 417.

Lane T. 2006. Crocodilians – Digestive System. In: D.R. Mader (ed). Reptile Medicine and Surgery. Elsiever Inc. Philadelphia. Pp 107-108.

Lanyon, J.M. and Marsh, H.1995. Digesta Passage Times in the Dugong. Australian Journal of Zoology 43, 119 – 127

Manfred, R. and Camilleri, M. 1992. Measurement of small bowel and colonic transit: Indications and methods. Clinic Proccedings 67, 1169-1179.

Meyer, J. 1998. Gastrofin as a gastrointestinal contrast agent in the Greek tortoise (*Testudo hermanni*). Journal of Zoo and Wildlife Medicine 29, 183-189.

Milton S. and Lutz, P. 2003. Natural and human impacts on sea turtles.. In: Gary Shigenaka (Ed.). Oil and sea turtles. Biology, planning, and response. NOAA OR&R technical document. Pp 27-34. Available on: http://archive.orr.noaa.gov/oilaids/turtles/turtles.html

Nelson, O.L., Jergens, A.E., Miles, K.G. and Christensen, W.F. 2001. Gastric emptying as assessed by barium-impregnated polyethylene spheres in healthy dogs consuming a commercial kibble ration Journal of the American Animal Hospital Association 37, 444-452.

Orós J., Torrent, A., Calabuig, P., Déniz, S. 2005. Diseases and causes of mortality among sea turtles stranded in the Canary Islands, Spain (1998-2001). Diseases of Aquatic Organisms 63, 13-24.

Pont S.G., Alegre, F. N. 2000. Work of the Foundation for the Conservation and Recovery of Marine Life. Marine Turtle Newsletter 87, 5-7.

Robbins CT. 1993. Wildlife Feeding and Nutrition. New York: Academic Press.352pp.

Sato, K., Matsuzawa, Y., Tanaka, H., Bando, T., Minamika-wa, S., Sakamoto, W., Naito, Y., 1998. Internesting intervals for loggerhead turtles, *Caretta caretta*, and green turtles, *Chelonia mydas*, are affected by temperature. Canadian Journal of Zoology 76, 1651–1662.

Skoczylas, R. 1978. Physiology of the digestive tract. In: C. Gans (Ed). Biology of the Reptilia.. Vol. 8, Physiol B. Academic press. Pp 589-717

Smith, D., Dobson, H. and Spence, E. 2001. Gastrointestinal studies in the green iguana: technique and reference values. Veterinary Radiology and Ultrasound 42, 515-520.

Southwood, A.L., Darveau, C.A. and Jones, D.R. 2003. Metabolic and cardiovascular adjustments of juvenile green turtles to seasonal changes in temperature and photoperiod. The Journal of Experimental Biology 206, 4521-4531.

Spencer, R., Thompson, M.B. and Hume, I.D. 1998. The diet and digestive energetics of an Australian short-necked turtle, *Emydura macquarii*. Comparative Biochemistry and physiology Part A 121, 341-349.

Taylor S.K., Citino, S.B., Zdziarski, M.Z. and Bush, M. 1996. Radiographic anatomy and barium sulphate transit time of the gastrointestinal tract of the Leopard tortoise (*Testudo pardalis*). Journal of Zoo and Wildlife Medicine 27, 180-186.

Thomas, C.A. and Dabo S. 2005. Determining the correlation between sea surface temperature, chlorophyll concentration, QuikSCAT wind data and the presence of *Caretta caretta* and *Chelonia mydas* in the Mid-Atlantic. Undergraduate Research Experience in Ocean, Marine and Space Science. Center for Excellence in Remote Sensing Education and Research. Available in: http://nia.ecsu.edu/ureoms2005/sp/thomas/index.htm

Tomás, J., Guitart, R., Mateo, R. and Raga, J.A. 2002. Marine debris ingestion in loggerhead sea turtles, *Caretta caretta*, from the Western Mediterranean. Marine Pollution Bulletin 44, 211-216.

Weber, M.P., Martin, L.J., Biourge, V.C., Nguyen, P.G., Dumon, H.J. 2003. Influence of age and body size on orocecal transit time as assessed by use of the sulfasalazine method in healthy dogs. American Journal of Veterinary Research 64, 1105-9.

Weber, M.P., Stambouli, F., Martin, L.J., Dumon, H.J., Biourge, V.C., Nguyen, P.G. 2002. Influence of age and body size on gastrointestinal transit time of radiopaque markers in healthy dogs. American Journal of Veterinary Research 63, 677–682.